

We are committed to providing [accessible customer service](#).

If you need accessible formats or communications supports, please [contact us](#).

Nous tenons à améliorer [l'accessibilité des services à la clientèle](#).

Si vous avez besoin de formats accessibles ou d'aide à la communication, veuillez [nous contacter](#).



11-17

Grass Roots

2020 Assessment Report

Ground Magnetics & VLF

Thunder Bay Mining District, Ontario

Soper (G-0749)

NTS 052A/12

Claims: 508413, 508414, 508415, 508416, 508417, 508418, 508419, 508420,
508421

White Metal Resources Corp.

864 Squire St.
Thunder Bay, ON
P7B 4A8

March 10, 2020

Cathy Salo

Table of Contents

1.0	Introduction	2
2.0	Property Description	2
3.0	Location, Access and Topography	5
4.0	Previous Exploration	6
5.0	Regional Geology.....	6
6.0	Property Geology	8
7.0	Ground Magnetic and VLF Survey	8
8.0	Recommendations and Conclusions.....	9
9.0	References	10
10.0	Certification of qualifications	11
	FIGURE 1: ONTARIO LOCATION MAP.....	1
	FIGURE 2: CLAIM MAP.....	4
	FIGURE 3: GENERAL LOCATION	5
	FIGURE 4: PROPERTY PHYSIOGRAPHY.....	6
	FIGURE 5: TERRANCE SUBDIVISION OF SUPERIOR PROVINCE IN ONTARIO.....	7
	FIGURE 6: REGIONAL GEOLOGY	8
	TABLE 1: PROPERTY CLAIMS.....	3
	APPENDIX A: LIST OF PERSONEL	
	APPENDIX B: TABLE OF VLF RAW DATA	
	APPENDIX C: TABLE OF GROUND MAGNETIC SURVEY RAW DATA	
	APPENDIX D: MAP 1, MAGNETIC & VLF SURVEY	
	APPENDIX E: GEM SYSTEMS GSM-19 SPECIFICATIONS	
	APPENDIX F: CRONE RADEM VLF-EM SPECIFICAITONS	



Figure 1: Ontario Location Map

1.0 INTRODUCTION

White Metal Resources staked the 11-17 property to follow-up on a dipolar feature on the Queitco Super grid Magnetics (data set 1037). This can be a signature for copper, nickel and PGEs.

Starting on November 17, 2018 a grid was cut which was followed by ground geophysics including magnetics and VLF starting on November 29, 2018 and continuing until December 11, 2018 covering a large area of the property. The results confirmed that in this area there is an area of very high magnetics immediately next to a very low magnetic area. The VLF resulted in a number of generally west-east trending cross overs.

Medium to coarse grain pyroxenite with, pyrrhotite, pyrite and chalcopyrite was located in both outcrop and boulders on the property.

2.0 PROPERTY DESCRIPTION

The Property is located approximately 74.3 kilometres west of Thunder Bay on highway 11-17. The turn off for the 3.0 kilometre logging road which goes to the bottom of the claim block is located about 8.3 kilometre north of Shabaqua Corners on highway 17. The logging road is located west of the highway and continues generally north through the center of the property.

The property is composed of 9 cells (single cell) making up 191 hectares. The yearly work required costs to keep the claims in good standing amounts to \$3,600. (See Table 1 for claim details and figure 2 for claim map).

Table 1: Property Claims

Claim No.	Type	Issue_date	Anniversary	Holder
508413	Single Cell Mining Claim	20180410	20200410	(100) WHITE METAL RESOURCES CORP.
508414	Single Cell Mining Claim	20180410	20200410	(100) WHITE METAL RESOURCES CORP.
508415	Single Cell Mining Claim	20180410	20200410	(100) WHITE METAL RESOURCES CORP.
508416	Single Cell Mining Claim	20180410	20200410	(100) WHITE METAL RESOURCES CORP.
508417	Single Cell Mining Claim	20180410	20200410	(100) WHITE METAL RESOURCES CORP.
508418	Single Cell Mining Claim	20180410	20200410	(100) WHITE METAL RESOURCES CORP.
508419	Single Cell Mining Claim	20180410	20200410	(100) WHITE METAL RESOURCES CORP.
508420	Single Cell Mining Claim	20180410	20200410	(100) WHITE METAL RESOURCES CORP.
508421	Single Cell Mining Claim	20180410	20200410	(100) WHITE METAL RESOURCES CORP.

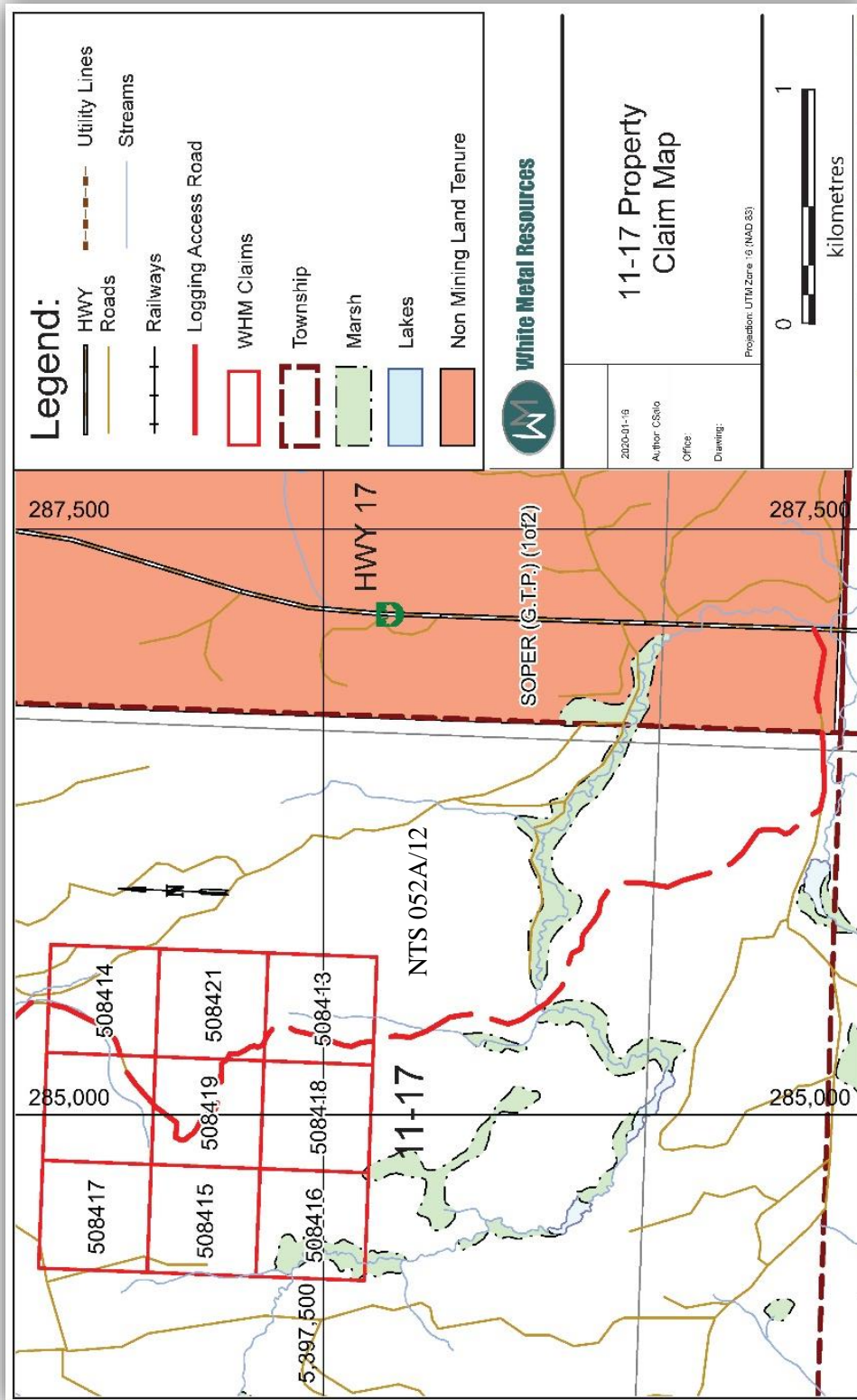


Figure 2: Claim Map

3.0 LOCATION, ACCESS AND TOPOGRAPHY

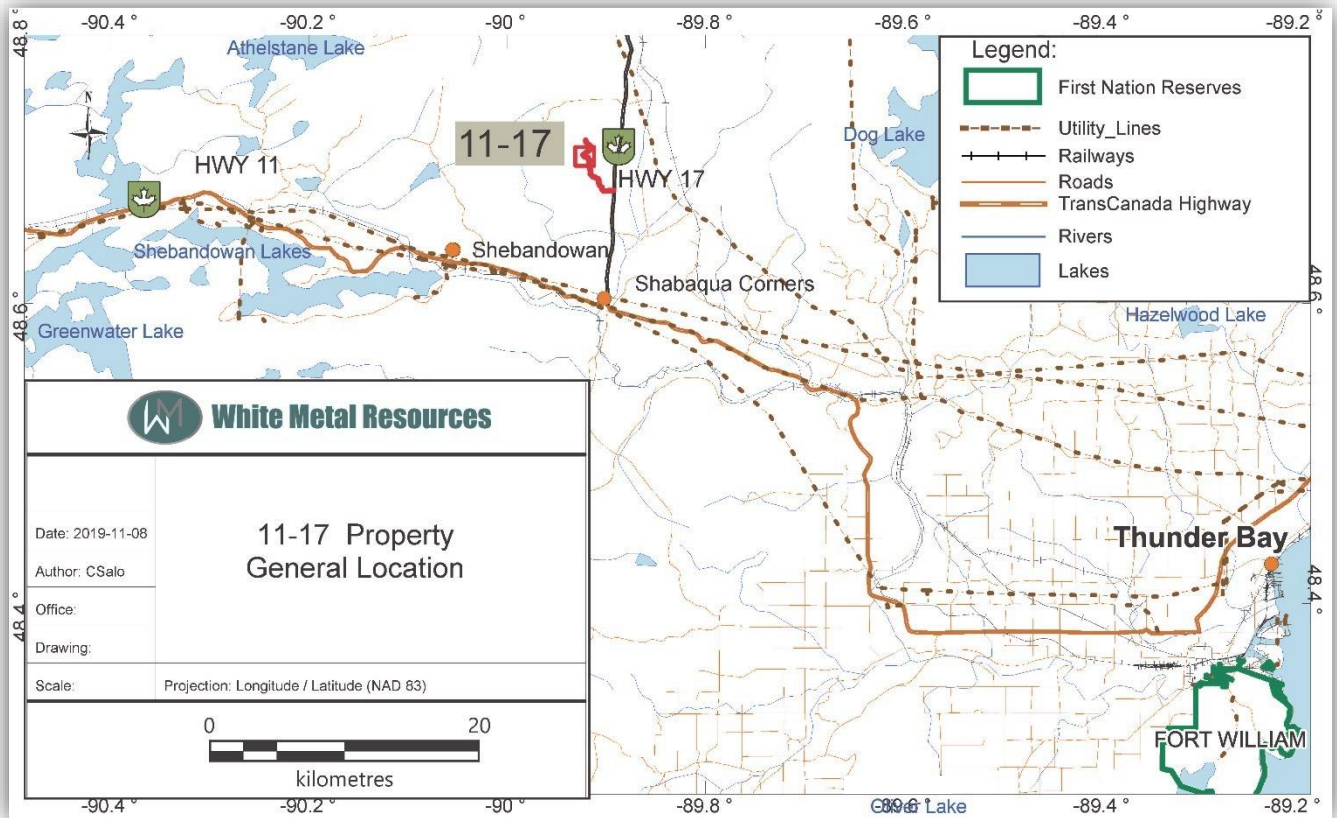


Figure 3: General Location

White Metal's 11-17 property is situated within the Thunder Bay Mining District in northern Ontario, Canada. The claims are located about 75 kilometres west of Thunder bay on TransCanada Highway 11-17, then a north Highway 17 for 8.3 kilometres and turning west on a logging Road for about another 3.0 kilometers. The property is located north of Blackwell Township and within NTS block 052A/12. The central point of the property is approximately 284,940E and 5,397,996N, (UTM Zone 16, NAD 83).

The property is mainly covered in trees (mostly spruce, with some poplar and alders) with minimal swamps. There are no lakes located on the property and minimal streams. A north-south logging road dissects the property. The topography is generally rolling hills. See Figure 4.

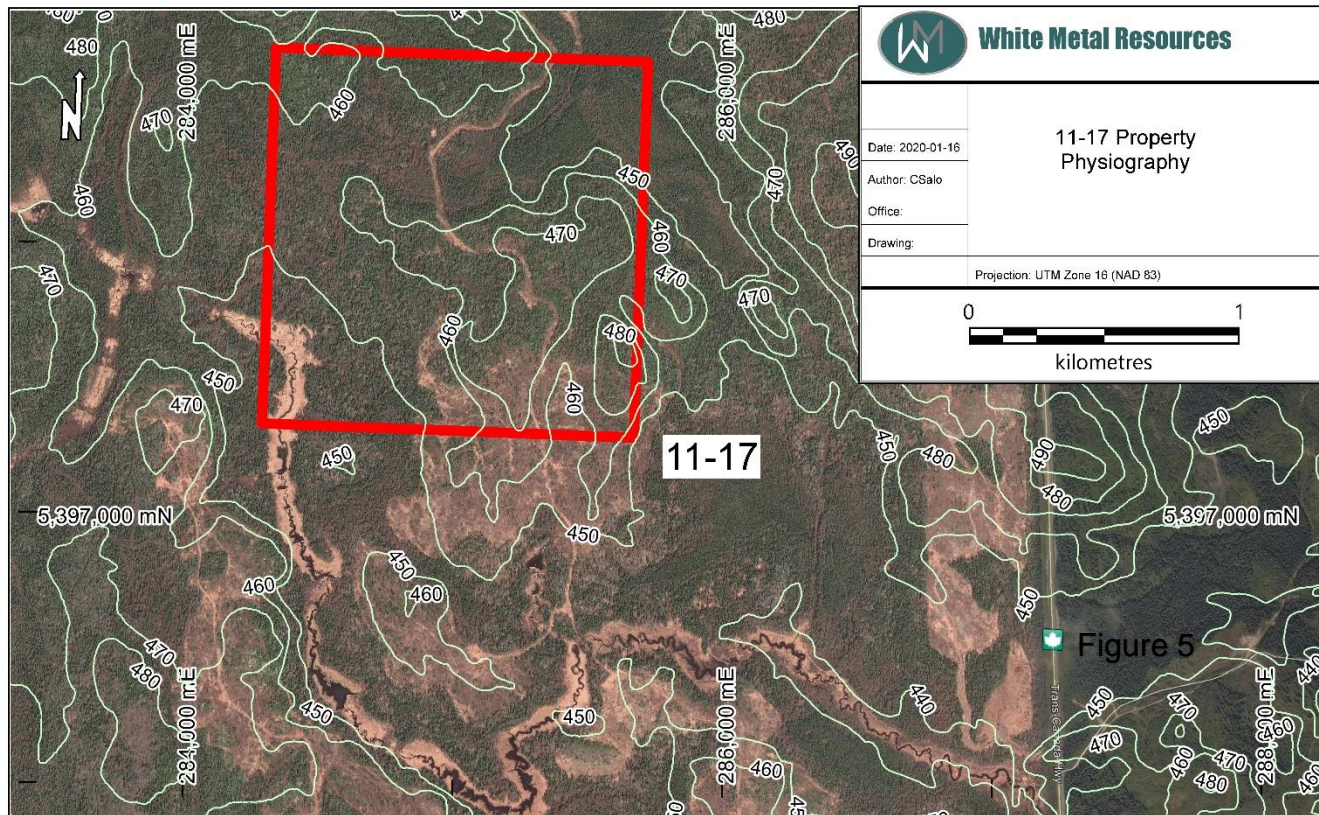


Figure 4: Property Physiography

4.0 PREVIOUS EXPLORATION

No Previous assessment work filed on this location.

5.0 REGIONAL GEOLOGY

The 11-17 property is part of the Quetico Belt which extends approximately 970 km across Ontario and parts of Minnesota. The dominant rocks within the belt are schists and gneisses produced by intense metamorphism of greywackes and minor amounts of other sedimentary rocks aged from 2,690 to 2,680 million years. The metamorphism is relatively low-grade on the margins and high-grade in the center. The low-grade components of the greywackes were derived primarily from volcanic rocks; the high-grade rocks are coarser-grained and contain minerals that reflect higher temperatures. The granitic intrusions within the high-grade metasediments were produced by subduction of the ocean crust and partial melting of metasedimentary rocks. Immediately south of Voyageurs National Park and extending to the Vermilion fault is a broad transition zone that contains migmatite

The Quetico gneiss belt represents an accretionary wedge that formed in a trench during the collision of several island arcs (greenstone belts). Boundaries between the gneiss belt and the

flanking greenstone belts to the north and south are major fault zones, the Vermilion and Rainy Lake – Seine River fault zones. (LaBerge, Gene L.,1994).

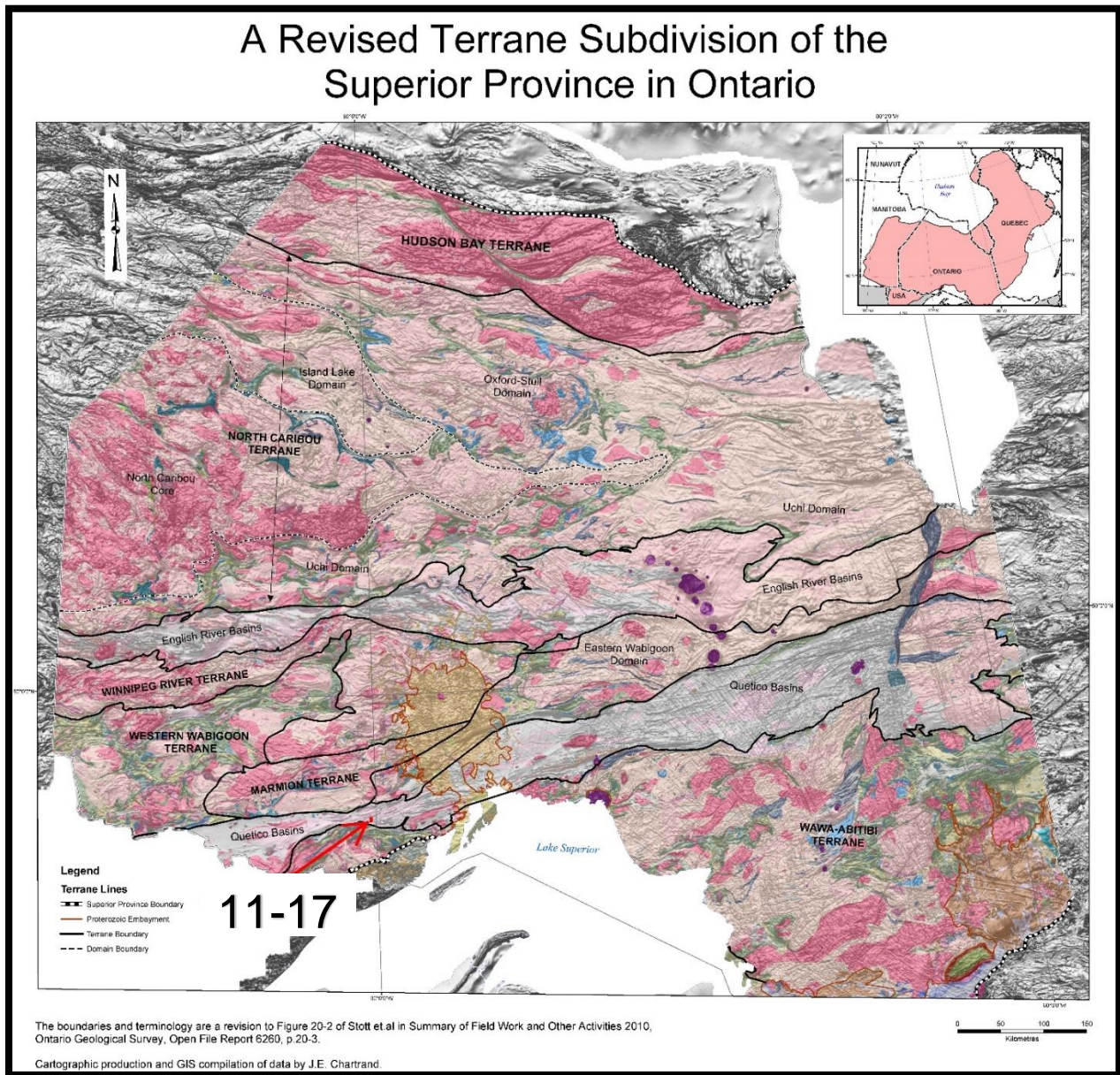


Figure 5: Terrane Subdivision of Superior Province in Ontario

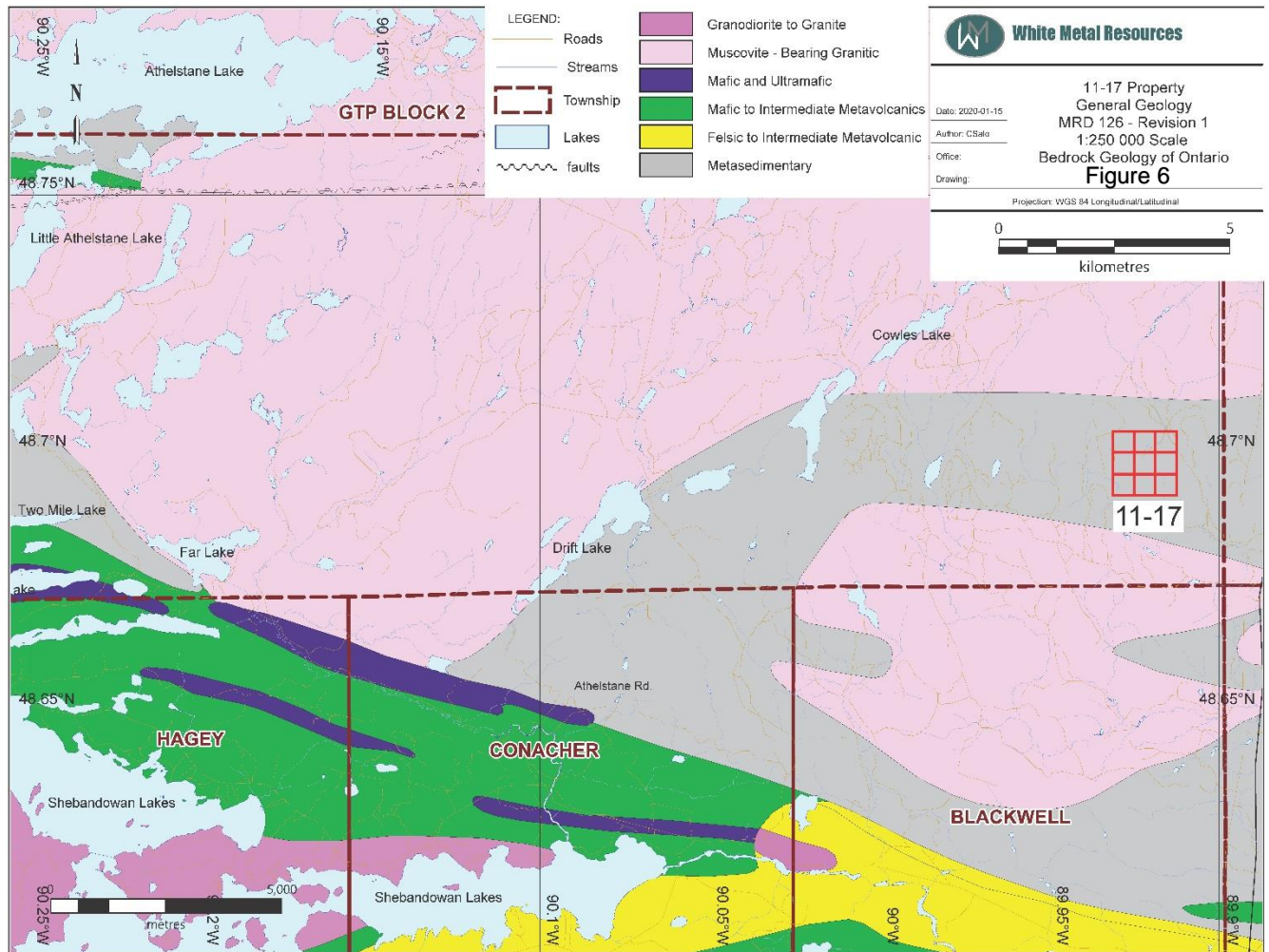


Figure 6: Regional Geology

6.0 PROPERTY GEOLOGY

Limited outcrops were located but all were identified as medium to coarse grain pyroxenite with pyrrhotite, pyrite and chalcopyrite.

7.0 GROUND MAGNETIC AND VLF SURVEY

The grid for the surveys were cut on a total of 18 north-south trending 1-kilometre lines and one east west base line. The line spacing is 100m. The project started on November 17 and was completed on December 11, 2018 by 4-man crew with Cliff Hickman in charge of the ground magnetics and Bob Heilman in charge of the VLF.

Cliff Hickman began the ground Magnetic survey on November 29 taking readings every 12.5 metres. On the same date Bob Heilman began the VLF survey taking readings every 25.0 metres. See Map 1 for results.

Below is a description of the equipment used for all the surveys along with specifications. See appendix for detail description of equipment used.

A Gem Systems GSM-19 over Hauser magnetometer serial no. 7052358 was one of the instruments used for the ground surveys. These units have an accuracy of +/- 1/100th of a gamma. In this phase of work 2.4 km was surveyed taking 194 readings at 12.5 metre intervals. A GSM-19 base station was used to monitor and correct for the diurnal variation during the survey. This instrument reads to 1/10th of a gamma resolution. The base station cycled at 15-second intervals. All survey Results have been gridded using MapInfo by Paul Nielsen and presented in plan form by Cathy Salo at 1:5,000 scale in Nad 83, UTM Zone 16 (Map 1). See appendix C for raw data.

The Crone Radem VLF-EM which was manufactured by Crone Geophysics Ltd. of Mississauga, Ontario was used for the VLF-EM survey. Cutler Maine, transmitting at 24.0 kHz and at an approximate azimuth of 246° from the survey area, was used as the transmitting station. The Crone Radem VLF-EM receiver measures both the total field strength and the dip angle. The VLF-EM uses a frequency range li-cm about 15 to 3X klz. whereas most EM instruments use frequencies ranging from a few hundred to a few thousand Hz. Because of its relatively high frequency, the VLF-EM can detect zones of relatively lower conductivity. This results in it being a useful tool for geologic mapping in areas of overburden but it also often results in detection of weak anomalies that are difficult to explain. However, the VLF-EM can also detect sulfide bodies that have too low a conductivity for other EM methods to pick up. A total of 5.5 kilometres were completed on the grid. Lines were orientated north South with readings being taken every 25 metres and 12.5m. All survey Results have been gridded using MapInfo by Cathy Salo and presented in plan form at 1:5,000 scale in Nad 83, UTM Zone 16 (Map 1). See appendix B for raw data.

8.0 RECOMMENDATIONS AND CONCLUSIONS

Ground magnetic survey confirms the Quectico supergrid survey (Data set 1037) a dipolar feature. The results of ground VLF survey shows an east-west VLF trend occurring at the boundary between the high and low magnetics. Another east-west trend occurs on the northern extents of the survey on the boundary between the magnetic low and moderate magnetics. Other minor east-west trends were also observed. (See Map 1).

It is recommended that additional prospecting be carried out with assaying of grab samples as well as soil sampling to cover the 2 main VLF trends.

9.0 REFERENCES

LaBerge, Gene L (1994). *Geology of the Lake Superior Region*. Geoscience Press, Inc.

W.O. MACKASEY, C.E. BLACKBURN AND N. F. TROWELL (1974); A Regional Approach to The Wabigoon-Quetico Belts and Its Bearing on Exploration In Northwestern Ontario, Miscellaneous Paper 58

ONTARIO GEOLOGICAL SURVEY Geophysical Data Set 1037—Revised Ontario Airborne Geophysical Surveys Magnetic Supergrids by Ontario Geological Survey 2017

ONTARIO GEOLOGICAL SURVEY MISCELLANEOUS RELEASE—DATA (MRD) 126-REVISION 1: 1:250 000 Scale Bedrock Geology of Ontario (MRD126-REV1)

10.0 CERTIFICATION OF QUALIFICATIONS

I, Cathy Salo, of 475 Francis St. East, Thunder Bay, Ontario, do hereby certify that:

1. I hold a Bachelor of Science Degree in Earth Science (1989) from Memorial University of Newfoundland, St. John's, Newfoundland and Labrador.
2. I have practised my profession in Ontario since 1989 and have been employed directing by Ontario mining exploration companies for the last 17 years as the sole proprietary of Salo Geoscience Services.

A handwritten signature in cursive script that reads "Cathy Salo". The signature is written in a light grey or blue ink.

Cathy Salo
Salo Geoscience Services
Date: March 10, 2020

Appendix A – List of Personnel

Employee/Contractor	Activities
Hickman Prospecting Services (Cliff Hickman)	Cut Grid and trails ground magnetics
Paul Nielsen (Paul Nielsen P.Geo Consulting)	Setup grid in MapInfo Geophysics data compiled in MapInfo
Bob Heilman	Cut Grid and trails VLF ground geophysics
Cathy Salo (Salo Geoscience)	GIS Compilation & Report
Alex Mainakouskang	Cut grid
Ghislain Gervais	Cut grid

Appendix B
Raw VLF Data

Appendix B
2018 VLF Data

Nad 83, Z16					
Line	Station		Easting	North	Results
10000	10500		285695.96	5398328.85	38
10000	10475		285696.06	5398302.62	30
10000	10450		285696.17	5398276.40	38
10000	10425		285696.28	5398250.18	44
10000	10400		285696.38	5398223.96	40
10000	10375		285696.49	5398197.73	40
10000	10350		285696.59	5398171.52	30
10000	10325		285696.70	5398145.29	25
10000	10300		285696.81	5398119.08	30
10000	10275		285696.91	5398092.85	25
10000	10250		285697.01	5398066.63	22
10000	10225		285697.12	5398040.41	24
10000	10200		285697.23	5398014.19	24
10000	10175		285697.33	5397987.97	20
10000	10150		285697.43	5397961.75	20
10000	10125		285697.54	5397935.53	16
10000	10100		285697.65	5397909.30	16
10000	10075		285697.75	5397883.09	16
10000	10050		285697.85	5397856.86	10
10000	10025		285697.96	5397830.65	0
10000	10000		285698.07	5397804.42	-10
10000	9975		285698.17	5397778.20	-8
10000	9950		285698.27	5397751.98	-12
10000	9925		285698.38	5397725.76	-18
10000	9900		285698.49	5397699.53	-18
10000	9875		285698.60	5397673.32	22
10000	9850		285698.69	5397647.10	28
10000	9825		285698.80	5397620.88	18
10000	9800		285698.91	5397594.66	8
10000	9775		285699.02	5397568.43	0
10000	9750		285699.12	5397542.22	-4
10000	9725		285699.22	5397515.99	-8
10000	9700		285699.33	5397489.77	-6
10000	9675		285699.44	5397463.55	-4
10000	9650		285699.54	5397437.33	-6
10000	9625		285699.64	5397411.10	-6
10000	9600		285699.75	5397384.89	-8
10000	9575		285699.86	5397358.66	-6
10000	9550		285699.96	5397332.45	-10
10000	9525		285700.06	5397306.22	-8
10000	9500		285700.17	5397280.00	0
9900	10500		285595.68	5398327.28	45
9900	10475		285595.78	5398301.06	40
9900	10450		285595.89	5398274.84	40
9900	10425		285595.99	5398248.62	50

Appendix B
2018 VLF Data

Nad 83, Z16					
Line	Station		Easting	North	Results
9900	10400		285596.10	5398222.40	32
9900	10375		285596.20	5398196.17	32
9900	10350		285596.31	5398169.96	30
9900	10325		285596.41	5398143.73	28
9900	10300		285596.52	5398117.51	25
9900	10275		285596.62	5398091.29	30
9900	10250		285596.73	5398065.07	20
9900	10225		285596.83	5398038.86	25
9900	10200		285596.94	5398012.63	18
9900	10175		285597.04	5397986.41	18
9900	10150		285597.15	5397960.19	16
9900	10125		285597.25	5397933.97	20
9900	10100		285597.36	5397907.74	20
9900	10075		285597.47	5397881.53	-12
9900	10050		285597.57	5397855.30	16
9900	10025		285597.68	5397829.08	22
9900	10000		285597.78	5397802.86	20
9900	9975		285597.89	5397776.64	14
9900	9950		285597.99	5397750.42	10
9900	9925		285598.10	5397724.20	8
9900	9900		285598.20	5397697.97	8
9900	9875		285598.31	5397671.76	2
9900	9850		285598.41	5397645.54	2
9900	9825		285598.52	5397619.31	0
9900	9800		285598.62	5397593.10	0
9900	9775		285598.73	5397566.87	0
9900	9750		285598.83	5397540.65	0
9900	9725		285598.94	5397514.43	0
9900	9700		285599.04	5397488.21	-6
9900	9675		285599.15	5397461.99	-8
9900	9650		285599.26	5397435.77	-10
9900	9625		285599.36	5397409.54	-10
9900	9600		285599.46	5397383.33	-12
9900	9575		285599.57	5397357.10	-14
9900	9550		285599.68	5397330.88	-16
9900	9525		285599.78	5397304.66	-14
9900	9500		285599.88	5397278.44	-8
9800	10500		285495.39	5398325.72	44
9800	10475		285495.49	5398299.50	42
9800	10450		285495.60	5398273.28	36
9800	10425		285495.71	5398247.05	36
9800	10400		285495.81	5398220.84	28
9800	10375		285495.92	5398194.61	28
9800	10350		285496.02	5398168.40	28
9800	10325		285496.13	5398142.17	30

Appendix B
2018 VLF Data

Nad 83, Z16					
Line	Station		Easting	North	Results
9800	10300		285496.23	5398115.95	26
9800	10275		285496.34	5398089.73	22
9800	10250		285496.44	5398063.51	22
9800	10225		285496.55	5398037.29	18
9800	10200		285496.66	5398011.07	18
9800	10175		285496.76	5397984.85	12
9800	10150		285496.86	5397958.63	14
9800	10125		285496.97	5397932.41	10
9800	10100		285497.08	5397906.18	10
9800	10075		285497.18	5397879.97	8
9800	10050		285497.28	5397853.74	10
9800	10025		285497.39	5397827.52	20
9800	10000		285497.50	5397801.30	14
9800	9975		285497.60	5397775.08	8
9800	9950		285497.70	5397748.85	0
9800	9925		285497.81	5397722.64	0
9800	9900		285497.92	5397696.42	10
9800	9875		285498.02	5397670.20	8
9800	9850		285498.13	5397643.98	8
9800	9825		285498.23	5397617.75	4
9800	9800		285498.34	5397591.54	2
9800	9775		285498.44	5397565.31	0
9800	9750		285498.55	5397539.09	0
9800	9725		285498.65	5397512.87	0
9800	9700		285498.76	5397486.65	-8
9800	9675		285498.87	5397460.42	-8
9800	9650		285498.97	5397434.21	-12
9800	9625		285499.07	5397407.98	-14
9800	9600		285499.18	5397381.77	-16
9800	9575		285499.29	5397355.54	-18
9800	9550		285499.39	5397329.32	-20
9800	9525		285499.49	5397303.11	-24
9800	9500		285499.60	5397276.88	-32
9700	10500		285395.11	5398324.16	30
9700	10475		285395.21	5398297.94	40
9700	10450		285395.31	5398271.72	40
9700	10425		285395.42	5398245.49	40
9700	10400		285395.53	5398219.28	44
9700	10375		285395.64	5398193.05	34
9700	10350		285395.73	5398166.83	40
9700	10325		285395.84	5398140.61	30
9700	10300		285395.95	5398114.39	26
9700	10275		285396.06	5398088.18	34
9700	10250		285396.15	5398061.95	22
9700	10225		285396.26	5398035.73	16

Appendix B
2018 VLF Data

Nad 83, Z16					
Line	Station		Easting	North	Results
9700	10200		285396.37	5398009.51	10
9700	10175		285396.48	5397983.29	20
9700	10150		285396.58	5397957.06	16
9700	10125		285396.68	5397930.85	12
9700	10100		285396.79	5397904.62	-10
9700	10075		285396.90	5397878.40	-16
9700	10050		285397.00	5397852.18	-10
9700	10025		285397.10	5397825.96	-24
9700	10000		285397.21	5397799.74	28
9700	9975		285397.32	5397773.52	24
9700	9950		285397.42	5397747.29	16
9700	9925		285397.52	5397721.08	16
9700	9900		285397.63	5397694.86	10
9700	9875		285397.74	5397668.63	10
9700	9850		285397.85	5397642.42	0
9700	9825		285397.94	5397616.19	0
9700	9800		285398.05	5397589.98	0
9700	9775		285398.16	5397563.75	0
9700	9750		285398.27	5397537.53	0
9700	9725		285398.37	5397511.31	-2
9700	9700		285398.47	5397485.09	-2
9700	9675		285398.58	5397458.86	0
9700	9650		285398.69	5397432.65	-4
9700	9625		285398.79	5397406.42	-8
9700	9600		285398.89	5397380.20	-16
9700	9575		285399.00	5397353.98	-20
9700	9550		285399.11	5397327.76	-8
9700	9525		285399.21	5397301.55	0
9700	9500		285399.31	5397275.32	10
9600	10500		285294.82	5398322.60	24
9600	10475		285294.93	5398296.38	24
9600	10450		285295.04	5398270.16	35
9600	10425		285295.14	5398243.93	44
9600	10400		285295.24	5398217.72	50
9600	10375		285295.35	5398191.49	38
9600	10350		285295.46	5398165.27	30
9600	10325		285295.56	5398139.05	26
9600	10300		285295.66	5398112.83	24
9600	10275		285295.77	5398086.61	20
9600	10250		285295.88	5398060.39	20
9600	10225		285295.98	5398034.17	20
9600	10200		285296.08	5398007.95	12
9600	10175		285296.19	5397981.73	10
9600	10150		285296.30	5397955.50	0
9600	10125		285296.40	5397929.29	10

Appendix B
2018 VLF Data

		Nad 83, Z16			
Line	Station		Easting	North	Results
9600	10100		285296.50	5397903.06	12
9600	10075		285296.61	5397876.84	10
9600	10050		285296.72	5397850.62	14
9600	10025		285296.82	5397824.40	12
9600	10000		285296.92	5397798.17	16
9600	9975		285297.03	5397771.96	10
9600	9950		285297.14	5397745.73	12
9600	9925		285297.25	5397719.52	10
9600	9900		285297.34	5397693.30	8
9600	9875		285297.45	5397667.07	8
9600	9850		285297.56	5397640.86	8
9600	9825		285297.67	5397614.63	6
9600	9800		285297.77	5397588.41	6
9600	9775		285297.87	5397562.19	6
9600	9750		285297.98	5397535.97	4
9600	9725		285298.09	5397509.75	2
9600	9700		285298.19	5397483.53	0
9600	9675		285298.29	5397457.30	0
9600	9650		285298.40	5397431.09	0
9600	9625		285298.51	5397404.86	0
9600	9600		285298.61	5397378.64	0
9600	9575		285298.71	5397352.43	0
9600	9550		285298.82	5397326.20	-2
9600	9525		285298.93	5397299.98	-4
9600	9500		285299.04	5397273.76	-8
9500	10500		285194.54	5398321.04	-16
9500	10475		285194.64	5398294.81	0
9500	10450		285194.75	5398268.60	20
9500	10425		285194.85	5398242.37	50
9500	10400		285194.96	5398216.16	48
9500	10375		285195.06	5398189.93	40
9500	10350		285195.17	5398163.71	36
9500	10325		285195.27	5398137.50	28
9500	10300		285195.38	5398111.27	25
9500	10275		285195.48	5398085.05	20
9500	10250		285195.59	5398058.83	18
9500	10225		285195.70	5398032.61	20
9500	10200		285195.80	5398006.38	15
9500	10175		285195.90	5397980.17	0
9500	10150		285196.01	5397953.94	-15
9500	10125		285196.12	5397927.73	-16
9500	10100		285196.22	5397901.50	16
9500	10075		285196.33	5397875.28	16
9500	10050		285196.43	5397849.06	20
9500	10025		285196.54	5397822.84	18

Appendix B
2018 VLF Data

Nad 83, Z16					
Line	Station		Easting	North	Results
9500	10000		285196.64	5397796.61	16
9400	10500		285094.25	5398319.48	-16
9400	10475		285094.36	5398293.25	-12
9400	10450		285094.46	5398267.04	20
9400	10425		285094.57	5398240.81	26
9400	10400		285094.67	5398214.59	32
9400	10375		285094.78	5398188.37	26
9400	10350		285094.88	5398162.15	38
9400	10325		285094.99	5398135.93	36
9400	10300		285095.09	5398109.71	26
9400	10275		285095.20	5398083.49	20
9400	10250		285095.31	5398057.27	16
9400	10225		285095.41	5398031.05	16
9400	10200		285095.51	5398004.82	-10
9400	10175		285095.62	5397978.61	-8
9400	10150		285095.73	5397952.38	-10
9400	10125		285095.83	5397926.16	-6
9400	10100		285095.93	5397899.94	6
9400	10075		285096.04	5397873.72	8
9400	10050		285096.15	5397847.50	14
9400	10025		285096.25	5397821.28	16
9400	10000		285096.36	5397795.05	10
9300	10500		284993.96	5398317.92	-30
9300	10475		284994.07	5398291.69	-36
9300	10450		284994.18	5398265.48	-20
9300	10425		284994.29	5398239.25	-20
9300	10400		284994.38	5398213.03	-10
9300	10375		284994.49	5398186.82	0
9300	10350		284994.60	5398160.59	14
9300	10325		284994.71	5398134.37	20
9300	10300		284994.81	5398108.15	24
9300	10275		284994.91	5398081.93	16
9300	10250		284995.02	5398055.70	0
9300	10225		284995.13	5398029.49	0
9300	10200		284995.23	5398003.26	-16
9300	10175		284995.33	5397977.05	0
9300	10150		284995.44	5397950.82	14
9300	10125		284995.55	5397924.60	14
9300	10100		284995.65	5397898.38	12
9300	10075		284995.75	5397872.16	14
9300	10050		284995.86	5397845.93	14
9300	10025		284995.97	5397819.72	24
9300	10000		284996.07	5397793.50	24
9200	10500		284893.69	5398316.36	-10
9200	10475		284893.79	5398290.13	0

Appendix B
2018 VLF Data

Nad 83, Z16					
Line	Station		Easting	North	Results
9200	10450		284893.89	5398263.91	-16
9200	10425		284894.00	5398237.69	-14
9200	10400		284894.11	5398211.47	8
9200	10375		284894.21	5398185.26	10
9200	10350		284894.31	5398159.03	16
9200	10325		284894.42	5398132.81	20
9200	10300		284894.53	5398106.59	14
9200	10275		284894.63	5398080.37	12
9200	10250		284894.73	5398054.14	-16
9200	10225		284894.84	5398027.93	-14
9200	10200		284894.95	5398001.70	-16
9200	10175		284895.05	5397975.48	-12
9200	10150		284895.15	5397949.26	0
9200	10125		284895.26	5397923.04	10
9200	10100		284895.37	5397896.82	10
9200	10075		284895.48	5397870.60	20
9200	10050		284895.57	5397844.37	20
9200	10025		284895.68	5397818.16	20
9200	10000		284895.79	5397791.94	8
9100	10500		284793.40	5398314.80	22
9100	10475		284793.50	5398288.57	16
9100	10450		284793.61	5398262.35	14
9100	10425		284793.71	5398236.14	14
9100	10400		284793.82	5398209.91	10
9100	10375		284793.93	5398183.69	10
9100	10350		284794.03	5398157.47	-10
9100	10325		284794.13	5398131.25	-12
9100	10300		284794.24	5398105.03	-16
9100	10275		284794.35	5398078.81	-12
9100	10250		284794.45	5398052.58	-18
9100	10225		284794.55	5398026.37	-16
9100	10200		284794.66	5398000.14	-20
9100	10175		284794.77	5397973.92	-20
9100	10150		284794.87	5397947.70	-14
9100	10125		284794.98	5397921.48	-16
9100	10100		284795.08	5397895.25	-8
9100	10075		284795.19	5397869.04	0
9100	10050		284795.29	5397842.82	24
9100	10025		284795.40	5397816.60	20
9100	10000		284795.50	5397790.38	16
9000	10500		284693.11	5398313.23	10
9000	10475		284693.22	5398287.01	26
9000	10450		284693.32	5398260.79	22
9000	10425		284693.43	5398234.58	16
9000	10400		284693.53	5398208.35	10

Appendix B
2018 VLF Data

Nad 83, Z16					
Line	Station		Easting	North	Results
9000	10375		284693.64	5398182.13	0
9000	10350		284693.74	5398155.91	-10
9000	10325		284693.85	5398129.69	-10
9000	10300		284693.96	5398103.46	-14
9000	10275		284694.06	5398077.25	-14
9000	10250		284694.16	5398051.02	-14
9000	10225		284694.27	5398024.80	-16
9000	10200		284694.38	5397998.58	-8
9000	10175		284694.48	5397972.36	-10
9000	10150		284694.59	5397946.14	-12
9000	10125		284694.69	5397919.92	-14
9000	10100		284694.80	5397893.69	-6
9000	10075		284694.90	5397867.48	-8
9000	10050		284695.01	5397841.26	-6
9000	10025		284695.11	5397815.03	-10
9000	10000		284695.22	5397788.82	10
8900	10500		284592.83	5398311.67	18
8900	10475		284592.94	5398285.46	32
8900	10450		284593.03	5398259.23	22
8900	10425		284593.14	5398233.01	18
8900	10400		284593.25	5398206.79	10
8900	10375		284593.36	5398180.57	10
8900	10350		284593.46	5398154.35	-10
8900	10325		284593.56	5398128.13	-12
8900	10300		284593.67	5398101.90	-16
8900	10275		284593.78	5398075.69	-16
8900	10250		284593.88	5398049.46	-18
8900	10225		284593.98	5398023.24	-16
8900	10200		284594.09	5397997.02	-12
8900	10175		284594.20	5397970.80	-10
8900	10150		284594.30	5397944.57	-10
8900	10125		284594.40	5397918.36	-8
8900	10100		284594.51	5397892.14	-6
8900	10075		284594.62	5397865.92	-8
8900	10050		284594.72	5397839.70	-10
8900	10025		284594.82	5397813.47	-14
8900	10000		284594.93	5397787.26	-10
8800	10500		284492.54	5398310.11	14
8800	10475		284492.65	5398283.90	10
8800	10450		284492.76	5398257.67	10
8800	10425		284492.86	5398231.45	14
8800	10400		284492.96	5398205.23	14
8800	10375		284493.07	5398179.01	20
8800	10350		284493.18	5398152.78	12
8800	10325		284493.28	5398126.57	0

Appendix B
2018 VLF Data

		Nad 83, Z16			
Line	Station		Easting	North	Results
8800	10300		284493.38	5398100.34	-10
8800	10275		284493.49	5398074.13	-14
8800	10250		284493.60	5398047.90	-14
8800	10225		284493.70	5398021.68	-18
8800	10200		284493.80	5397995.46	-16
8800	10175		284493.91	5397969.24	-18
8800	10150		284494.02	5397943.01	-20
8800	10125		284494.13	5397916.80	-18
8800	10100		284494.22	5397890.58	-24
8800	10075		284494.33	5397864.35	-16
8800	10050		284494.44	5397838.14	-10
8800	10025		284494.55	5397811.91	-12
8800	10000		284494.64	5397785.70	-10
8700	10500		284392.26	5398308.55	-32
8700	10475		284392.36	5398282.33	0
8700	10450		284392.47	5398256.11	8
8700	10425		284392.58	5398229.89	6
8700	10400		284392.68	5398203.67	14
8700	10375		284392.78	5398177.45	16
8700	10350		284392.89	5398151.22	10
8700	10325		284393.00	5398125.01	-12
8700	10300		284393.10	5398098.78	-12
8700	10275		284393.20	5398072.56	-16
8700	10250		284393.31	5398046.34	-18
8700	10225		284393.42	5398020.12	-16
8700	10200		284393.52	5397993.90	-16
8700	10175		284393.63	5397967.68	-20
8700	10150		284393.73	5397941.46	-30
8700	10125		284393.84	5397915.24	-20
8700	10100		284393.94	5397889.02	-20
8700	10075		284394.05	5397862.79	-30
8700	10050		284394.15	5397836.58	-20
8700	10025		284394.26	5397810.35	-12
8700	10000		284394.37	5397784.13	-18

Appendix C
Raw Magnetic Data



Appendix C
Magnetic Data

Nad 83, Z16				
East	North		Field_nT	Corr_nT
285296.81	5397799.83		56170.41	56101.30
285309.34	5397799.88		56150.67	56081.58
285321.88	5397799.93		56150.53	56081.59
285334.42	5397799.98		56050.89	55981.81
285346.95	5397800.03		56070.12	56001.04
285359.49	5397800.08		55913.52	55844.33
285372.03	5397800.13		55804.70	55735.82
285384.56	5397800.18		55927.74	55858.93
285397.10	5397800.23		55936.83	55867.97
285409.63	5397800.28		55954.00	55885.28
285422.17	5397800.34		55999.68	55930.84
285434.71	5397800.39		56025.29	55956.67
285447.24	5397800.44		56044.56	55975.95
285459.78	5397800.49		56120.80	56052.30
285472.32	5397800.54		55855.00	55786.62
285484.85	5397800.59		56124.68	56056.32
285497.39	5397800.64		56161.79	56093.42
285509.92	5397800.69		56176.92	56108.68
285522.46	5397800.74		56209.63	56141.35
285535.00	5397800.79		56251.50	56183.17
285547.53	5397800.84		56166.98	56098.73
285560.07	5397800.89		56160.09	56091.67
285572.61	5397800.94		56178.82	56110.58
285585.14	5397801.00		56270.70	56202.53
285597.68	5397801.05		56138.28	56070.16
285610.21	5397801.10		56119.94	56051.98
285622.75	5397801.15		56267.25	56199.23
285635.29	5397801.20		56142.90	56075.21
285647.82	5397801.25		56082.65	56014.96
285660.36	5397801.30		56046.98	55979.17
285672.90	5397801.35		56068.24	56000.37
285685.43	5397801.40		56089.88	56022.14
285697.97	5397801.45		56177.66	56110.04
285697.92	5397813.99		56208.13	56140.82
285697.87	5397826.53		56137.79	56070.38
285697.82	5397839.06		56097.48	56030.41
285697.77	5397851.60		56163.88	56096.72
285697.72	5397864.13		56228.15	56160.94
285697.66	5397876.67		56221.12	56153.85
285697.61	5397889.21		56169.35	56102.50
285697.56	5397901.74		56079.00	56012.08
285697.51	5397914.28		56029.14	55962.13
285697.46	5397926.82		56029.69	55962.66
285697.41	5397939.35		55997.97	55931.22
285697.36	5397951.89		56002.35	55935.55

Appendix C
Magnetic Data

Nad 83, Z16				
East	North		Field_nT	Corr_nT
285697.31	5397964.42		56667.37	56600.65
285697.26	5397976.96		56157.63	56090.85
285697.21	5397989.50		56167.38	56100.54
285697.16	5398002.03		56026.26	55959.55
285697.11	5398014.57		56070.75	56004.13
285697.06	5398027.11		56164.45	56097.94
285697.00	5398039.64		56150.60	56084.34
285696.95	5398052.18		56226.40	56159.88
285696.90	5398064.71		56132.61	56066.21
285696.85	5398077.25		56129.08	56062.88
285696.80	5398089.79		56068.54	56002.30
285696.75	5398102.32		56083.87	56018.00
285696.70	5398114.86		56119.93	56053.89
285696.65	5398127.40		56006.89	55940.95
285696.60	5398139.93		56002.64	55936.79
285696.55	5398152.47		56043.25	55977.18
285696.50	5398165.01		55996.00	55930.11
285696.45	5398177.54		56004.51	55938.81
285696.40	5398190.08		55994.40	55928.56
285696.34	5398202.61		56042.80	55977.00
285696.29	5398215.15		56019.67	55953.74
285696.24	5398227.69		56054.45	55988.82
285696.19	5398240.22		56027.38	55961.74
285696.14	5398252.76		56078.15	56012.68
285696.09	5398265.30		56066.19	56000.47
285696.04	5398277.83		56072.97	56007.30
285695.99	5398290.37		56144.90	56079.56
285695.94	5398302.90		56161.01	56095.88
285595.65	5398302.50		56202.60	56137.82
285595.70	5398289.96		56126.67	56062.80
285595.75	5398277.43		56079.36	56015.36
285595.80	5398264.89		56097.94	56033.89
285595.85	5398252.35		56061.23	55997.33
285595.90	5398239.82		56089.44	56025.04
285595.95	5398227.28		56045.82	55981.88
285596.00	5398214.74		56024.43	55960.12
285596.05	5398202.21		55974.38	55910.36
285596.10	5398189.67		55960.18	55895.84
285596.16	5398177.14		56092.57	56028.29
285596.21	5398164.60		56086.17	56022.16
285596.26	5398152.06		56038.51	55974.17
285596.31	5398139.53		56014.75	55950.31
285596.36	5398126.99		56126.75	56062.07
285596.41	5398114.45		56178.83	56114.36
285596.46	5398101.92		56176.95	56112.34

Appendix C
Magnetic Data

Nad 83, Z16				
East	North		Field_nT	Corr_nT
285596.51	5398089.38		56198.11	56133.49
285596.56	5398076.85		56147.31	56082.67
285596.61	5398064.31		56239.36	56174.68
285596.66	5398051.77		56208.97	56144.18
285596.71	5398039.24		56157.69	56092.92
285596.76	5398026.70		56112.88	56048.41
285596.82	5398014.16		56177.40	56113.04
285596.87	5398001.63		56167.27	56103.05
285596.92	5397989.09		56205.73	56141.14
285596.97	5397976.55		56184.88	56120.55
285597.02	5397964.02		56145.29	56081.10
285597.07	5397951.48		56063.01	55998.61
285597.12	5397938.95		56138.03	56073.37
285597.17	5397926.41		56105.09	56040.29
285597.22	5397913.87		56194.83	56130.15
285597.27	5397901.34		56109.90	56045.19
285597.32	5397888.80		56021.16	55956.44
285597.37	5397876.26		56064.18	55999.41
285597.42	5397863.73		56064.01	55999.24
285597.48	5397851.19		56069.57	56004.79
285597.53	5397838.66		56167.94	56103.33
285597.58	5397826.12		56103.87	56039.36
285597.63	5397813.58		56147.59	56082.90
285597.68	5397801.05		56121.34	56056.55
285597.73	5397788.51		56057.08	55992.50
285597.78	5397775.97		56181.73	56116.93
285597.83	5397763.44		56130.63	56066.03
285597.88	5397750.90		56147.99	56083.43
285597.93	5397738.36		56375.85	56311.62
285597.98	5397725.83		56177.98	56113.80
285598.03	5397713.29		56531.97	56467.66
285598.08	5397700.76		56304.62	56240.23
285598.14	5397688.22		56295.40	56231.15
285598.19	5397675.68		56261.99	56197.81
285598.24	5397663.15		56219.54	56155.25
285598.29	5397650.61		56176.52	56112.21
285598.34	5397638.07		56198.58	56134.38
285598.39	5397625.54		56194.45	56130.25
285598.44	5397613.00		56192.27	56128.00
285598.49	5397600.47		56205.34	56141.30
285598.54	5397587.93		56174.82	56110.83
285598.59	5397575.39		56171.81	56107.84
285598.64	5397562.86		56168.52	56104.55
285598.69	5397550.32		56182.38	56118.40
285598.74	5397537.78		56222.47	56158.50

Appendix C
Magnetic Data

Nad 83, Z16				
East	North		Field_nT	Corr_nT
285598.80	5397525.25		56244.53	56180.76
285598.85	5397512.71		56233.60	56169.75
285598.90	5397500.17		56310.40	56246.70
285598.95	5397487.64		56301.44	56237.79
285599.00	5397475.10		56248.46	56184.79
285599.05	5397462.57		56152.29	56088.56
285599.10	5397450.03		56152.31	56088.54
285599.15	5397437.49		56169.35	56105.58
285599.20	5397424.96		56153.33	56089.45
285599.25	5397412.42		55780.18	55716.26
285599.30	5397399.88		56130.64	56066.77
285599.35	5397387.35		55974.49	55910.84
285599.40	5397374.81		56091.24	56027.37
285599.46	5397362.28		55948.11	55884.32
285599.51	5397349.74		55991.22	55927.49
285599.56	5397337.20		55994.91	55931.35
285599.61	5397324.67		55986.78	55923.18
285599.66	5397312.13		56001.59	55938.00
285599.71	5397299.59		56096.48	56033.04
285700.00	5397300.00		56042.93	55978.82
285699.95	5397312.54		56122.67	56058.40
285699.90	5397325.07		56163.18	56098.45
285699.85	5397337.61		56177.77	56113.42
285699.80	5397350.15		56148.86	56084.44
285699.75	5397362.68		56163.36	56099.30
285699.70	5397375.22		56094.38	56029.76
285699.64	5397387.75		56163.12	56098.77
285699.59	5397400.29		56165.47	56101.30
285699.54	5397412.83		56146.60	56082.09
285699.49	5397425.36		56325.49	56260.90
285699.44	5397437.90		56189.49	56125.05
285699.39	5397450.44		56219.84	56155.65
285699.34	5397462.97		55955.05	55890.52
285699.29	5397475.51		56249.12	56184.60
285699.24	5397488.04		56254.50	56190.09
285699.19	5397500.58		56281.21	56216.51
285699.14	5397513.12		56255.96	56191.42
285699.09	5397525.65		56287.80	56223.32
285699.04	5397538.19		56353.09	56288.49
285698.98	5397550.73		56313.54	56248.65
285698.93	5397563.26		56317.00	56252.20
285698.88	5397575.80		56290.56	56226.09
285698.83	5397588.34		56251.98	56187.36
285698.78	5397600.87		56062.20	55997.44
285698.73	5397613.41		56251.24	56186.38

Appendix C
Magnetic Data

Nad 83, Z16				
East	North		Field_nT	Corr_nT
285698.68	5397625.94		56246.76	56182.30
285698.63	5397638.48		56195.37	56130.47
285698.58	5397651.02		56000.74	55935.86
285698.53	5397663.55		56155.82	56090.57
285698.48	5397676.09		56236.20	56170.77
285698.43	5397688.63		56079.07	56014.16
285698.38	5397701.16		56104.56	56039.37
285698.32	5397713.70		56145.19	56080.38
285698.27	5397726.23		56267.96	56203.09
285698.22	5397738.77		56405.03	56340.19
285698.17	5397751.31		56202.64	56137.32
285698.12	5397763.84		56156.29	56091.80
285698.07	5397776.38		56136.34	56071.32
285698.02	5397788.92		56172.54	56107.49
285697.97	5397801.45		56174.20	56109.40
285497.39	5397800.64		56145.79	56079.76
285497.44	5397788.10		56161.47	56095.99
285497.49	5397775.57		56132.18	56066.53
285497.54	5397763.03		56075.48	56008.08
285497.59	5397750.49		56095.28	56027.86
285497.64	5397737.96		56099.74	56032.55
285497.69	5397725.42		56094.55	56027.55
285497.74	5397712.89		56063.90	55997.28
285497.79	5397700.35		56173.72	56106.81
285497.85	5397687.81		56129.01	56061.57
285497.90	5397675.28		56187.16	56119.45
285497.95	5397662.74		56200.42	56133.01
285498.00	5397650.20		56191.78	56124.06
285498.05	5397637.67		56143.02	56075.62
285498.10	5397625.13		56163.09	56096.14
285498.15	5397612.60		56171.97	56104.53
285498.20	5397600.06		56186.45	56119.35
285498.25	5397587.52		56129.68	56062.09
285498.30	5397574.99		56021.33	55953.94
285498.35	5397562.45		56044.36	55976.81
285498.40	5397549.91		56056.21	55988.75
285498.45	5397537.38		56068.77	56001.00
285498.51	5397524.84		56112.63	56045.06
285498.56	5397512.30		56148.28	56081.20
285498.61	5397499.77		56019.32	55952.10
285498.66	5397487.23		55993.71	55926.85
285498.71	5397474.70		56038.98	55970.68
285498.76	5397462.16		56008.84	55940.15
285498.81	5397449.62		55978.51	55910.22
285498.86	5397437.09		55892.28	55823.74

Appendix C
Magnetic Data

Nad 83, Z16				
East	North		Field_nT	Corr_nT
285498.91	5397424.55		55903.89	55835.92
285498.96	5397412.01		56386.40	56318.82
285499.01	5397399.48		56018.96	55951.01
285499.06	5397386.94		56239.93	56172.55
285499.11	5397374.41		56114.11	56046.50
285499.17	5397361.87		56128.44	56061.07
285499.22	5397349.33		56409.88	56342.77
285499.22	5397349.33		56408.76	56341.53
285499.27	5397336.80		56817.86	56750.55
285499.32	5397324.26		56788.71	56721.11
285499.37	5397311.72		56912.27	56843.87
285499.42	5397299.19		57011.37	56943.00
285399.13	5397298.78		56417.87	56348.79
285399.08	5397311.32		56404.46	56335.65
285399.03	5397323.85		56404.95	56335.62
285398.98	5397336.39		56436.32	56367.33
285398.93	5397348.93		56567.92	56498.55
285398.87	5397361.46		56600.68	56531.65
285398.82	5397374.00		56600.10	56531.15
285398.77	5397386.54		56601.97	56532.89
285398.72	5397399.07		56518.51	56449.63
285398.67	5397411.61		56330.95	56261.53
285398.62	5397424.14		56228.86	56159.57
285398.57	5397436.68		56082.34	56012.38
285398.52	5397449.22		56100.47	56030.71
285398.47	5397461.75		56155.78	56085.85
285398.42	5397474.29		56181.95	56112.04
285398.37	5397486.83		56206.33	56136.97
285398.32	5397499.36		56292.08	56222.12
285398.27	5397511.90		56271.55	56202.32
285398.21	5397524.44		56350.15	56280.25
285398.16	5397536.97		56426.27	56356.94
285398.11	5397549.51		56670.23	56600.67
285398.06	5397562.04		56197.67	56128.45
285398.01	5397574.58		55969.02	55899.49
285397.96	5397587.12		55977.26	55907.82
285397.91	5397599.65		55975.90	55906.25
285397.86	5397612.19		56019.29	55949.29
285397.81	5397624.73		56066.38	55996.78
285397.76	5397637.26		56098.93	56029.88
285397.71	5397649.80		56112.87	56043.14
285397.66	5397662.33		56158.21	56088.43
285397.61	5397674.87		56175.73	56106.03
285397.55	5397687.41		56191.58	56121.82
285397.50	5397699.94		56146.06	56076.20

Appendix C
Magnetic Data

Nad 83, Z16				
East	North		Field_nT	Corr_nT
285397.45	5397712.48		56165.72	56096.11
285397.40	5397725.02		56406.42	56336.85
285397.35	5397737.55		56181.65	56111.17
285397.30	5397750.09		56024.77	55954.46
285397.25	5397762.63		55978.94	55909.08
285397.20	5397775.16		55923.92	55854.62
285397.15	5397787.70		55947.49	55877.60
285397.05	5397812.77		55921.72	55853.99
285397.00	5397825.31		55979.22	55911.55
285396.95	5397837.84		55925.12	55857.74
285396.89	5397850.38		55880.48	55813.10
285396.84	5397862.92		55826.69	55759.17
285396.79	5397875.45		55826.82	55759.24
285396.74	5397887.99		55848.25	55780.84
285396.69	5397900.52		55829.94	55762.65
285396.64	5397913.06		55648.50	55581.29
285396.59	5397925.60		55518.96	55451.72
285396.54	5397938.13		55254.09	55186.85
285396.49	5397950.67		55444.38	55377.19
285396.44	5397963.21		55668.85	55602.05
285396.39	5397975.74		55754.62	55687.81
285396.34	5397988.28		55763.79	55697.07
285396.29	5398000.81		55807.99	55741.33
285396.23	5398013.35		55817.87	55751.34
285396.18	5398025.89		55787.72	55720.95
285396.13	5398038.42		55835.53	55768.58
285396.08	5398050.96		55878.28	55811.38
285396.03	5398063.50		55915.10	55848.40
285395.98	5398076.03		55927.16	55860.52
285395.93	5398088.57		55939.75	55873.11
285395.88	5398101.11		55969.05	55902.51
285395.83	5398113.64		56009.64	55943.27
285395.78	5398126.18		55980.59	55914.18
285395.73	5398138.71		56007.96	55941.55
285395.68	5398151.25		56009.59	55943.24
285395.63	5398163.79		56041.19	55974.82
285395.57	5398176.32		56097.11	56030.78
285395.52	5398188.86		56078.70	56012.41
285395.47	5398201.40		56135.42	56069.15
285395.42	5398213.93		56033.39	55967.20
285395.37	5398226.47		56068.06	56001.88
285395.32	5398239.00		56000.10	55933.94
285395.27	5398251.54		56016.08	55949.94
285395.22	5398264.08		56025.85	55959.77
285395.17	5398276.61		56029.61	55963.66

Appendix C
Magnetic Data

Nad 83, Z16				
East	North		Field_nT	Corr_nT
285395.12	5398289.15		56026.46	55960.56
285395.07	5398301.69		56042.06	55976.20
285495.36	5398302.09		55921.68	55856.39
285495.41	5398289.56		55897.52	55832.25
285495.46	5398277.02		56826.57	56761.33
285495.51	5398264.48		56646.69	56581.48
285495.56	5398251.95		56502.06	56437.02
285495.61	5398239.41		56031.89	55966.82
285495.66	5398226.87		56058.66	55993.52
285495.71	5398214.34		55964.99	55899.77
285495.76	5398201.80		55973.42	55908.26
285495.81	5398189.27		56169.99	56105.01
285495.87	5398176.73		56116.57	56051.60
285495.92	5398164.19		56041.37	55976.39
285495.97	5398151.66		56011.23	55946.26
285496.02	5398139.12		56038.61	55973.23
285496.07	5398126.58		56200.38	56135.13
285496.12	5398114.05		56090.98	56025.92
285496.17	5398101.51		56055.36	55990.36
285496.22	5398088.98		56061.05	55996.15
285496.27	5398076.44		56022.47	55957.56
285496.32	5398063.90		56033.87	55968.93
285496.37	5398051.37		56018.09	55953.08
285496.42	5398038.83		56010.41	55945.39
285496.47	5398026.29		55876.55	55811.60
285496.53	5398013.76		56123.79	56058.86
285496.58	5398001.22		58574.40	58509.84
285496.63	5397988.68		56569.07	56504.44
285496.68	5397976.15		56283.21	56218.47
285496.73	5397963.61		56203.75	56139.00
285496.78	5397951.08		56130.71	56065.98
285496.83	5397938.54		56140.81	56076.14
285496.88	5397926.00		56125.65	56060.96
285496.93	5397913.47		56196.68	56131.97
285496.98	5397900.93		56107.99	56043.29
285497.03	5397888.39		56135.87	56071.25
285497.08	5397875.86		56203.77	56139.10
285497.13	5397863.32		56175.27	56110.58
285497.19	5397850.79		56139.84	56075.10
285497.24	5397838.25		56104.56	56039.79
285497.29	5397825.71		56107.22	56042.48
285497.34	5397813.18		56147.20	56082.47
285497.39	5397800.64		56152.01	56087.26
285296.81	5397799.83		56168.01	56103.60
285296.86	5397787.29		56059.76	55995.23

Appendix C
Magnetic Data

Nad 83, Z16				
East	North		Field_nT	Corr_nT
285296.91	5397774.76		56012.93	55948.44
285296.96	5397762.22		55932.17	55867.64
285297.01	5397749.68		55895.63	55831.08
285297.06	5397737.15		55952.69	55888.08
285297.11	5397724.61		56059.37	55994.79
285297.16	5397712.07		55974.53	55910.05
285297.21	5397699.54		56060.35	55995.88
285297.26	5397687.00		55944.08	55879.70
285297.31	5397674.46		56086.53	56021.94
285297.37	5397661.93		56111.12	56046.41
285297.42	5397649.39		56070.32	56005.53
285297.47	5397636.86		56028.19	55963.47
285297.52	5397624.32		56061.95	55997.32
285297.57	5397611.78		55949.29	55884.71
285297.62	5397599.25		56105.04	56040.38
285297.67	5397586.71		56169.73	56104.96
285297.72	5397574.17		56150.57	56085.80
285297.77	5397561.64		56081.73	56016.94
285297.82	5397549.10		56191.24	56126.40
285297.87	5397536.57		56204.26	56139.20
285297.92	5397524.03		56120.81	56055.64
285297.97	5397511.49		56134.53	56069.36
285298.03	5397498.96		56205.80	56140.69
285298.08	5397486.42		56330.58	56265.53
285298.13	5397473.88		56404.95	56340.00
285298.18	5397461.35		56493.64	56428.78
285298.23	5397448.81		56475.56	56410.77
285298.28	5397436.27		56443.02	56378.31
285298.33	5397423.74		56383.29	56318.51
285298.38	5397411.20		56445.86	56381.02
285298.43	5397398.67		56457.29	56392.30
285298.48	5397386.13		56438.11	56372.82
285298.53	5397373.59		56557.21	56491.84
285298.58	5397361.06		56245.51	56180.24
285298.63	5397348.52		56172.27	56106.93
285298.69	5397335.98		56267.69	56202.35
285298.74	5397323.45		56226.62	56161.31
285298.79	5397310.91		56250.78	56185.34
285298.84	5397298.38		56271.60	56206.11
285198.55	5397297.97		56245.05	56179.49
285198.50	5397310.51		56185.77	56119.35
285198.45	5397323.04		56151.76	56085.25
285198.40	5397335.58		56346.75	56280.30
285198.34	5397348.11		56123.06	56056.59
285198.29	5397360.65		56174.04	56107.55

Appendix C
Magnetic Data

Nad 83, Z16				
East	North		Field_nT	Corr_nT
285198.24	5397373.19		56108.34	56042.13
285198.19	5397385.72		56093.33	56026.93
285198.14	5397398.26		56200.54	56134.12
285198.09	5397410.80		56259.81	56193.24
285198.04	5397423.33		56281.24	56214.53
285197.99	5397435.87		56272.35	56205.41
285197.94	5397448.40		56241.16	56174.01
285197.89	5397460.94		56003.03	55935.94
285197.84	5397473.48		56213.41	56146.46
285197.79	5397486.01		56210.51	56143.72
285197.74	5397498.55		56186.00	56119.30
285197.68	5397511.09		56168.93	56102.21
285197.63	5397523.62		56127.96	56061.63
285197.58	5397536.16		56084.06	56017.88
285197.53	5397548.70		56051.35	55984.97
285197.48	5397561.23		56070.38	56003.99
285197.43	5397573.77		55928.74	55862.30
285197.38	5397586.30		55994.34	55927.68
285197.33	5397598.84		56027.77	55960.90
285197.28	5397611.38		56155.30	56088.30
285197.23	5397623.91		56037.53	55970.54
285197.18	5397636.45		56058.46	55991.48
285197.13	5397648.99		56081.77	56014.57
285197.08	5397661.52		56171.72	56104.80
285197.02	5397674.06		56204.42	56137.37
285196.97	5397686.59		56285.27	56218.11
285196.92	5397699.13		56440.69	56373.60
285196.87	5397711.67		56635.09	56567.86
285196.82	5397724.20		56926.20	56858.88
285196.77	5397736.74		56772.80	56705.43
285196.72	5397749.28		56211.58	56144.36
285196.67	5397761.81		56246.93	56180.00
285196.62	5397774.35		56227.05	56160.07
285196.57	5397786.89		55896.67	55829.74
285196.52	5397799.42		55905.33	55838.27
285196.47	5397811.96		56264.64	56197.29
285196.42	5397824.49		57124.25	57057.24
285196.36	5397837.03		56982.99	56915.80
285196.31	5397849.57		57452.15	57384.89
285196.26	5397862.10		56795.95	56728.47
285196.21	5397874.64		57231.02	57163.55
285196.16	5397887.18		56356.27	56288.70
285196.11	5397899.71		57322.23	57254.58
285196.06	5397912.25		60184.12	60116.30
285196.01	5397924.78		56520.30	56452.56

Appendix C
Magnetic Data

Nad 83, Z16				
East	North		Field_nT	Corr_nT
285195.96	5397937.32		57739.49	57671.64
285195.91	5397949.86		56867.81	56800.11
285195.86	5397962.39		57949.32	57882.02
285195.81	5397974.93		55617.99	55550.23
285195.76	5397987.47		55572.75	55505.18
285195.70	5398000.00		55508.60	55440.02
285195.65	5398012.54		55475.47	55406.75
285195.60	5398025.08		55561.68	55493.22
285195.55	5398037.61		55716.96	55648.59
285195.50	5398050.15		55468.52	55400.18
285195.45	5398062.68		55641.35	55573.04
285195.40	5398075.22		55749.71	55681.24
285195.35	5398087.76		55641.41	55573.34
285195.30	5398100.29		55836.15	55767.57
285195.25	5398112.83		55852.40	55783.83
285195.20	5398125.37		55538.52	55469.77
285195.15	5398137.90		55715.91	55646.81
285195.10	5398150.44		55895.24	55826.34
285195.04	5398162.97		55731.25	55662.24
285194.99	5398175.51		55840.62	55771.68
285194.94	5398188.05		55735.33	55666.63
285194.89	5398200.58		55866.82	55798.18
285194.84	5398213.12		55933.47	55864.58
285194.79	5398225.66		55799.63	55730.67
285194.74	5398238.19		56039.83	55970.85
285194.69	5398250.73		56086.04	56016.96
285194.64	5398263.27		55983.83	55914.65
285194.59	5398275.80		55982.90	55913.50
285194.54	5398288.34		55991.62	55922.25
285194.49	5398300.87		55986.31	55917.26
285294.78	5398301.28		56033.22	55963.75
285294.83	5398288.74		56026.55	55956.80
285294.88	5398276.21		56030.23	55960.58
285294.93	5398263.67		56015.28	55945.44
285294.98	5398251.13		56003.19	55933.19
285295.03	5398238.60		56025.90	55955.66
285295.08	5398226.06		55955.69	55885.69
285295.13	5398213.53		55972.21	55902.54
285295.18	5398200.99		55975.71	55905.60
285295.23	5398188.45		55969.38	55899.20
285295.28	5398175.92		55960.52	55890.52
285295.33	5398163.38		55844.49	55774.96
285295.39	5398150.84		55727.43	55657.53
285295.44	5398138.31		55929.71	55859.43
285295.49	5398125.77		55821.41	55751.25

Appendix C
Magnetic Data

Nad 83, Z16				
East	North		Field_nT	Corr_nT
285295.54	5398113.24		55735.07	55664.82
285295.59	5398100.70		55761.02	55690.78
285295.64	5398088.16		55713.09	55642.64
285295.69	5398075.63		55594.43	55523.94
285295.74	5398063.09		55497.40	55426.54
285295.79	5398050.55		55320.65	55250.01
285295.84	5398038.02		54867.10	54796.26
285295.84	5398038.02		54865.09	54794.32
285295.89	5398025.48		54445.30	54374.47
285295.94	5398012.95		57811.86	57741.14
285295.94	5398012.95		57841.43	57770.79
285295.94	5398012.95		56448.62	56378.05
285295.94	5398012.95		55629.57	55559.00
285295.94	5398012.95		55636.43	55565.92
285295.94	5398012.95		57886.16	57815.65
285295.94	5398012.95		57876.38	57805.80
285295.94	5398012.95		57740.10	57669.43
285295.99	5398000.41		58699.72	58628.98
285295.99	5398000.41		58550.46	58479.75
285295.99	5398000.41		58648.53	58577.94
285295.99	5398000.41		58302.46	58232.02
285295.99	5398000.41		57653.17	57582.75
285295.99	5398000.41		57012.51	56942.21
285295.99	5398000.41		58113.72	58043.24
285295.99	5398000.41		58448.68	58377.98
285295.99	5398000.41		58448.12	58377.58
285295.99	5398000.41		58450.22	58379.74
285296.05	5397987.87		56683.27	56612.23
285296.05	5397987.87		56683.21	56612.12
285296.05	5397987.87		56687.41	56616.39
285296.10	5397975.34		55301.81	55230.92
285296.10	5397975.34		55303.04	55232.25
285296.10	5397975.34		55306.93	55236.13
285296.15	5397962.80		55933.04	55862.36
285296.20	5397950.26		56242.86	56171.99
285296.25	5397937.73		55632.73	55561.54
285296.30	5397925.19		55900.80	55829.51
285296.35	5397912.65		56651.32	56580.29
285296.40	5397900.12		57311.92	57241.03
285296.40	5397900.12		57311.89	57241.13
285296.45	5397887.58		57097.46	57026.51
285296.50	5397875.05		56512.46	56441.35
285296.55	5397862.51		57322.16	57251.19
285296.60	5397849.97		58297.69	58226.61
285296.65	5397837.44		58435.15	58363.82

Appendix C
Magnetic Data

Nad 83, Z16				
East	North		Field_nT	Corr_nT
285296.71	5397824.90		56658.14	56586.21
285296.76	5397812.36		56199.99	56128.50
285296.81	5397799.83		56176.30	56110.76
285296.81	5397799.83		56157.62	56094.64
285284.27	5397799.78		56057.24	55994.13
285271.73	5397799.73		56137.33	56074.25
285259.20	5397799.68		55935.88	55872.87
285246.66	5397799.62		55632.90	55570.08
285234.13	5397799.57		55672.25	55609.38
285221.59	5397799.52		55895.80	55832.88
285209.05	5397799.47		55975.16	55912.27
285196.52	5397799.42		55812.00	55749.28
285183.98	5397799.37		54985.68	54923.64
285171.44	5397799.32		56025.82	55964.09
285158.91	5397799.27		57556.20	57495.21
285146.37	5397799.22		57401.09	57339.74
285133.84	5397799.17		56893.99	56832.26
285121.30	5397799.12		57273.57	57211.72
285108.76	5397799.07		57520.69	57458.86
285096.23	5397799.02		60264.99	60204.14
285083.69	5397798.96		58233.14	58172.25
285071.15	5397798.91		57872.91	57812.02
285058.62	5397798.86		58351.99	58291.31
285046.08	5397798.81		58669.00	58608.67
285033.54	5397798.76		58279.49	58219.18
285021.01	5397798.71		57688.37	57628.11
285008.47	5397798.66		57738.72	57678.68
284995.94	5397798.61		57501.72	57441.55
284995.94	5397798.61		57539.33	57478.79
284995.88	5397811.15		57873.86	57813.64
284995.83	5397823.68		58358.68	58298.63
284995.78	5397836.22		58210.47	58150.58
284995.73	5397848.75		58485.85	58426.37
284995.68	5397861.29		58533.14	58474.57
284995.63	5397873.83		59787.22	59726.80
284995.58	5397886.36		59484.23	59424.54
284995.53	5397898.90		59088.62	59029.71
284995.48	5397911.44		57941.49	57882.53
284995.43	5397923.97		57542.81	57483.47
284995.38	5397936.51		57566.38	57506.59
284995.33	5397949.04		57657.39	57597.45
284995.28	5397961.58		57835.25	57775.90
284995.22	5397974.12		58090.52	58031.20
284995.17	5397986.65		58070.55	58011.20
284995.12	5397999.19		57384.29	57325.06

Appendix C
Magnetic Data

Nad 83, Z16				
East	North		Field_nT	Corr_nT
284995.07	5398011.73		55721.14	55662.40
284995.02	5398024.26		54630.94	54571.87
284994.97	5398036.80		54902.93	54843.67
284994.92	5398049.34		55100.79	55041.51
284994.87	5398061.87		55397.16	55338.47
284994.82	5398074.41		55462.04	55403.87
284994.77	5398086.94		55370.07	55311.70
284994.72	5398099.48		55419.33	55360.84
284994.67	5398112.02		55335.19	55277.20
284994.62	5398124.55		55377.21	55319.33
284994.56	5398137.09		55448.02	55390.26
284994.51	5398149.63		55512.40	55454.97
284994.46	5398162.16		55580.74	55522.29
284994.41	5398174.70		55631.95	55572.78
284994.36	5398187.23		55703.74	55643.97
284994.31	5398199.77		55743.70	55683.94
284994.26	5398212.31		55794.10	55734.64
284994.21	5398224.84		55831.99	55772.84
284994.16	5398237.38		55874.65	55815.83
284994.11	5398249.92		55897.50	55838.93
284994.06	5398262.45		55920.93	55862.14
284994.01	5398274.99		55952.08	55892.99
284993.96	5398287.53		55951.19	55892.65
284993.90	5398300.06		55944.79	55886.07
285094.20	5398300.47		55938.45	55881.17
285094.25	5398287.93		55938.01	55881.03
285094.30	5398275.40		55961.93	55904.91
285094.35	5398262.86		55972.11	55915.96
285094.40	5398250.32		55985.60	55929.35
285094.45	5398237.79		55952.22	55896.08
285094.50	5398225.25		55903.65	55847.24
285094.55	5398212.71		55847.27	55790.65
285094.60	5398200.18		55819.41	55762.57
285094.65	5398187.64		55758.21	55701.39
285094.70	5398175.10		55702.05	55645.58
285094.75	5398162.57		55603.42	55547.09
285094.80	5398150.03		55561.66	55505.37
285094.86	5398137.50		55481.32	55425.22
285094.91	5398124.96		55481.51	55426.00
285094.96	5398112.42		55521.29	55465.77
285095.01	5398099.89		55542.57	55487.14
285095.06	5398087.35		55466.39	55410.81
285095.11	5398074.81		55362.45	55306.95
285095.16	5398062.28		55480.22	55425.15
285095.21	5398049.74		55518.10	55462.94

Appendix C
Magnetic Data

Nad 83, Z16				
East	North		Field_nT	Corr_nT
285095.26	5398037.21		55463.18	55407.60
285095.31	5398024.67		55686.10	55629.98
285095.36	5398012.13		55516.55	55459.88
285095.41	5397999.60		55359.21	55302.29
285095.46	5397987.06		55807.75	55751.79
285095.52	5397974.52		56771.20	56715.42
285095.57	5397961.99		58012.13	57956.24
285095.62	5397949.45		57467.66	57411.21
285095.67	5397936.91		60623.40	60566.41
285095.72	5397924.38		62647.67	62590.64
285095.77	5397911.84		60807.01	60748.99
285095.82	5397899.31		57472.88	57414.99
285095.87	5397886.77		58899.19	58840.39
285095.92	5397874.23		59316.67	59256.99
285095.97	5397861.70		58055.08	57995.75
285096.02	5397849.16		58314.15	58254.22
285096.07	5397836.62		57936.40	57876.37
285096.12	5397824.09		57860.69	57801.17
285096.18	5397811.55		57662.49	57602.81
285096.23	5397799.02		59963.16	59903.03
285096.28	5397786.48		60072.72	60012.62
285096.33	5397773.94		58228.76	58167.65
285096.38	5397761.41		57432.85	57370.89
285096.43	5397748.87		57141.88	57080.44
285096.48	5397736.33		56702.06	56641.55
285096.53	5397723.80		56827.97	56767.18
285096.58	5397711.26		56775.31	56714.52
285096.63	5397698.72		56913.36	56852.76
285096.68	5397686.19		56480.27	56419.81
285096.73	5397673.65		56162.55	56101.74
285096.78	5397661.12		56598.26	56536.39
285096.84	5397648.58		56474.25	56412.57
285096.89	5397636.04		56759.78	56697.72
285096.94	5397623.51		56768.74	56706.93
285096.99	5397610.97		56278.14	56216.41
285097.04	5397598.43		56256.37	56194.86
285097.09	5397585.90		56001.29	55940.17
285097.14	5397573.36		56952.67	56890.97
285097.19	5397560.83		56720.61	56658.47
285097.24	5397548.29		56499.41	56437.28
285097.29	5397535.75		56447.26	56384.66
285097.34	5397523.22		56126.41	56063.91
285097.39	5397510.68		56132.69	56070.19
285097.44	5397498.14		56138.21	56075.45
285097.50	5397485.61		56130.86	56068.17

Appendix C
Magnetic Data

Nad 83, Z16				
East	North		Field_nT	Corr_nT
285097.55	5397473.07		56135.00	56072.53
285097.60	5397460.54		56196.93	56134.59
285097.65	5397448.00		56203.19	56140.61
285097.70	5397435.46		56222.06	56159.64
285097.75	5397422.93		56162.66	56100.44
285097.80	5397410.39		56190.51	56128.21
285097.85	5397397.85		56209.93	56147.16
285097.90	5397385.32		56169.38	56106.72
285097.95	5397372.78		56084.78	56022.46
285098.00	5397360.24		56093.80	56031.17
285098.05	5397347.71		56082.89	56020.17
285098.10	5397335.17		56061.11	55998.37
285098.16	5397322.64		56091.93	56029.46
285098.21	5397310.10		56083.10	56020.72
285098.26	5397297.56		56189.29	56127.19
284997.97	5397297.16		56133.40	56069.89
284997.92	5397309.69		56123.09	56060.66
284997.87	5397322.23		56193.89	56131.66
284997.81	5397334.77		56174.84	56112.53
284997.76	5397347.30		56170.08	56107.98
284997.71	5397359.84		56121.33	56059.23
284997.66	5397372.37		56129.56	56067.33
284997.61	5397384.91		56171.26	56108.91
284997.56	5397397.45		56148.59	56085.94
284997.51	5397409.98		56099.83	56036.84
284997.46	5397422.52		56134.40	56071.01
284997.41	5397435.06		56123.36	56059.15
284997.36	5397447.59		56190.25	56125.95
284997.31	5397460.13		56088.00	56023.82
284997.26	5397472.67		56106.07	56041.91
284997.21	5397485.20		56057.67	55993.42
284997.15	5397497.74		56131.19	56067.02
284997.10	5397510.27		56062.63	55998.85
284997.05	5397522.81		56158.78	56095.30
284997.00	5397535.35		56186.80	56123.39
284996.95	5397547.88		56081.94	56018.80
284996.90	5397560.42		56187.81	56124.74
284996.85	5397572.96		56673.07	56609.48
284996.80	5397585.49		56428.51	56365.18
284996.75	5397598.03		56174.18	56110.87
284996.70	5397610.56		56427.41	56363.87
284996.65	5397623.10		56308.03	56244.32
284996.60	5397635.64		56281.04	56217.77
284996.54	5397648.17		56354.28	56291.01
284996.49	5397660.71		56859.09	56795.72

Appendix C
Magnetic Data

Nad 83, Z16				
East	North		Field_nT	Corr_nT
284996.44	5397673.25		56057.66	55994.36
284996.39	5397685.78		56180.95	56118.48
284996.34	5397698.32		56283.10	56221.15
284996.29	5397710.86		56262.07	56199.71
284996.24	5397723.39		56161.28	56097.68
284996.19	5397735.93		56519.28	56454.69
284996.14	5397748.46		56569.75	56504.94
284996.09	5397761.00		56882.12	56817.37
284996.04	5397773.54		56977.60	56912.42
284995.99	5397786.07		57125.26	57060.00
284995.94	5397798.61		57526.65	57461.30
284995.94	5397798.61		57523.43	57458.59
284983.40	5397798.56		57826.52	57762.38
284970.86	5397798.51		57536.79	57472.93
284958.33	5397798.46		57472.58	57408.76
284945.79	5397798.41		57389.47	57325.71
284933.25	5397798.36		57657.60	57593.83
284920.72	5397798.30		57349.03	57285.57
284908.18	5397798.25		57179.17	57114.93
284895.65	5397798.20		57149.72	57084.64
284883.11	5397798.15		57230.73	57165.51
284870.57	5397798.10		57674.87	57609.42
284858.04	5397798.05		57280.29	57214.24
284845.50	5397798.00		57384.11	57318.20
284832.96	5397797.95		57003.62	56938.17
284820.43	5397797.90		57215.58	57150.62
284807.89	5397797.85		57287.55	57222.75
284795.35	5397797.80		56726.53	56662.13
284782.82	5397797.75		57419.11	57353.88
284795.35	5397797.80		56808.27	56742.17
284795.41	5397785.26		57094.69	57029.12
284795.46	5397772.72		56978.46	56912.96
284795.51	5397760.19		56666.75	56601.36
284795.56	5397747.65		56585.75	56520.67
284795.61	5397735.12		56495.19	56430.20
284795.66	5397722.58		56267.96	56203.06
284795.71	5397710.04		56195.03	56130.34
284795.76	5397697.51		55982.61	55918.41
284795.81	5397684.97		56135.92	56071.92
284795.86	5397672.43		56129.81	56066.08
284795.91	5397659.90		56005.35	55941.75
284795.96	5397647.36		56101.72	56038.11
284796.01	5397634.82		56075.20	56011.58
284796.07	5397622.29		56061.17	55997.80
284796.12	5397609.75		56022.04	55959.10

Appendix C
Magnetic Data

Nad 83, Z16				
East	North		Field_nT	Corr_nT
284796.17	5397597.22		51654.74	51591.55
284796.22	5397584.68		56096.28	56032.44
284796.27	5397572.14		56135.26	56071.12
284796.32	5397559.61		56106.03	56042.27
284796.37	5397547.07		56165.84	56102.45
284796.42	5397534.53		56263.65	56199.91
284796.47	5397522.00		56234.41	56170.74
284796.52	5397509.46		56369.86	56305.75
284796.57	5397496.93		56227.11	56162.97
284796.62	5397484.39		56160.80	56096.59
284796.67	5397471.85		56170.06	56106.17
284796.73	5397459.32		56162.65	56098.51
284796.78	5397446.78		56166.63	56102.11
284796.83	5397434.24		56157.93	56093.25
284796.88	5397421.71		56146.00	56081.19
284796.93	5397409.17		56142.99	56078.11
284796.98	5397396.63		56124.40	56059.26
284797.03	5397384.10		56133.74	56068.11
284797.08	5397371.56		56135.95	56070.18
284797.13	5397359.03		56135.73	56070.05
284797.18	5397346.49		56145.01	56079.38
284797.23	5397333.95		56131.36	56065.93
284797.28	5397321.42		56139.78	56073.95
284797.33	5397308.88		56174.61	56109.13
284797.39	5397296.34		56198.99	56133.84
284897.68	5397296.75		56100.90	56035.12
284897.63	5397309.29		56155.34	56088.97
284897.57	5397321.82		56160.85	56094.21
284897.52	5397334.36		56190.68	56123.78
284897.47	5397346.90		56147.86	56081.38
284897.42	5397359.43		56165.57	56098.87
284897.37	5397371.97		56157.87	56091.39
284897.32	5397384.50		56137.15	56070.60
284897.27	5397397.04		56124.16	56057.39
284897.22	5397409.58		56154.42	56087.74
284897.17	5397422.11		56157.55	56091.18
284897.12	5397434.65		56173.49	56106.79
284897.07	5397447.19		56179.72	56113.28
284897.02	5397459.72		56220.43	56153.85
284896.97	5397472.26		56181.98	56115.04
284896.91	5397484.80		56197.01	56129.88
284896.86	5397497.33		56229.62	56162.36
284896.81	5397509.87		56271.52	56204.34
284896.76	5397522.40		56422.28	56355.50
284896.71	5397534.94		56041.49	55974.53

Appendix C
Magnetic Data

Nad 83, Z16				
East	North		Field_nT	Corr_nT
284896.66	5397547.48		56132.20	56065.02
284896.61	5397560.01		56176.97	56110.11
284896.56	5397572.55		56290.44	56223.91
284896.51	5397585.09		56251.26	56184.28
284896.46	5397597.62		56147.74	56081.10
284896.41	5397610.16		56144.32	56077.82
284896.36	5397622.69		56056.30	55989.45
284896.31	5397635.23		56019.60	55952.58
284896.25	5397647.77		56163.70	56096.97
284896.20	5397660.30		56066.97	55999.88
284896.15	5397672.84		56110.42	56043.56
284896.10	5397685.38		56134.18	56067.46
284896.05	5397697.91		56142.04	56075.85
284896.00	5397710.45		56199.43	56132.96
284895.95	5397722.99		56289.92	56223.11
284895.90	5397735.52		56334.90	56268.14
284895.85	5397748.06		56351.51	56284.46
284895.80	5397760.59		56535.10	56467.51
284895.75	5397773.13		56603.22	56535.37
284895.70	5397785.67		56840.93	56773.53
284895.65	5397798.20		57147.98	57080.81
284895.59	5397810.74		57248.89	57180.90
284895.54	5397823.28		57484.75	57416.69
284895.49	5397835.81		58699.48	58630.92
284895.44	5397848.35		59387.63	59318.27
284895.39	5397860.88		58351.10	58282.12
284895.34	5397873.42		57572.83	57504.61
284895.29	5397885.96		57383.15	57314.80
284895.24	5397898.49		57003.64	56935.31
284895.19	5397911.03		57469.05	57401.77
284895.14	5397923.57		58462.59	58393.89
284895.09	5397936.10		58369.46	58300.64
284895.04	5397948.64		58054.60	57985.36
284894.99	5397961.18		57748.67	57679.44
284894.93	5397973.71		57837.66	57768.01
284894.88	5397986.25		56630.82	56562.24
284894.83	5397998.78		55421.55	55352.38
284894.78	5398011.32		55378.45	55309.43
284894.73	5398023.86		54638.45	54569.37
284894.68	5398036.39		54981.75	54912.88
284894.63	5398048.93		55247.22	55177.73
284894.58	5398061.47		55794.37	55724.92
284894.53	5398074.00		55555.11	55485.78
284894.48	5398086.54		55328.54	55259.97
284894.43	5398099.07		55377.70	55309.11

Appendix C
Magnetic Data

Nad 83, Z16				
East	North		Field_nT	Corr_nT
284894.38	5398111.61		55403.28	55335.32
284894.33	5398124.15		55402.88	55334.10
284894.27	5398136.68		55458.95	55390.82
284894.22	5398149.22		55480.07	55411.78
284894.17	5398161.76		55551.88	55483.53
284894.12	5398174.29		55604.85	55536.15
284894.07	5398186.83		55672.83	55603.74
284894.02	5398199.37		55709.57	55640.53
284893.97	5398211.90		55752.75	55683.42
284893.92	5398224.44		55864.37	55794.96
284893.87	5398236.97		56013.15	55943.16
284893.82	5398249.51		56033.63	55963.26
284893.77	5398262.05		55925.73	55854.40
284893.72	5398274.58		55897.49	55826.06
284893.67	5398287.12		55908.32	55836.78
284795.35	5397797.80		56875.30	56809.85
284795.30	5397810.33		58050.32	57985.62
284795.25	5397822.87		57786.20	57721.38
284795.20	5397835.41		58251.10	58186.65
284795.15	5397847.94		58820.40	58755.74
284795.10	5397860.48		60704.74	60639.35
284795.05	5397873.01		61381.33	61315.54
284795.00	5397885.55		61174.42	61108.09
284794.95	5397898.09		61103.16	61038.17
284794.90	5397910.62		60099.61	60034.99
284794.85	5397923.16		59067.93	59003.47
284794.80	5397935.70		58264.10	58199.85
284794.75	5397948.23		58005.92	57941.71
284794.69	5397960.77		58475.00	58410.63
284794.64	5397973.31		58144.01	58079.85
284794.59	5397985.84		56843.38	56778.40
284794.54	5397998.38		56407.76	56342.49
284794.49	5398010.91		55416.21	55350.83
284794.44	5398023.45		55858.29	55792.74
284794.39	5398035.99		54772.23	54706.66
284794.34	5398048.52		54769.98	54704.45
284794.29	5398061.06		55123.91	55058.34
284794.24	5398073.60		55515.51	55449.97
284794.19	5398086.13		55226.35	55160.63
284794.14	5398098.67		55152.62	55086.86
284794.09	5398111.20		55259.01	55193.15
284794.03	5398123.74		55702.55	55637.23
284793.98	5398136.28		55572.93	55507.97
284793.93	5398148.81		55606.04	55540.21
284793.88	5398161.35		55510.81	55444.24

Appendix C
Magnetic Data

Nad 83, Z16				
East	North		Field_nT	Corr_nT
284793.83	5398173.89		55511.46	55448.06
284793.78	5398186.42		55699.58	55634.35
284793.73	5398198.96		55697.67	55631.59
284793.68	5398211.50		55717.69	55651.61
284793.63	5398224.03		55996.28	55931.02
284793.58	5398236.57		56168.11	56102.45
284793.53	5398249.10		56030.25	55964.53
284793.48	5398261.64		56080.81	56014.79
284793.43	5398274.18		55820.21	55754.21
284793.37	5398286.71		55913.31	55847.39
284793.32	5398299.25		55944.43	55878.49
284693.03	5398298.84		55841.61	55776.61
284693.08	5398286.31		55756.16	55690.95
284693.13	5398273.77		55753.72	55688.24
284693.19	5398261.23		55782.16	55716.18
284693.24	5398248.70		55819.57	55753.81
284693.29	5398236.16		55788.39	55723.15
284693.34	5398223.63		55785.99	55720.84
284693.39	5398211.09		55740.66	55675.30
284693.44	5398198.55		55897.77	55832.39
284693.49	5398186.02		56120.26	56054.68
284693.54	5398173.48		55537.82	55472.24
284693.59	5398160.94		55608.03	55542.55
284693.64	5398148.41		55688.67	55623.15
284693.69	5398135.87		55619.32	55553.98
284693.74	5398123.33		55830.31	55764.93
284693.79	5398110.80		55533.08	55467.49
284693.85	5398098.26		55392.05	55326.32
284693.90	5398085.73		55256.47	55190.90
284693.95	5398073.19		55522.59	55457.24
284694.00	5398060.65		56836.79	56771.51
284694.05	5398048.12		56293.13	56227.77
284694.10	5398035.58		56995.48	56929.91
284694.15	5398023.04		57114.19	57048.83
284694.20	5398010.51		56348.67	56283.70
284694.25	5397997.97		56271.84	56206.75
284694.30	5397985.44		55922.09	55857.13
284694.35	5397972.90		55953.71	55889.11
284694.40	5397960.36		55925.17	55860.69
284694.46	5397947.83		56083.44	56018.55
284694.51	5397935.29		56021.72	55957.65
284694.56	5397922.75		55702.91	55639.19
284694.61	5397910.22		56002.23	55938.27
284694.66	5397897.68		57175.81	57112.03
284694.71	5397885.14		58228.77	58164.95

Appendix C
Magnetic Data

Nad 83, Z16				
East	North		Field_nT	Corr_nT
284694.76	5397872.61		58747.58	58684.04
284694.81	5397860.07		58207.92	58144.18
284694.86	5397847.54		57741.99	57678.01
284694.91	5397835.00		57494.39	57430.37
284694.96	5397822.46		57095.53	57031.54
284695.01	5397809.93		56886.48	56822.58
284695.06	5397797.39		56769.07	56705.18
284695.12	5397784.85		56633.49	56569.98
284695.17	5397772.32		56602.05	56538.59
284695.22	5397759.78		56584.44	56520.80
284695.27	5397747.25		56394.40	56331.11
284695.32	5397734.71		56329.17	56265.81
284695.37	5397722.17		56244.31	56180.81
284695.42	5397709.64		56234.98	56171.42
284695.47	5397697.10		56254.65	56190.94
284695.52	5397684.56		56144.08	56080.14
284695.57	5397672.03		56149.49	56085.89
284695.62	5397659.49		56105.39	56041.87
284695.67	5397646.96		56110.89	56047.47
284695.72	5397634.42		56149.89	56086.23
284695.78	5397621.88		56130.66	56066.94
284695.83	5397609.35		56127.85	56064.31
284695.88	5397596.81		56100.24	56036.71
284695.93	5397584.27		56089.07	56025.28
284695.98	5397571.74		56089.97	56026.19
284696.03	5397559.20		56120.06	56056.02
284696.08	5397546.66		56124.57	56060.40
284696.13	5397534.13		56127.41	56063.12
284696.18	5397521.59		56159.40	56094.86
284696.23	5397509.06		56182.36	56117.73
284696.28	5397496.52		56182.45	56117.91
284696.33	5397483.98		56184.45	56120.41
284696.38	5397471.45		56171.93	56108.04
284696.44	5397458.91		56155.70	56091.92
284696.49	5397446.37		56157.39	56093.64
284696.54	5397433.84		56172.79	56109.11
284696.59	5397421.30		56172.30	56108.68
284696.64	5397408.77		56156.90	56093.25
284696.69	5397396.23		56160.90	56097.35
284696.74	5397383.69		56150.02	56086.26
284696.79	5397371.16		56147.41	56083.80
284696.84	5397358.62		56148.26	56084.39
284696.89	5397346.08		56155.09	56091.28
284696.94	5397333.55		56171.14	56107.56
284696.99	5397321.01		56184.43	56121.05

Appendix C
Magnetic Data

Nad 83, Z16				
East	North		Field_nT	Corr_nT
284697.04	5397308.47		56208.41	56145.38
284697.10	5397295.94		56234.74	56171.78
284596.80	5397295.53		56224.08	56162.83
284596.75	5397308.07		56234.34	56173.58
284596.70	5397320.60		56175.53	56114.71
284596.65	5397333.14		56155.67	56094.77
284596.60	5397345.68		56149.11	56087.93
284596.55	5397358.21		56148.82	56087.65
284596.50	5397370.75		56167.71	56106.54
284596.45	5397383.29		56166.92	56105.48
284596.40	5397395.82		56160.21	56098.63
284596.35	5397408.36		56139.54	56077.83
284596.30	5397420.90		56138.29	56076.69
284596.25	5397433.43		56122.87	56061.54
284596.20	5397445.97		56129.08	56067.52
284596.14	5397458.50		56129.92	56068.33
284596.09	5397471.04		56147.79	56086.50
284596.04	5397483.58		56158.76	56097.55
284595.99	5397496.11		56191.75	56130.33
284595.94	5397508.65		56211.79	56150.54
284595.89	5397521.19		56220.88	56159.81
284595.84	5397533.72		56222.81	56161.64
284595.79	5397546.26		56186.23	56125.10
284595.74	5397558.79		56162.21	56100.69
284595.69	5397571.33		56159.30	56097.75
284595.64	5397583.87		56148.22	56086.62
284595.59	5397596.40		56125.58	56063.87
284595.54	5397608.94		56110.94	56049.47
284595.48	5397621.48		56130.01	56068.52
284595.43	5397634.01		56127.01	56065.22
284595.38	5397646.55		56137.18	56075.23
284595.33	5397659.09		56065.09	56003.02
284595.28	5397671.62		56060.45	55998.84
284595.23	5397684.16		56071.22	56009.22
284595.18	5397696.69		56082.17	56020.50
284595.13	5397709.23		56047.16	55985.95
284595.08	5397721.77		56167.13	56105.58
284595.03	5397734.30		56218.10	56156.80
284594.98	5397746.84		56115.23	56053.91
284594.93	5397759.38		56116.86	56055.52
284594.88	5397771.91		56137.20	56075.44
284594.82	5397784.45		56406.90	56345.58
284594.77	5397796.98		56172.76	56111.06
284594.72	5397809.52		56282.79	56221.16
284594.67	5397822.06		56508.67	56446.99

Appendix C
Magnetic Data

Nad 83, Z16				
East	North		Field_nT	Corr_nT
284594.62	5397834.59		56597.85	56536.07
284594.57	5397847.13		56807.45	56745.91
284594.52	5397859.67		57170.59	57109.20
284594.47	5397872.20		57784.43	57723.00
284594.42	5397884.74		58306.67	58245.38
284594.37	5397897.28		58930.17	58869.14
284594.32	5397909.81		60103.46	60042.52
284594.27	5397922.35		59590.25	59529.25
284594.22	5397934.88		57019.71	56958.73
284594.16	5397947.42		58345.18	58284.23
284594.11	5397959.96		60098.52	60038.75
284594.06	5397972.49		61288.37	61227.29
284594.01	5397985.03		61364.95	61304.23
284593.96	5397997.57		60176.21	60115.92
284593.91	5398010.10		60038.62	59977.64
284593.86	5398022.64		60015.99	59955.58
284593.81	5398035.17		59617.75	59557.56
284593.76	5398047.71		59205.13	59144.98
284593.71	5398060.25		56167.10	56107.01
284593.66	5398072.78		56224.47	56164.87
284593.61	5398085.32		56605.57	56546.81
284593.56	5398097.86		56471.07	56412.42
284593.50	5398110.39		56269.41	56210.68
284593.45	5398122.93		55565.41	55506.58
284593.40	5398135.46		55029.18	54969.74
284593.35	5398148.00		55771.04	55711.71
284593.30	5398160.54		55617.31	55557.98
284593.25	5398173.07		55447.84	55388.50
284593.20	5398185.61		55236.50	55176.85
284593.15	5398198.15		55473.14	55413.42
284593.10	5398210.68		55733.58	55673.73
284593.05	5398223.22		55595.41	55535.71
284593.00	5398235.76		55898.49	55838.70
284592.95	5398248.29		55631.58	55571.70
284592.90	5398260.83		55919.11	55859.39
284592.84	5398273.36		55843.52	55784.04
284592.79	5398285.90		55759.54	55700.39
284592.74	5398298.44		55819.16	55760.22
284492.45	5398298.03		55733.99	55673.56
284492.50	5398285.49		55745.30	55683.27
284492.55	5398272.96		55673.65	55611.13
284492.60	5398260.42		55647.50	55584.96
284492.66	5398247.89		55492.46	55430.01
284492.71	5398235.35		55364.57	55302.24
284492.76	5398222.81		55314.14	55251.81

Appendix C
Magnetic Data

Nad 83, Z16				
East	North		Field_nT	Corr_nT
284492.81	5398210.28		54821.52	54759.35
284492.86	5398197.74		54591.56	54529.32
284492.91	5398185.20		55655.06	55592.65
284492.96	5398172.67		55920.26	55857.73
284493.01	5398160.13		57245.24	57182.19
284493.06	5398147.60		56040.31	55977.06
284493.11	5398135.06		56612.95	56549.75
284493.16	5398122.52		54975.79	54912.51
284493.21	5398109.99		56546.43	56482.74
284493.26	5398097.45		54706.52	54642.01
284493.32	5398084.91		56822.44	56757.64
284493.37	5398072.38		54436.45	54371.81
284493.42	5398059.84		54687.70	54623.15
284493.47	5398047.30		56007.47	55942.70
284493.52	5398034.77		56977.60	56912.83
284493.57	5398022.23		59194.31	59130.13
284493.62	5398009.70		60124.71	60060.38
284493.67	5397997.16		60283.29	60218.53
284493.72	5397984.62		58837.21	58771.93
284493.77	5397972.09		58510.33	58444.72
284493.82	5397959.55		58030.58	57964.77
284493.87	5397947.01		57199.41	57133.72
284493.92	5397934.48		56613.04	56547.54
284493.98	5397921.94		56337.97	56272.23
284494.03	5397909.41		56244.39	56178.24
284494.08	5397896.87		56200.31	56133.74
284494.13	5397884.33		56111.43	56044.42
284494.18	5397871.80		56009.18	55941.96
284494.23	5397859.26		55993.91	55926.61
284494.28	5397846.72		55999.32	55931.79
284494.33	5397834.19		56019.00	55951.35
284494.38	5397821.65		55991.18	55923.35
284494.43	5397809.11		55999.15	55931.11
284494.48	5397796.58		56007.62	55939.42
284494.53	5397784.04		55996.73	55928.03
284494.58	5397771.51		56002.33	55933.71
284494.64	5397758.97		56017.66	55948.83
284494.69	5397746.43		56015.46	55946.90
284494.74	5397733.90		56011.64	55942.99
284494.79	5397721.36		56041.37	55972.35
284494.84	5397708.82		56082.35	56012.81
284494.89	5397696.29		56095.89	56026.14
284494.94	5397683.75		56059.41	55989.44
284494.99	5397671.22		56068.15	55997.91
284495.04	5397658.68		56081.10	56010.66

Appendix C
Magnetic Data

Nad 83, Z16				
East	North		Field_nT	Corr_nT
284495.09	5397646.14		56082.19	56011.13
284495.14	5397633.61		56044.96	55973.61
284495.19	5397621.07		56068.60	55997.40
284495.24	5397608.53		56080.64	56009.81
284495.30	5397596.00		56099.41	56028.88
284495.35	5397583.46		56109.91	56039.60
284495.40	5397570.92		56105.35	56034.94
284495.45	5397558.39		56184.38	56113.78
284495.50	5397545.85		56287.04	56216.59
284495.55	5397533.32		56253.69	56183.37
284495.60	5397520.78		56218.41	56148.19
284495.65	5397508.24		56206.29	56136.15
284495.70	5397495.71		56173.24	56103.07
284495.75	5397483.17		56147.08	56076.83
284495.80	5397470.63		56140.17	56070.17
284495.85	5397458.10		56163.11	56093.26
284495.90	5397445.56		56160.50	56090.86
284495.96	5397433.03		56149.32	56079.73
284496.01	5397420.49		56140.05	56070.79
284496.06	5397407.95		56155.91	56086.90
284496.11	5397395.42		56130.67	56061.76
284496.16	5397382.88		56126.49	56057.82
284496.21	5397370.34		56134.12	56065.57
284496.26	5397357.81		56131.49	56062.90
284496.31	5397345.27		56146.77	56077.91
284496.36	5397332.73		56148.77	56079.66
284496.41	5397320.20		56151.52	56082.30
284496.46	5397307.66		56155.85	56086.76
284496.51	5397295.13		56167.67	56098.41
284396.22	5397294.72		56131.52	56063.77
284396.17	5397307.26		56136.75	56069.56
284396.12	5397319.79		56139.90	56072.36
284396.07	5397332.33		56128.46	56061.02
284396.02	5397344.87		56162.89	56096.06
284395.97	5397357.40		56163.95	56097.56
284395.92	5397369.94		56152.09	56085.80
284395.87	5397382.47		56107.44	56040.83
284395.82	5397395.01		56032.81	55965.58
284395.77	5397407.55		56077.00	56009.16
284395.72	5397420.08		56075.73	56007.84
284395.67	5397432.62		56052.71	55984.95
284395.61	5397445.16		56057.62	55990.10
284395.56	5397457.69		56054.57	55987.13
284395.51	5397470.23		56051.07	55983.55
284395.46	5397482.76		56091.22	56023.63

Appendix C
Magnetic Data

Nad 83, Z16				
East	North		Field_nT	Corr_nT
284395.41	5397495.30		56122.74	56055.07
284395.36	5397507.84		56150.30	56082.54
284395.31	5397520.37		56145.89	56078.14
284395.26	5397532.91		56132.42	56064.58
284395.21	5397545.45		56181.47	56113.58
284395.16	5397557.98		56181.55	56113.34
284395.11	5397570.52		56125.98	56057.05
284395.06	5397583.05		56099.90	56031.43
284395.01	5397595.59		56063.79	55996.71
284394.95	5397608.13		56049.53	55982.24
284394.90	5397620.66		56044.75	55977.39
284394.85	5397633.20		56052.96	55985.59
284394.80	5397645.74		56058.88	55992.64
284394.75	5397658.27		56061.50	55994.88
284394.70	5397670.81		56058.33	55991.22
284394.65	5397683.35		56097.95	56030.94
284394.60	5397695.88		56088.12	56021.01
284394.55	5397708.42		56072.66	56005.45
284394.50	5397720.95		56028.87	55961.56
284394.45	5397733.49		55999.67	55932.17
284394.40	5397746.03		56021.37	55953.57
284394.35	5397758.56		56021.15	55954.02
284394.29	5397771.10		56026.34	55959.52
284394.24	5397783.64		56039.05	55972.20
284394.19	5397796.17		56039.56	55972.51
284394.19	5397796.17		56039.36	55972.56
284406.73	5397796.22		56023.97	55957.42
284419.27	5397796.27		56005.14	55938.68
284431.80	5397796.32		55998.52	55932.03
284444.34	5397796.38		56003.05	55936.42
284456.87	5397796.43		56000.85	55933.86
284469.41	5397796.48		55970.97	55903.87
284481.95	5397796.53		55982.64	55915.36
284494.48	5397796.58		56008.58	55941.02
284507.02	5397796.63		55994.83	55927.05
284519.56	5397796.68		56044.39	55976.46
284532.09	5397796.73		56019.22	55951.16
284544.63	5397796.78		56035.26	55967.41
284557.16	5397796.83		56093.35	56025.68
284569.70	5397796.88		56101.16	56034.23
284582.24	5397796.93		56135.81	56068.76
284594.77	5397796.98		56171.38	56104.20
284607.31	5397797.04		56167.66	56100.51
284619.85	5397797.09		56166.03	56098.90
284632.38	5397797.14		56332.39	56265.18

Appendix C
Magnetic Data

Nad 83, Z16				
East	North		Field_nT	Corr_nT
284644.92	5397797.19		56596.09	56528.70
284657.46	5397797.24		56591.22	56523.73
284669.99	5397797.29		56782.57	56715.15
284682.53	5397797.34		56308.60	56241.09
284695.06	5397797.39		56772.93	56705.28
284707.60	5397797.44		56966.39	56898.58
284720.14	5397797.49		57200.17	57132.56
284732.67	5397797.54		57347.76	57280.21
284745.21	5397797.59		57424.39	57356.77
284757.75	5397797.64		57237.69	57169.99
284770.28	5397797.70		57067.41	56999.75
284782.82	5397797.75		57343.43	57275.85
284394.19	5397796.17		56043.85	55971.62
284394.14	5397808.71		56041.69	55969.13
284394.09	5397821.24		56039.39	55965.57
284394.04	5397833.78		55988.95	55915.43
284393.99	5397846.32		56002.33	55928.75
284393.94	5397858.85		55995.65	55921.93
284393.89	5397871.39		55978.01	55904.80
284393.84	5397883.93		55939.12	55865.94
284393.79	5397896.46		55927.39	55854.54
284393.74	5397909.00		56043.29	55970.63
284393.69	5397921.54		55947.56	55874.98
284393.63	5397934.07		55900.55	55827.93
284393.58	5397946.61		55911.50	55839.41
284393.53	5397959.14		55993.49	55921.89
284393.48	5397971.68		56025.81	55954.35
284393.43	5397984.22		56123.56	56051.06
284393.38	5397996.75		56116.34	56043.75
284393.33	5398009.29		56133.27	56060.72
284393.28	5398021.83		56279.02	56206.59
284393.23	5398034.36		57549.34	57476.85
284393.18	5398046.90		61316.29	61243.63
284393.13	5398059.43		67058.07	66985.11
284393.08	5398071.97		61277.59	61204.78
284393.03	5398084.51		61461.19	61388.24
284392.97	5398097.04		61542.65	61470.63
284392.92	5398109.58		59754.02	59682.16
284392.87	5398122.12		56677.92	56605.59
284392.82	5398134.65		55103.12	55030.40
284392.77	5398147.19		55480.44	55408.11
284392.72	5398159.73		55041.10	54968.80
284392.67	5398172.26		55036.15	54963.69
284392.62	5398184.80		56306.81	56235.06
284392.57	5398197.33		55372.15	55299.77

Appendix C
Magnetic Data

Nad 83, Z16				
East	North		Field_nT	Corr_nT
284392.52	5398209.87		55314.02	55241.61
284392.47	5398222.41		55525.29	55453.12
284392.42	5398234.94		55734.98	55663.16
284392.37	5398247.48		55826.51	55754.81
284392.31	5398260.02		55679.41	55607.56
284392.26	5398272.55		55763.22	55691.37
284392.21	5398285.09		55828.84	55757.48
284392.16	5398297.62		55934.00	55862.92
284291.87	5398297.22		56005.82	55934.58
284291.92	5398284.68		55995.48	55923.58
284291.97	5398272.15		55990.54	55918.49
284292.02	5398259.61		55974.19	55902.32
284292.07	5398247.07		55962.80	55891.01
284292.13	5398234.54		55892.68	55820.93
284292.18	5398222.00		55872.00	55800.13
284292.23	5398209.46		55833.90	55762.42
284292.28	5398196.93		55847.76	55776.48
284292.33	5398184.39		55743.17	55672.71
284292.38	5398171.86		55724.24	55653.53
284292.43	5398159.32		55749.03	55678.02
284292.48	5398146.78		55877.84	55806.85
284292.53	5398134.25		55787.92	55716.40
284292.58	5398121.71		55773.93	55703.42
284292.63	5398109.17		55733.58	55663.03
284292.68	5398096.64		55854.16	55783.80
284292.73	5398084.10		56437.29	56366.73
284292.79	5398071.56		56230.31	56160.02
284292.84	5398059.03		55890.48	55820.29
284292.89	5398046.49		55916.55	55845.97
284292.94	5398033.96		55870.74	55800.14
284292.99	5398021.42		55944.37	55873.47
284293.04	5398008.88		56014.85	55944.21
284293.09	5397996.35		55970.76	55900.68
284293.14	5397983.81		56202.95	56132.68
284293.19	5397971.27		56119.75	56049.32
284293.24	5397958.74		56304.84	56234.03
284293.29	5397946.20		56096.18	56025.06
284293.34	5397933.67		56118.54	56047.44
284293.39	5397921.13		56332.70	56261.88
284293.45	5397908.59		56543.35	56472.83
284293.50	5397896.06		56325.21	56254.70
284293.55	5397883.52		56006.56	55935.75
284293.60	5397870.98		55985.71	55914.84
284293.65	5397858.45		55976.96	55906.29
284293.70	5397845.91		56039.08	55968.48

Appendix C
Magnetic Data

Nad 83, Z16				
East	North		Field_nT	Corr_nT
284293.75	5397833.38		56012.62	55942.10
284293.80	5397820.84		56028.49	55958.10
284293.85	5397808.30		56036.06	55965.59
284293.90	5397795.77		56049.03	55978.70
284293.95	5397783.23		56041.08	55972.41
284294.00	5397770.69		56041.37	55972.46
284294.05	5397758.16		56054.70	55986.13
284294.11	5397745.62		56013.76	55945.06
284294.16	5397733.08		56028.91	55960.07
284294.21	5397720.55		56055.36	55986.44
284294.26	5397708.01		56051.22	55982.70
284294.31	5397695.48		56061.18	55992.51
284294.36	5397682.94		56118.65	56050.08
284294.41	5397670.40		56110.23	56041.84
284294.46	5397657.87		56074.60	56005.82
284294.51	5397645.33		56067.64	55998.62
284294.56	5397632.79		56036.48	55967.70
284294.61	5397620.26		56007.20	55938.60
284294.66	5397607.72		56021.42	55952.94
284294.71	5397595.19		56073.17	56004.41
284294.77	5397582.65		56141.22	56072.22
284294.82	5397570.11		56167.01	56097.83
284294.87	5397557.58		56157.82	56088.74
284294.92	5397545.04		56149.37	56080.25
284294.97	5397532.50		56141.56	56072.38
284295.02	5397519.97		56152.16	56083.22
284295.07	5397507.43		56134.30	56065.35
284295.12	5397494.89		56057.30	55988.29
284295.17	5397482.36		56061.69	55992.63
284295.22	5397469.82		56087.37	56018.59
284295.27	5397457.29		56050.76	55981.47
284295.32	5397444.75		56072.61	56004.35
284295.37	5397432.21		56110.16	56040.96
284295.43	5397419.68		56013.31	55943.71
284295.48	5397407.14		56169.43	56100.06
284295.53	5397394.60		56009.61	55941.00
284295.58	5397382.07		56144.92	56075.81
284295.63	5397369.53		56158.31	56089.44
284295.68	5397357.00		56129.72	56061.22
284295.73	5397344.46		56124.24	56056.38
284295.78	5397331.92		55253.51	55185.00
284295.83	5397319.39		56144.86	56075.97
284295.73	5397344.46		56121.11	56052.32
284295.78	5397331.92		56130.48	56061.58
284295.83	5397319.39		56145.87	56077.16

Appendix C
Magnetic Data

Nad 83, Z16				
East	North		Field_nT	Corr_nT
284295.88	5397306.85		56162.64	56094.15
284295.93	5397294.31		56174.75	56106.28
284195.64	5397293.91		56105.66	56035.97
284195.59	5397306.44		56120.87	56050.69
284195.54	5397318.98		56124.93	56055.37
284195.49	5397331.52		56111.58	56042.33
284195.44	5397344.05		56101.45	56033.07
284195.39	5397356.59		56107.92	56038.42
284195.34	5397369.13		56121.85	56052.93
284195.29	5397381.66		56106.02	56037.01
284195.24	5397394.20		56150.90	56081.73
284195.19	5397406.73		56157.21	56087.65
284195.13	5397419.27		56155.81	56086.32
284195.08	5397431.81		56151.30	56082.40
284195.03	5397444.34		56138.59	56070.31
284194.98	5397456.88		56083.12	56015.51
284194.93	5397469.42		56062.25	55994.27
284194.88	5397481.95		56068.26	55999.43
284194.83	5397494.49		56067.02	55997.98
284194.78	5397507.02		56102.18	56032.67
284194.73	5397519.56		56135.58	56065.99
284194.68	5397532.10		56205.27	56135.56
284194.63	5397544.63		56205.66	56135.83
284194.58	5397557.17		56226.60	56156.45
284194.53	5397569.71		56178.22	56107.72
284194.47	5397582.24		56155.85	56085.00
284194.42	5397594.78		56130.60	56059.76
284194.37	5397607.32		56130.07	56059.38
284194.32	5397619.85		56128.31	56058.00
284194.27	5397632.39		56094.48	56023.51
284194.22	5397644.92		56086.81	56015.98
284194.17	5397657.46		56118.22	56047.46
284194.12	5397670.00		56106.01	56035.35
284194.07	5397682.53		56118.51	56048.57
284194.02	5397695.07		56109.90	56040.45
284193.97	5397707.61		56115.90	56046.45
284193.92	5397720.14		56091.74	56022.18
284193.87	5397732.68		56087.33	56017.59
284193.81	5397745.21		56078.65	56008.84
284193.76	5397757.75		56085.47	56016.03
284193.71	5397770.29		56088.05	56018.89
284193.66	5397782.82		56085.17	56015.59
284193.61	5397795.36		56096.37	56026.86
284193.56	5397807.90		56156.63	56086.10
284193.51	5397820.43		56269.94	56199.94

Appendix C
Magnetic Data

Nad 83, Z16				
East	North		Field_nT	Corr_nT
284193.46	5397832.97		56303.39	56233.74
284193.41	5397845.51		56177.53	56107.83
284193.36	5397858.04		56161.72	56091.62
284193.31	5397870.58		56156.58	56087.58
284193.26	5397883.11		56035.01	55966.20
284193.21	5397895.65		56103.62	56034.43
284193.15	5397908.19		56164.66	56096.32
284193.10	5397920.72		56217.46	56149.07
284193.05	5397933.26		56199.67	56131.21
284193.00	5397945.80		56076.97	56008.14
284192.95	5397958.33		56328.98	56259.73
284192.90	5397970.87		56153.38	56084.32
284192.85	5397983.40		56155.09	56086.11
284192.80	5397995.94		56124.22	56055.03
284192.75	5398008.48		56087.50	56018.39
284192.70	5398021.01		56129.40	56060.20
284192.65	5398033.55		56124.94	56055.83
284192.60	5398046.09		56111.80	56042.69
284192.55	5398058.62		56096.15	56026.97
284192.49	5398071.16		56067.04	55998.12
284192.44	5398083.70		56020.01	55951.00
284192.39	5398096.23		56056.42	55987.89
284192.34	5398108.77		56103.08	56034.47
284192.29	5398121.30		56201.76	56133.13
284192.24	5398133.84		56130.82	56062.18
284192.19	5398146.38		56130.93	56062.24
284192.14	5398158.91		56051.83	55982.92
284192.09	5398171.45		56070.57	56001.84
284192.04	5398183.99		56074.34	56004.98
284191.99	5398196.52		56019.60	55950.49
284191.94	5398209.06		55995.71	55926.78
284191.89	5398221.59		55966.47	55896.70
284191.83	5398234.13		55925.99	55856.34
284191.78	5398246.67		55893.02	55823.25
284191.73	5398259.20		56161.14	56092.17
284191.68	5398271.74		56174.79	56105.30
284191.63	5398284.28		56060.43	55990.68
284191.58	5398296.81		56102.85	56032.97
284091.29	5398296.41		56190.50	56120.34
284091.34	5398283.87		56181.44	56111.07
284091.39	5398271.33		56122.76	56052.40
284091.44	5398258.80		56078.05	56008.17
284091.49	5398246.26		56055.33	55985.28
284091.54	5398233.72		56084.83	56015.00
284091.60	5398221.19		56106.81	56037.31

Appendix C
Magnetic Data

Nad 83, Z16				
East	North		Field_nT	Corr_nT
284091.65	5398208.65		56113.14	56043.26
284091.70	5398196.12		56115.38	56045.41
284091.75	5398183.58		56128.51	56058.65
284091.80	5398171.04		56120.00	56049.88
284091.85	5398158.51		56129.35	56059.44
284091.90	5398145.97		56141.13	56071.19
284091.95	5398133.43		56188.07	56118.14
284092.00	5398120.90		56164.49	56094.54
284092.05	5398108.36		56292.03	56222.10
284092.10	5398095.83		56271.21	56201.19
284092.15	5398083.29		56181.22	56111.39
284092.20	5398070.75		56115.25	56045.22
284092.26	5398058.22		56170.93	56101.04
284092.31	5398045.68		56193.81	56123.84
284092.36	5398033.14		56159.64	56089.64
284092.41	5398020.61		56124.80	56054.76
284092.46	5398008.07		55986.86	55916.50
284092.51	5397995.53		56148.89	56078.70
284092.56	5397983.00		56094.60	56024.40
284092.61	5397970.46		56087.91	56017.92
284092.66	5397957.93		56076.61	56006.86
284092.71	5397945.39		56081.79	56011.67
284092.76	5397932.85		56122.14	56051.99
284092.81	5397920.32		56132.86	56062.88
284092.86	5397907.78		56140.08	56069.81
284092.92	5397895.24		56177.67	56107.71
284092.97	5397882.71		56206.68	56136.67
284093.02	5397870.17		56136.00	56065.91
284093.07	5397857.64		56128.18	56058.20
284093.12	5397845.10		56177.45	56107.45
284093.17	5397832.56		56166.67	56096.59
284093.22	5397820.03		56147.64	56077.34
284093.27	5397807.49		56142.16	56072.01
284093.32	5397794.95		56218.92	56148.96
284093.37	5397782.42		56211.35	56141.17
284093.42	5397769.88		56114.37	56044.09
284093.47	5397757.34		56134.85	56064.65
284093.52	5397744.81		56194.57	56124.41
284093.58	5397732.27		56090.61	56020.29
284093.63	5397719.74		56067.17	55996.96
284093.68	5397707.20		56069.84	55999.42
284093.73	5397694.66		56107.92	56037.72
284093.78	5397682.13		56160.90	56090.69
284093.83	5397669.59		56173.95	56103.73
284093.88	5397657.05		56181.79	56111.44

Appendix C
Magnetic Data

Nad 83, Z16				
East	North		Field_nT	Corr_nT
284093.93	5397644.52		56185.16	56114.99
284093.98	5397631.98		56170.02	56099.91
284094.03	5397619.45		56180.35	56110.16
284094.08	5397606.91		56158.82	56088.51
284094.13	5397594.37		56182.39	56112.25
284094.18	5397581.84		56196.10	56125.81
284094.24	5397569.30		56227.57	56157.30
284094.29	5397556.76		56290.97	56220.53
284094.34	5397544.23		56251.44	56180.71
284094.39	5397531.69		56142.00	56071.37
284094.44	5397519.15		56108.75	56038.15
284094.49	5397506.62		56083.41	56013.04
284094.54	5397494.08		56145.67	56075.17
284094.59	5397481.55		56139.17	56068.62
284094.64	5397469.01		56185.81	56115.23
284094.69	5397456.47		56195.85	56125.61
284094.74	5397443.94		56230.47	56160.32
284094.79	5397431.40		56197.96	56127.65
284094.84	5397418.86		56283.07	56212.75
284094.90	5397406.33		56079.85	56009.81
284094.95	5397393.79		56671.69	56601.50
284095.00	5397381.26		56111.93	56041.73
284095.05	5397368.72		56110.96	56040.77
284095.10	5397356.18		56115.54	56045.10
284095.15	5397343.65		56113.11	56042.24
284095.20	5397331.11		56114.12	56043.88
284095.25	5397318.57		56097.08	56027.21
284095.30	5397306.04		56115.37	56045.49
284095.35	5397293.50		56059.46	55989.66
283995.06	5397293.10		56208.07	56136.28
283995.01	5397305.63		56224.60	56152.77
283994.96	5397318.17		56078.06	56005.97
283994.91	5397330.70		56124.05	56051.59
283994.86	5397343.24		56145.07	56072.53
283994.81	5397355.78		56116.26	56043.77
283994.76	5397368.31		56113.31	56040.98
283994.71	5397380.85		56105.17	56032.64
283994.66	5397393.39		56103.60	56031.31
283994.60	5397405.92		56134.37	56061.83
283994.55	5397418.46		56126.03	56053.64
283994.50	5397430.99		56199.25	56126.83
283994.45	5397443.53		56216.44	56144.24
283994.40	5397456.07		56196.66	56124.36
283994.35	5397468.60		56138.34	56065.78
283994.30	5397481.14		56114.49	56042.02

Appendix C
Magnetic Data

Nad 83, Z16				
East	North		Field_nT	Corr_nT
283994.25	5397493.68		56116.44	56044.19
283994.20	5397506.21		56149.63	56077.64
283994.15	5397518.75		56075.76	56004.06
283994.10	5397531.29		56096.77	56025.07
283994.05	5397543.82		56098.73	56026.90
283994.00	5397556.36		56216.57	56145.07
283993.94	5397568.89		56216.85	56145.86
283993.89	5397581.43		56363.37	56291.99
283993.84	5397593.97		56301.24	56229.70
283993.79	5397606.50		56200.04	56128.28
283993.74	5397619.04		56209.00	56137.04
283993.69	5397631.58		56173.51	56101.37
283993.64	5397644.11		56179.70	56107.45
283993.59	5397656.65		56133.13	56060.73
283993.54	5397669.18		56108.73	56036.59
283993.49	5397681.72		56104.72	56032.59
283993.44	5397694.26		56142.27	56070.06
283993.39	5397706.79		56131.71	56059.19
283993.34	5397719.33		56082.21	56009.78
283993.28	5397731.87		56081.98	56009.30
283993.23	5397744.40		56123.17	56050.53
283993.18	5397756.94		56181.87	56109.04
283993.13	5397769.47		56186.68	56113.78
283993.08	5397782.01		56088.38	56015.42
283993.03	5397794.55		56083.67	56010.66
283992.98	5397807.08		56070.74	55997.90
283992.93	5397819.62		56133.04	56059.87
283992.88	5397832.16		56175.62	56102.20
283992.83	5397844.69		56155.65	56082.37
283992.78	5397857.23		56124.34	56050.96
283992.73	5397869.77		56116.92	56043.31
283992.68	5397882.30		56082.87	56009.19
283992.62	5397894.84		56123.99	56050.15
283992.57	5397907.37		56117.91	56043.99
283992.52	5397919.91		56054.94	55980.99
283992.47	5397932.45		56098.00	56023.88
283992.42	5397944.98		56137.66	56063.81
283992.37	5397957.52		56194.54	56120.80
283992.32	5397970.06		56170.12	56096.34
283992.27	5397982.59		56166.48	56092.60
283992.22	5397995.13		56206.68	56132.66
283992.17	5398007.66		56266.16	56191.95
283992.12	5398020.20		56199.09	56125.21
283992.07	5398032.74		56137.86	56064.02
283992.02	5398045.27		56168.15	56094.34

Appendix C
Magnetic Data

Nad 83, Z16				
East	North		Field_nT	Corr_nT
283991.96	5398057.81		56196.12	56122.96
283991.91	5398070.35		56210.51	56137.45
283991.86	5398082.88		56205.28	56132.37
283991.81	5398095.42		56153.22	56080.19
283991.76	5398107.96		56079.36	56006.23
283991.71	5398120.49		56031.87	55958.67
283991.66	5398133.03		56080.61	56007.20
283991.61	5398145.56		56092.03	56018.40
283991.56	5398158.10		56197.45	56123.74
283991.51	5398170.64		56534.86	56461.12
283991.46	5398183.17		56109.48	56035.49
283991.41	5398195.71		56205.02	56130.66
283991.36	5398208.25		56202.69	56128.06
283991.30	5398220.78		56249.75	56175.06
283991.25	5398233.32		56254.86	56179.97
283991.20	5398245.85		56271.07	56196.09
283991.15	5398258.39		56270.33	56195.53
283991.10	5398270.93		56271.84	56197.04
283991.05	5398283.46		56270.07	56194.97
283991.00	5398296.00		56278.93	56203.75
283993.03	5397794.55		56084.78	56007.50
284005.57	5397794.60		56066.62	55990.59
284018.10	5397794.65		56109.70	56033.55
284030.64	5397794.70		56071.58	55994.63
284043.18	5397794.75		56134.06	56056.43
284055.71	5397794.80		56127.69	56050.23
284068.25	5397794.85		56122.37	56045.15
284080.79	5397794.90		56245.86	56168.72
284093.32	5397794.95		56221.93	56144.31
284105.86	5397795.00		56250.21	56172.37
284118.39	5397795.06		56308.92	56231.28
284130.93	5397795.11		56318.75	56241.47
284143.47	5397795.16		56262.50	56185.36
284156.00	5397795.21		56215.32	56138.27
284168.54	5397795.26		56166.10	56089.10
284181.08	5397795.31		56127.16	56050.06
284193.61	5397795.36		56104.88	56027.65
284206.15	5397795.41		56093.90	56016.76
284218.68	5397795.46		56087.25	56009.97
284231.22	5397795.51		56075.99	55998.53
284243.76	5397795.56		56082.88	56005.23
284256.29	5397795.61		56073.43	55995.85
284268.83	5397795.66		56059.34	55981.82
284281.37	5397795.72		56049.05	55971.60
284293.90	5397795.77		56055.48	55978.06

Appendix C
Magnetic Data

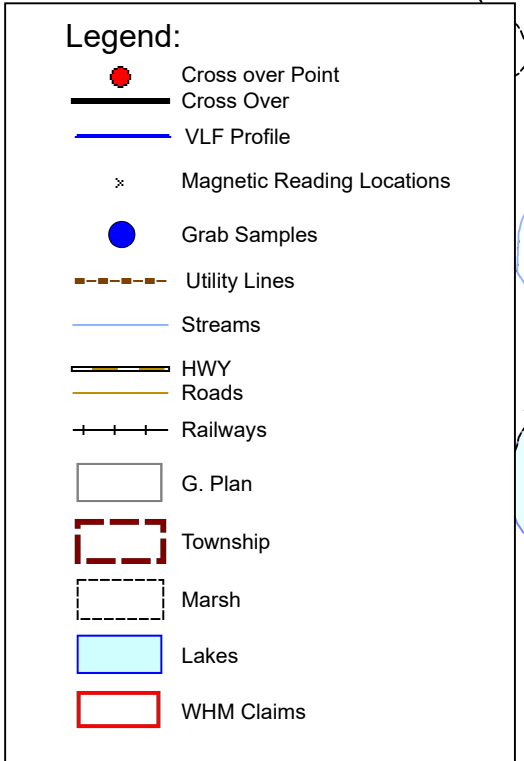
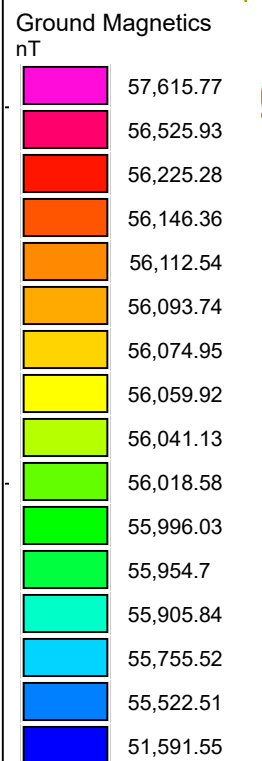
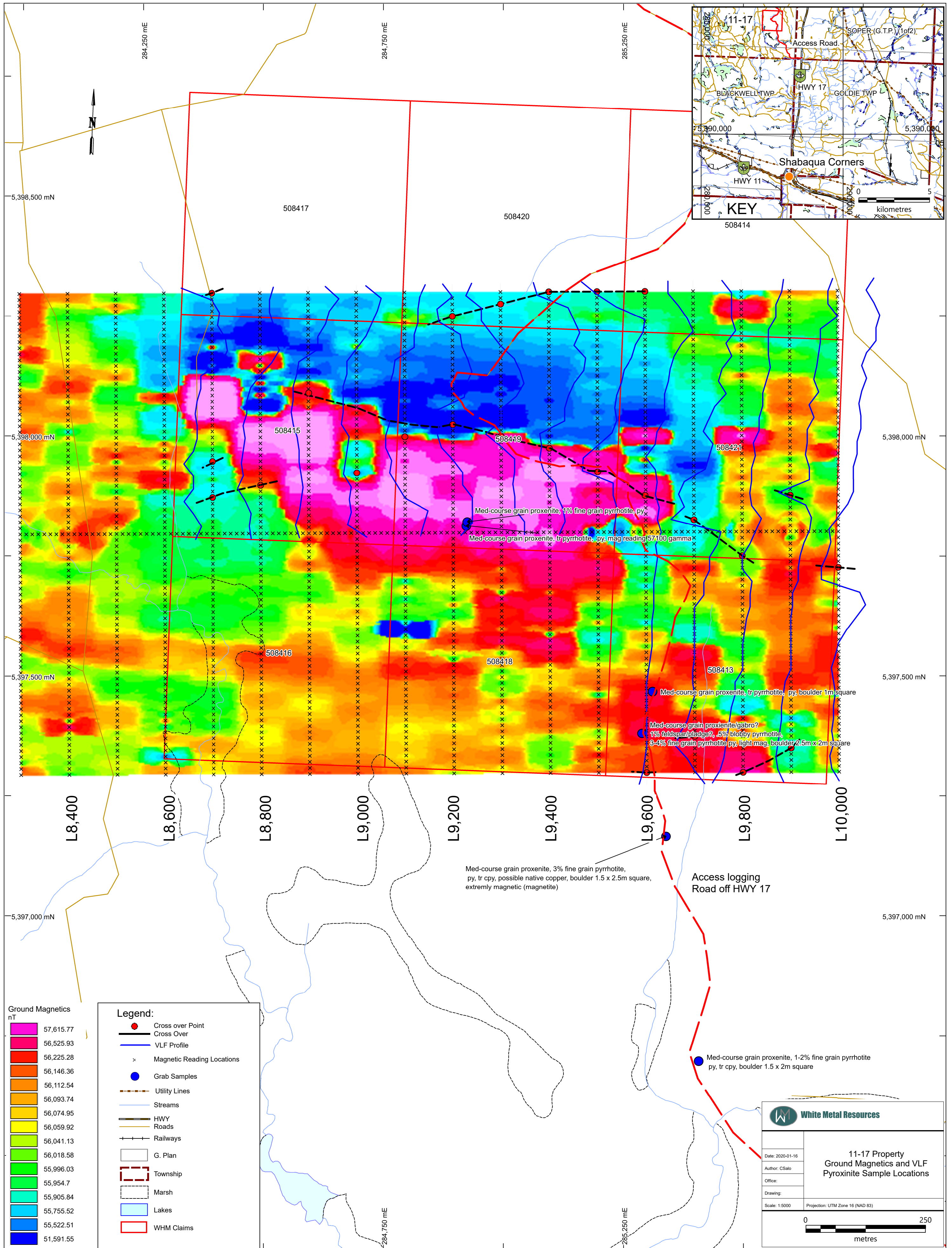
Nad 83, Z16

East	North		Field_nT	Corr_nT
284306.44	5397795.82		56054.46	55977.18
284318.97	5397795.87		56029.70	55952.59
284331.51	5397795.92		56017.71	55940.92
284344.05	5397795.97		56025.89	55949.16
284356.58	5397796.02		56018.24	55941.52
284369.12	5397796.07		56061.72	55984.76
284381.66	5397796.12		56042.26	55965.14

Appendix D

Map





White Metal Resources

**11-17 Property
Ground Magnetics and VLF
Pyroxinite Sample Locations**

Date: 2020-01-16
 Author: CSalo
 Office:
 Drawing:
 Scale: 1:5000
 Projection: UTM Zone 16 (NAD 83)

0 250 metres

APPENDIX E: GEM SYSTEMS GSM-19 SPECIFICATIONS





Overhauser Magnetometers

Magnetometer (GSM-19) - Walking Magnetometer (GSM-19W)
Gradiometer (GSM-19G) - Walking Gradiometer (GSM-19GW)

Since 1980

Leading the World of **Magnetics**

GEM Systems is the global leader in the manufacture and sale of high precision magnetometers.

GEM Systems is the only commercial manufacturer of Overhauser magnetometers, that are accepted and used at Magnetic Observatories over the world.

Our Potassium Magnetometers are the most precise magnetometers in the world.

Our Proton sensors are considered the most practical and robust magnetometers for general field use.

Proven reliability based on R+D since 1980.

We deliver fully integrated systems with GPS and additional survey capability with VLF-EM for convenience and high productivity.

Today we are creating the absolute best in airborne sensors and are leading the way with smaller and lighter sensors for practical UAV applications.

GEM Systems large potassium sensors offer the highest sensitivity (20-50 fT) for use in natural hazard research and global ionospheric studies.

Our Leadership and Success in the World of Magnetics is your key to success in applications from Archeology, Volcanology and UXO detection to Exploration and Magnetic Observations Globally.



GEM Systems Overhauser Magnetometer system. It can be configured with additional survey sensors for simultaneous gradiometer readings as well as VLF. System configurations can also include walking mode and GPS.

The Overhauser

GEM Systems GSM-19 Overhauser total field magnetometer and the GSM-19G Gradiometer provide improved data quality and greater absolute accuracy than Proton magnetometers, while providing a robust and comparable system to costlier Cs magnetometers for ground applications.

Technically Superior

The GSM-19 Overhauser instrument is the total field magnetometer / gradiometer of choice in today's earth science environment. GEM Overhauser technology provides a unique blend of physics, chemistry and engineering. Sophisticated system design and solid experience in the field of magnetics help to clearly differentiate it from other quantum magnetometers.

The GSM-19 is a standard in many fields, including:

- **Mineral exploration**
- **Environmental and engineering**
- **Pipeline mapping**
- **Airborne basestation**
- **Unexploded Ordnance Detection**
- **Archaeology**
- **Magnetic observatory measurements**
- **Volcanology and earthquake prediction**

Taking Advantage of the Overhauser Effect

Overhauser effect magnetometers are essentially proton precession devices - except that they produce an order-of magnitude greater sensitivity.

The Overhauser effect occurs when a special liquid (with unpaired electrons) is combined with hydrogen atoms and then exposed to secondary polarization from a radio frequency (RF) magnetic field. The unpaired electrons transfer their stronger polarization to hydrogen atoms, thereby generating a strong precession signal that is **ideal for very high sensitivity total field measurements.**

In comparison with proton precession methods, RF signal generation also keeps **power consumption to an absolute minimum.** RF frequencies are well out of the bandwidth of the precession signal and they do not impair the sensitivity i.e. polarization and signal measurement can occur simultaneously - which enables **faster, sequential measurements** and increased cycling rates (i.e. sampling speeds). Measurements can therefore be near continuous.

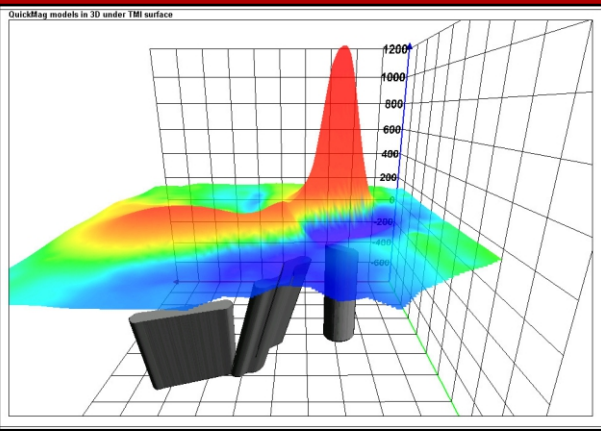
GEM Systems, Inc.

135 Spy Court Markham, ON Canada L3R 5H6

Phone: 1 905 752 2202 • Fax: 1 905 752 2205

Email: info@gemsystems.ca • Web: www.gemsystems.ca

Our World is **Magnetics.**



Single sensor and gradiometer modes provide flexibility and fast sampling and are used for detecting changes in the magnetic field. Applications include; alteration mapping, structural geology, archeology and UXO applications.

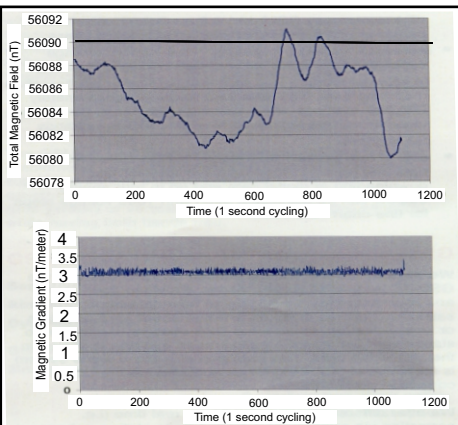
GEM Systems Sensor Technology

GEM Systems sensors represent a **proprietary innovation** that combines advances in electronics design and quantum magnetometer chemistry. Each sensor head houses a **proprietary** hydrogen-rich liquid solvent which is combined with free electrons (free radicals) in the GEM laboratory to increase the signal intensity under RF polarization.



GEM Systems GSM-19

Small and light weight. Rugged plastic housing protects the internal components during operation and transport.



Sample data

Gradiometer data shows very low noise level (<0.2nT. peak to peak)

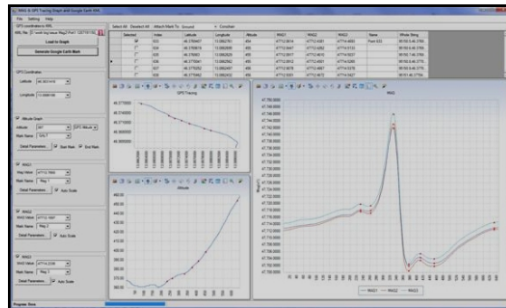
GPS and Navigation

Along with basic GPS tracking, GEM provides a Navigation feature with real-time coordinate transformation to UTM and local grid. A survey "lane" guidance system with cross track display coupled with automatic end-of-line flag and guidance to the next line allows the operator to navigate seamlessly while carrying out the magnetic survey. Operators can define a complete survey on PC and download points to the magnetometer via RS-232 before leaving for the field.

GEMLink+

Software for Processing Magnetic Data

GEMLink+ processing software is provided with every GEM magnetometer system. **GEMLink+** provides all of the data visualization needed by the geoscientist to quickly assess the data quality in the field. The software provides diurnal correction, profile plotting, line path maps and some basic mapping and modeling functions. Files can be imported/exported to Google (.kmz) format and coordinate transformations can be made.



GEMLink+ Data QAQC software with multi window data processing and plotting.

Specifications

Performance

Sensitivity: Standard GSM 19 0.022 nT @ 1 Hz
 GSM 19PRO 0.015 nT @ 1 Hz
 Resolution: 0.01 nT
 Absolute Accuracy: 0.1 nT
 Dynamic Range: 20,000 to 120,000 nT
 Gradient Tolerance: up to 10,000 nT/m
 Samples at: 60+, 5, 3, 2, 1, 0.5, 0.2 sec
 Operating Temperature: -40°C to +50°C

Operating Modes

Manual: Coordinates, time, date and reading stored automatically at upto 0.2 sec.

Base Station: Time, date and reading stored at 1 to 60 second intervals.

Remote Control: Optional remote control using RS-232 interface.

Input / Output: Input/Output: RS-232 using 6-pin weatherproof connector with USB adapter.

Memory - (# of Readings in millions)

Mobile: 1.4M, Base Station: 5.3M,
 Gradiometer: 1.2M, Walking Mag: 2.6M

Dimensions

Console: 223mm x 69mm x 240 mm
 (8.7x2.7x9.5in)
 Sensor: 175mm x 75mm diameter cylinder
 (6.8in long by 3 in diameter)

Weights

Console with Belt: 2.1 kg
 Sensor and Staff Assembly: 1.0 kg

Standard Components

GSM-19 console, GEMLink software, battery, harness, charger, sensor with cable, RS-232 cable and USB adapter, staff, instruction manual, and shipping case.

Options

Gradient Magnetometer, Walking Mode, Multi sensor

Available GPS

GPS Time Only (Option A)

Standard GPS (Option B):

- 0.7m SBAS (WAAS, EGNOS, MSAS)
- < 1.5m non-SBAS

Enhanced GPS (Option C):

- 0.6m SBAS (WAAS, EGNOS, MSAS), GLONASS, BeiDou, Galileo
- Consult GEM for availability

High resolution GPS (Option D):

- 0.6m SBAS (WAAS, EGNOS, MSAS), GLONASS, BeiDou, Galileo
- 40 cm or 4cm accuracy with NovaTel Correct (TerraStar Subscription required)
- Consult GEM for availability

VLF Option : Frequency Range: 15 to 30.0 kHz with up to 3 stations. Parameters: Vertical in-phase and out-of-phase components as % of total field.

The GSM 19,19G,19W and 19GW systems come complete with an industry leading three year warranty



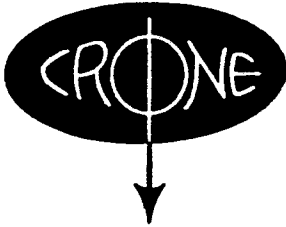
GEM Systems, Inc.

135 Spy Court Markham, ON Canada L3R 5H6

Phone: 1 905 752 2202 • Fax: 1 905 752 2205

Email: info@gemsystems.ca • Web: www.gemsystems.ca

APPENDIX F: CRONE RADEM VLF-EM SPECIFICAITONS



CRONE GEOPHYSICS LIMITED

3607 WOLFEDALE ROAD, MISSISSAUGA, ONTARIO, CANADA L5C 1V8
TELEPHONE: (416) 270-0096 CABLE: CRONGEO, TORONTO TELEX: 06-961260.

Australian Branch: 244 Newbridge Road, MOOREBANK, N.S.W. 2170 Telephone: (02) 602-0937, Telex: 71-22922

INSTRUCTIONS FOR OPERATION OF THE RADEM VLF-EM RECEIVER

(1) Transmitter Stations

The VLF Communication Broadcast stations are positioned throughout the world. At present, 13 of these stations broadcast steadily except for maintenance periods usually of 1/2 to 1/3 days per week. The RADEM receives any 7 of these stations with selection by means of a switch. The usable range of the stations varies widely with power and transmission conditions but is usually between 1000 and 5000 miles. Two types of signals are broadcast "keyed" (on and off) and "frequency shift" (FM).

A station should be selected that is located in the same direction as the regional strike. For example, if the geological strike is east-west then a station located east or west of the operator should be used. If in doubt of the geological strike two orthogonal stations should be read.

(2) Field Measurements

(a) Dip Angle of Resultant Field

This is the angle of inclination, measured from the horizontal in degrees, of the direction of the resultant VLF field. The VLF field is normally horizontal (0° dip). The dip angle measurement is independent of the strength of the field and the gain setting of the RADEM receiver. When plotted on a profile the dip angles usually form a cross-over pattern above the conductor as with the standard vertical loop EM method.

To measure the dip angle the RADEM is first held with the instrument face horizontal and rotated until a null is obtained (visual minimum on the field strength meter and audio null).

direction of the VLF field. The RADEM is then held vertically and tilted from right to left until another null is obtained. The instrument is held steady in this null position and the dip angle read from the inclinometer. Note that the arrow in CRONE points towards the conductor if the arrow points north the dip angle is recorded as say 10°N . In making the dip angle measurement the Normal-K switch must be in the NORM position.

(b) Out-Of-Phase Measurement
(Usually Not Measured)

The secondary field from a ground conductor often is not in the same phase as the primary field, therefore the resultant field will have an out-of-phase component.

To measure the out-of-phase component as a percent of the normal primary field the volume control of the amplifier must be set up as a standard. This is achieved at a base station in a normal area. The Field Strength range switch is placed in the 0 - 300 position. The RADEM held with the face horizontal and the body rotated until a maximum Field Strength reading is obtained. In this position the Volume control is adjusted until the meter reads "100". The Volume control is left at this setting until the base station is read again usually one to several hours later. The Out-Of-Phase reading is the minimum position of the Field Strength meter when the dip angle of the resultant field is being measured. It is read at the same time as the dip angle is being read with the RADEM in the vertical null position.

The Out-Of-Phase measurement is sensitive to a lower order of conductivity than the dip angle measurement. For this reason it is often not recorded unless very poor conductors are being sought.

(c) Horizontal Component of the Field Strength

This is simply the strength of the field in the horizontal plane. It is the maximum reading obtained from the Field Strength meter when the instrument is rotated in the horizontal plane. It is therefore at right angles to the null position. It is usually read after the dip angle measurement simply by holding the RADEM horizontal, the CRONE arrow pointing at right angles to the operator, and adjusting position for maximum reading in the horizontal plane.

If the signal is keyed the Normal-K switch is moved to the "K" position for the field strength reading. It must be returned to the normal position for dip angle measurement.

The field strength of VLF stations drifts with time. This drift is particularly severe during sunrise and sunset periods. A base station should be established in a normal area and the RADEM adjusted to a Horizontal Field Strength of "100" on the "0 - 300" scale by means of the volume control pot. This base or subsidiary base station should be read every one to two hours as in a magnetic survey.

Fraser's Method

Reference: Geophysics, Volume 34, No. 6, December 1969.
"Contouring of VLF-EM Data"

This is a simple operation on the dip angle readings that more clearly defines anomalous areas. It requires a consistent reading interval usually 50' or 100'. It produces a survey in which the conductors are contoured much the same as a Horizontal Field Strength survey although lacking the detail possible with the Field Strength measurement.

Example of Field Sheet

Station	Out-Of-Phase-%	Dip Angle Degrees	Reading	Field Strength	Time Drift	Corr.	Remarks
10N-Base	2	0	100	9:00	0	100	
10+50N	2	0	100	:02	0	100	Lake
11N	0	2N	99	:04	-1	98	Lake
11+50N	0	6N	101	:06	-1	100	
12N	0	12N	102	:08	-2	100	Road
12+50N	4	22N	118	:10	-2	116	
13N	6	20N	185	:12	-2	183	
13+50N	6	8N	263	:14	-3	260	X' Ov
14N	0	1S	247	:17	-3	244	
14+50N	0	12S	164	:20	-4	160	
/							
10N-Base			114	10:10	-14	100	

Reprint from Geophysics, Vol. 34, No.6 (December 1969) p.958-967

"Contouring of VLF-EM Data (Dip Angle Measurements)"

by Frazer, D.C.

CONTOURING OF VLF-EM DATA†

D. C. FRASER*

Prospecting for conductive deposits with ground VLF-EM instruments has received considerable impetus with the recent development of lightweight receivers. The large geologic noise component, which results from the relatively high-transmitted frequency, has caused some critics to avoid use of the technique. Those who routinely perform surveys with a VLF-EM unit find that, in some areas, a 5-degree peak-to-peak anomaly can be significant, whereas anomalies having amplitudes in excess of 100 degrees may occur as well. Consequently, there is a dynamic range problem when presenting the results as profiles

plotted on a field map.

A data manipulation procedure is described which transforms noisy noncontourable data into less noisy contourable data, thereby eliminating the dynamic range problem and reducing the noise problem. The manipulation is the result of the application of a difference operator to transform zero-crossings into peaks, and a low-pass smoothing operator to reduce noise. Experience has shown that field personnel can routinely perform the calculations which simply involve additions and subtractions.

INTRODUCTION

VLF-EM data can be exceedingly difficult to interpret because a large geologic noise component can result from the relatively high-transmitted frequency of about 20,000 Hz. Routine surveys can yield useless data unless special care is taken both in survey procedure and in data presentation.

The purpose of this paper is to describe the survey procedure and the method of data presentation in use by the Keevil Mining Group and to illustrate the advantages of this approach.

VLF-EM GROUND SURVEY PROCEDURE AND DATA TREATMENT

The primary field

VLF-EM transmitter stations are located at several points around the globe. They broadcast at frequencies close to 20,000 Hz, which is low compared to the normal broadcast band. The purpose of these stations is to allow governmental communication with submarines, and the low frequency allows some penetration of the conduc-

tive ocean water. Skin depth is approximately $3.6\sqrt{P}$ meters, where P is the resistivity of a homogeneous halfspace in ohm-m, on the assumption that the frequency is 20,000 Hz and that the halfspace is magnetically nonpolarizable. Consequently, depth of exploration is severely restricted for overburden resistivities less than 200 ohm-m.

Since the area to be prospected normally is of considerable distance from the transmitter stations, the primary field is uniform in the area, allowing rather simple mathematics to be used in anomaly prediction and analysis.

Survey procedure and data treatment

The survey procedure first consists of selecting a transmitter station which provides a field approximately parallel to the traverse direction, i.e., approximately perpendicular to the expected strike of a conductor. The following points relate to the method of data treatment.

1. Readings should be taken every 50 ft, as will be shown below.
2. Transmitter stations should not be changed

† Manuscript received by the Editor April 24, 1969; revised manuscript received August 18, 1969.

* Keevil Mining Group Limited, Geophysical Engineering & Surveys Limited, Teck Corporation Limited, Toronto, Ontario, Canada.

Copyright ©1970 by the Society of Exploration Geophysicists.

for a given block of ground, to avoid distortion in the contour presentation. Hence, fill-in lines should be run with the same transmitter station as other lines in the block. The field direction of this station should be shown on the data map.

3. List the dip angle¹ data in tabular form, as follows:
 - a) list in the direction of north (top of paper) to south, or from west to east;
 - b) designate south or east dips as negative; and
 - c) perform calculations as shown in Table 1.

Thus, the filtered output or contourable quantity simply consists of the sum of the observations at two consecutive data stations subtracted from the sum at the next two consecutive data stations. The theoretical basis for this procedure will be described below.

4. The right-hand column (filtered data) is

¹ This paper assumes that data is recorded as for the Crone Radem which defines a north-dipping field as a south "dip" on the instrument. This convention was chosen because a south reading is interpreted as arising from a conductor to the south.

suitable for contouring. Normally, negative values are not contoured since, being caused by dip angle flanks, they do not aid interpretation but only confuse the picture. The positive values generally are contoured at 10-unit intervals, and the zero contour is shown only when it brackets an anomaly. In quiet areas, 5-unit contours may be meaningful.

Example

Figure 1 presents dip-angle data, according to the Crone convention, in the vicinity of the Temagami mine of Copperfields Mining Corporation Limited in Ontario. This figure illustrates that several conductors are present yielding large dip angles. A complex pattern has resulted which requires some thought to interpret properly.

Figure 2 presents the filtered data in contoured form where only the 0, 20, and 40 contours are shown for simplicity. The conductor pattern is immediately apparent, even to exploration personnel untrained in VLF-EM interpretation. The three anomalies correlate with a zone of nearly massive pyrite and two brecciated fault zones. Depth to bedrock is 15 ft.

In practice, all the data of Figures 1 and 2 are

Table 1. Example of calculations

Location	Measured dips	Apply sign and form the moving sum of pairs of entries	Take first differences of alternate entries
3+00S	6S	-6	
3+50S	7S	-7	
4+00S	8S	-8	
4+50S	15S	-15	
5+00S	24S	-24	
5+50S	8N	+8	
6+00S	10N	+10	
6+50S	12N	+12	
7+00S	14N	+14	
7+50S	14N	+14	
8+00S	20N	+20	
		$(-6) + (-7) = -13$ $(-7) + (-8) = -15$ $(-15) + (-24) = -39$ $(+8) + (+10) = +18$ $(+10) + (+12) = +22$ $(+12) + (+14) = +26$ $(+14) + (+14) = +28$ $(+14) + (+20) = +34$	$(-23) - (-13) = -10$ $(-39) - (-15) = -24$ $(+34) - (+26) = +8$

Fraser

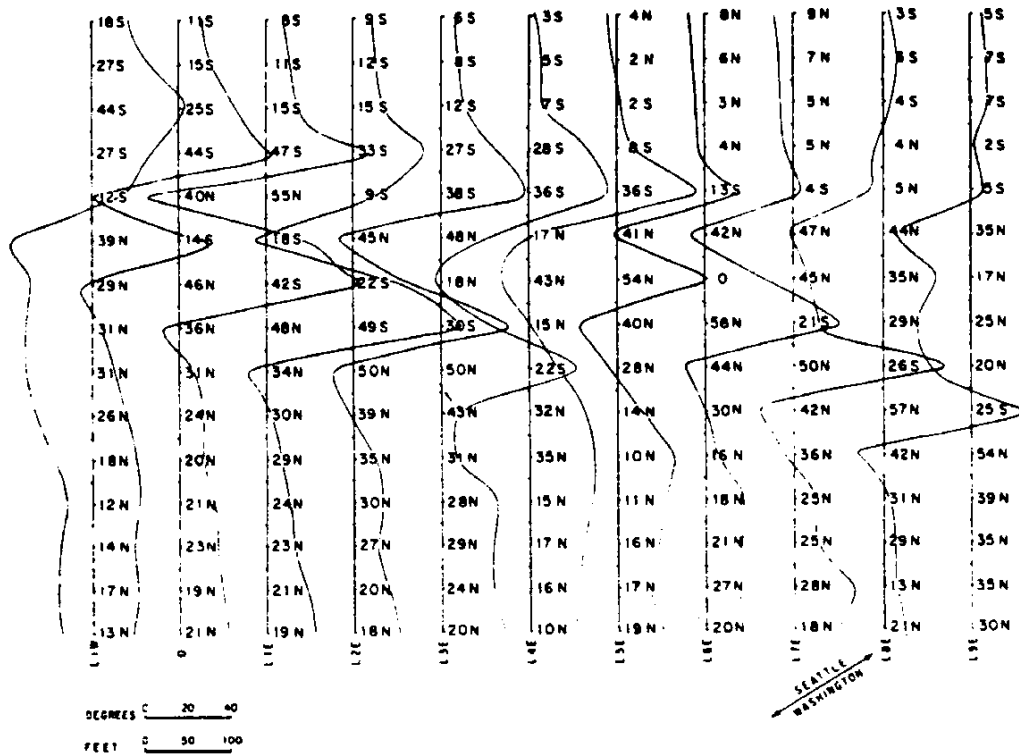


FIG. 1. Dip-angle data in the vicinity of the Temagami mine. The arrow defines the VLF-EM primary field direction from the transmitter at Seattle, Washington.

placed on a single map. The above example illustrates that this very simple one-dimensional filtering scheme yields a practical and effective approach to VLF-EM data handling.

The filter improves the resolution of anomalies, thereby making them easier to recognize. An inflection on the dip profile from a conductor subordinate to a larger one yields a positive peak, thereby emphasizing the presence of such a conductor. Figure 3 illustrates this effect where nine lines were run over an SP (self-potential) anomaly in the Temagami area. The dip-angle anomaly is very poorly resolved due to the regional south dips produced by an areally large conductor to the south of the map area. The contoured VLF-EM data yields a clearly defined anomaly which was located over the negative center of the SP.

THE FILTER AND ITS EFFECT ON ANOMALIES

The filter operator

The filter operator was designed to meet the

following criteria:

1. It must phase shift the dip-angle data by 90 degrees so that crossovers and inflections will be transformed into peaks to yield contourable quantities.
2. It must completely remove dc and attenuate long spatial wavelengths to increase resolution of local anomalies.
3. It must not exaggerate the station-to-station random noise.
4. It must be simple to apply so that field personnel can make the calculations without difficulty.

The first two criteria are met by using a simple difference operator, i.e.

$$M_2 - M_1,$$

where M_1 and M_2 are any two consecutive data points.

The third criterion is met by applying a smoothing or low-pass operator to the differences, i.e.

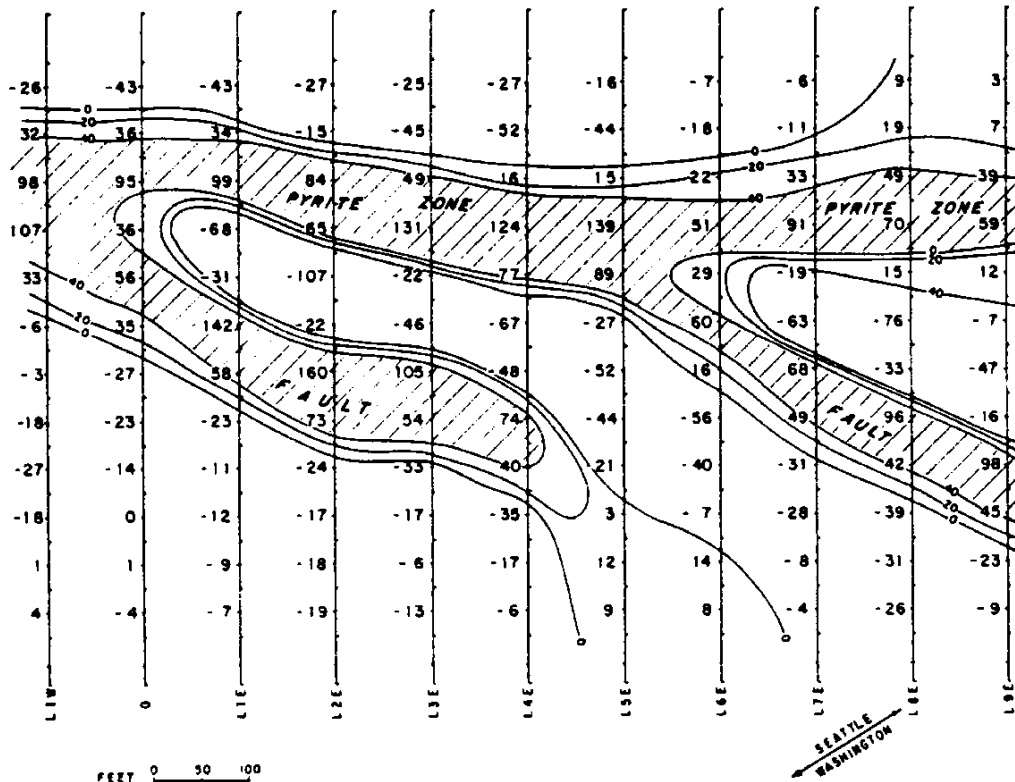


FIG. 2. Filtered data computed from the map of Figure 1.

$$\frac{1}{4}(M_2 - M_1) + \frac{1}{2}(M_3 - M_2) + \frac{1}{4}(M_4 - M_1),$$

where $M_1, M_2, M_3,$ and M_4 are any four consecutive data points. The filtered output then is

$$\frac{1}{4}(M_2 - M_1) + \frac{1}{2}(M_3 - M_2) + \frac{1}{4}(M_4 - M_1) = \frac{1}{4}[M_3 + M_4 - M_1 - M_2].$$

The final criterion is enhanced by eliminating the constant, so that the plotted function becomes

$$f_{2,3} = (M_3 + M_4) - (M_1 + M_2),$$

which is plotted midway between the M_2 and M_3 dip-angle stations.

This filter has its frequency (wavenumber) response displayed in Figure 4, for a station spacing of 50 ft. Its characteristics are as follows:

1. All frequencies are shifted by 90 degrees.
2. Noise having a wavelength equal to the station spacing and dc bias are completely removed.

3. Maximum amplitude occurs for wavelengths of 250 ft, or five times the station spacing.

The frequency (wavenumber) response of the filter is shown for a station spacing of 50 ft, because this is the most suitable spacing for defining sulfide bodies within a few hundred feet of surface. This will be demonstrated below.

The dike model

A conducting dike in a VLF-EM field will produce a secondary induction field from eddy currents maintained in it by the primary field. These eddy currents will tend to flow in such a manner as to form line sources concentrated near the outer edges of the dike since the field is uniform (Figure 5a). This dike may be replaced by a loop of wire of dimensions traced out by the main current concentration in the dike. The secondary field geometry of the loop and dike then will be practically identical, as has been shown by Fraser (1966), Parry (1966), and Parry et al (1965). This

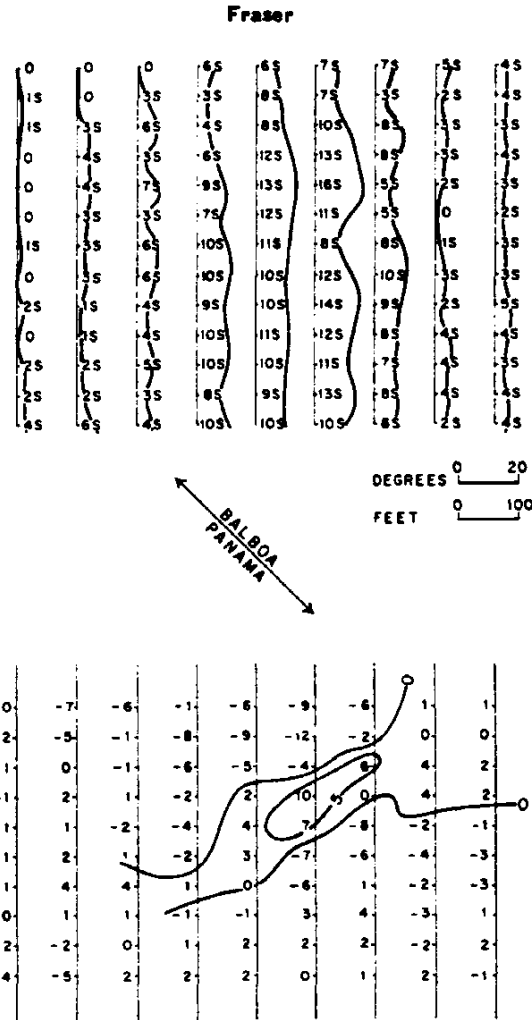


FIG. 3. Dip-angle (upper map) and filtered data (lower map) over a small grid in the Temagami area. The arrow defines the VLF-EM primary field direction from the transmitter at Balboa, Panama.

allows a mathematical model of a dike to be constructed because the field from a line source is known.

For brevity, only a dike which is large in depth extent and in length will be considered herein. Only the top line source of Figure 5a will contribute to the measured dip angles because the other current line sources are very far away.

The horizontal H_{s_x} and vertical H_{s_z} secondary fields are (Figure 5b)

$$H_{s_x} = kH_0 \frac{z}{x^2 + z^2}$$

$$H_{s_z} = kH_0 \frac{x}{x^2 + z^2}$$

where k is a positive constant having the dimension of length and is related to the conductivity and dimensions of the dike, and where H_0 is the primary VLF-EM strength at the dike. The measured dip angle is

$$\begin{aligned} \alpha &= \tan^{-1} \left[\frac{H_{s_z}}{H_{s_x} + H_0} \right] \\ &= \tan^{-1} \left[\frac{kx}{kz + x^2 + z^2} \right] \end{aligned}$$

Model dip profiles can be computed for various depths z only by assuming a value for k .

As a means of testing the effect of the filter operator, a single k value was chosen to yield a

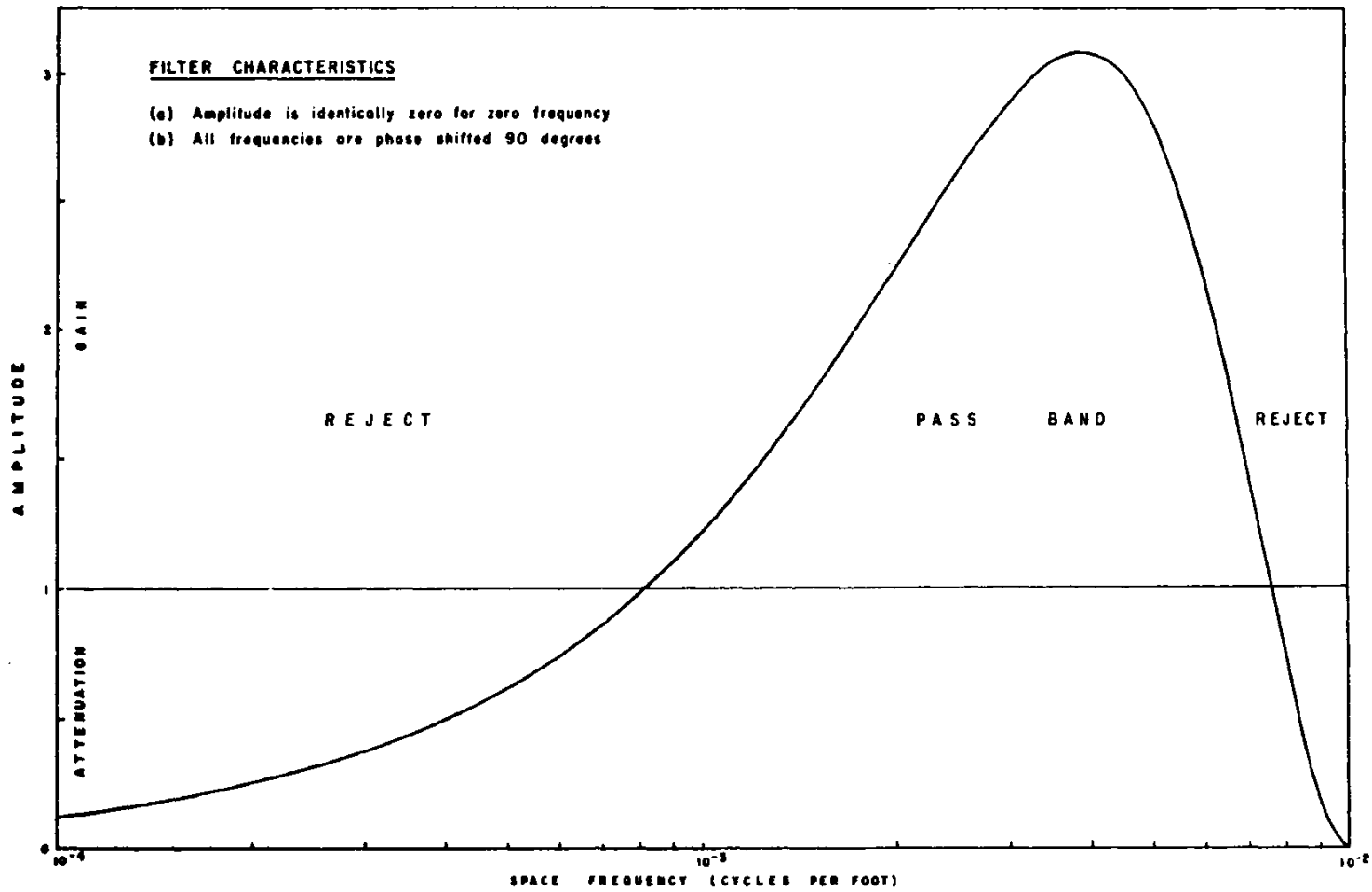


FIG. 4. Frequency response of filter operator for station spacing of 50 ft.

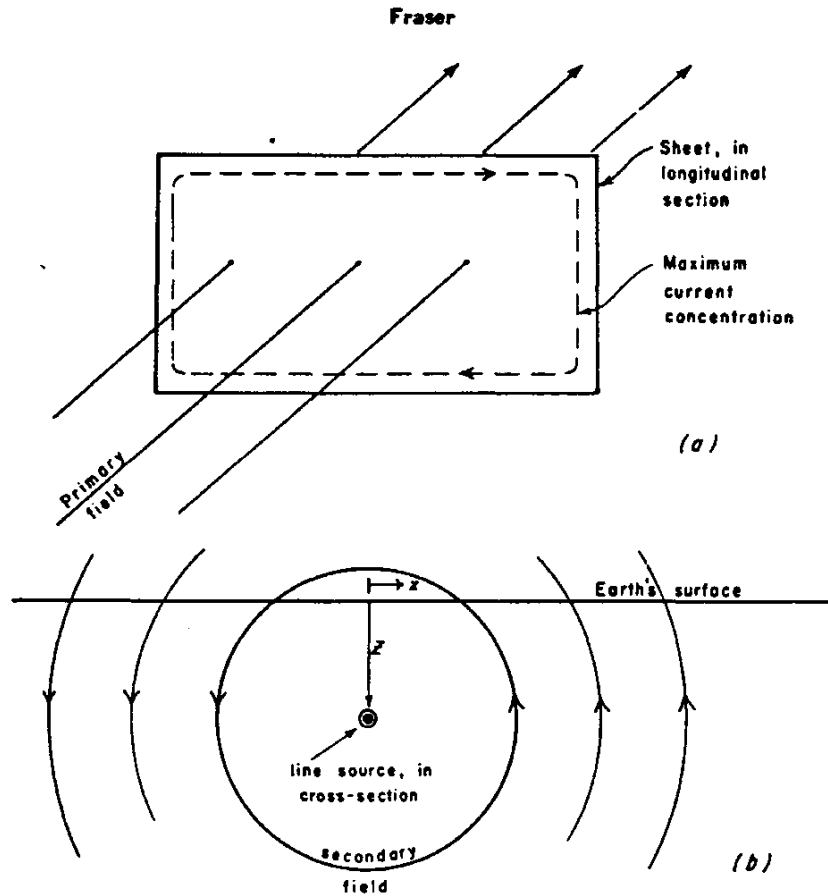


FIG. 5. (a) A sheet in a uniform primary field will have maximum current concentrated near its edges. (b) A line source, corresponding to the upper current concentration in (a), yields a secondary magnetic field of cylindrical shape.

maximum dip angle of 35 degrees when depth z to top of dike (or line source) was 100 ft. Figure 6 illustrates the dip angle and filtered profiles for this case for a station spacing of 50 ft and for several depth values.

The following are the main characteristics of these dike and filtered anomalies:

1. Peak-to-peak angles vary from 93 degrees for $z=50$ ft to 25 degrees for $z=500$ ft. Filtered peaks vary from 118 degrees for $z=50$ ft to 8 degrees for $z=500$ ft. Thus, the filter amplifies near-surface anomalies and attenuates deep-source anomalies. There is neither amplification nor attenuation when z is 100 ft.
2. On the basis of anomaly resolution and usual noise levels, dip angle data can detect dike-like conductors in a resistive medium to a

depth of 500 ft, while filtered data can detect such bodies to a depth of 300 ft. Conductors in the upper 200 ft generally will be more easily recognized on the filtered data.

VLF-EM data commonly is measured at 100-ft intervals in Canada. A change in the sample interval from the 50 ft recommended herein to 100 ft causes the passband curve of Figure 4 to shift to the left, such that the peak is at 2×10^{-3} cpf rather than 4×10^{-3} cpf. Similarly, the anomaly curves of Figure 6 remain correct in shape provided all distance dimensions are doubled. Consequently, detection of conductors to a depth of 500 ft, when utilizing the filter operator, might appear facilitated by use of a 100-ft station interval rather than a 50-ft interval. However, anomalies from near-surface conductors will have poorly defined waveforms for a 100-ft

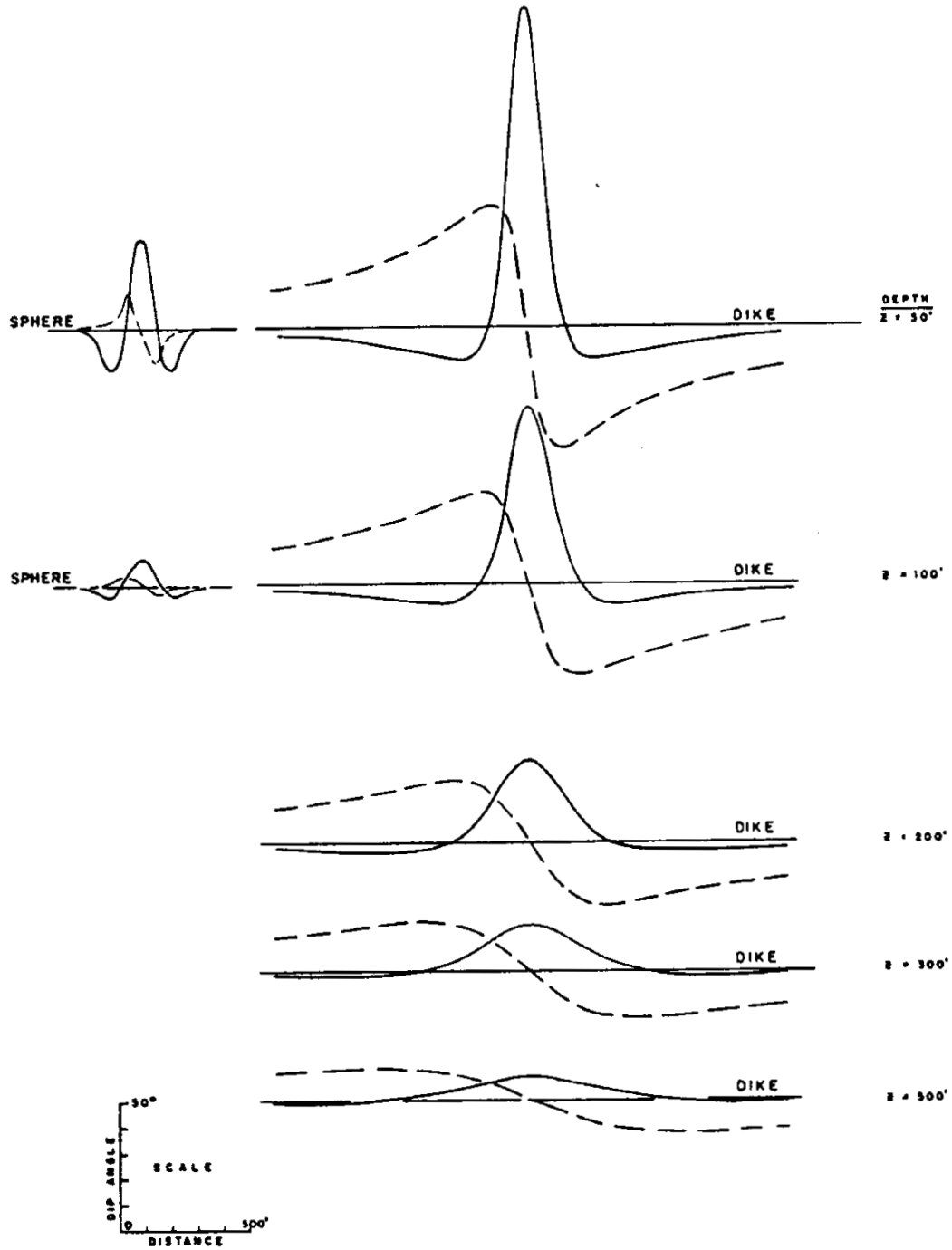


FIG. 6. Dip-angle (dashed) and filtered (solid) curves for model dike and sphere for several depths of burial, where z is depth to top of dike and to center of sphere.

data station interval, and will alias as deeper conductors. This "geologic noise" will somewhat confuse the contoured output. Generally, a comparison of the 50-ft data station dip angle profiles with the contoured filtered output suffices to indicate approximate depth to source and to allow recognition of sources deeper than 300 ft.

As an aside, some geophysicists have claimed that a reasonable dike model depth estimate can be obtained directly as half the distance between dip angle peaks, because the vertical field H_s peaks at $x = \pm z$. However, this formula is not applicable to dip-angle data, as can be seen by the dike curves of Figure 6. For this example, the formula provides erroneous depth estimates of 150, 200, 325, 425, and 625 for true depths of 50, 100, 200, 300, and 500 ft.

The sphere model

A conducting sphere in a VLF-EM field will produce an anomaly according to equations in Ward (1967). For a traverse directly over a sphere having its center at depth z , and run in the direction of the primary field H_0 , the anomaly is,

$$H_{s_z} = kH_0 \frac{(2x^2 - z^2)}{(x^2 + z^2)^{3/2}}$$

$$H_{s_x} = kH_0 \frac{3xz}{(x^2 + z^2)^{3/2}}$$

where k is a positive constant which saturates at $R^3/2$, where R is the sphere radius, and where quadrature is ignored. The measured dip angle as a function of station location x is (where x is zero directly over the sphere center),

$$\alpha = \tan^{-1} \left(\frac{H_{s_x}}{H_{s_z} + H_0} \right)$$

$$= \tan^{-1} \left[\frac{3kxz}{k(2x^2 - z^2) + (x^2 + z^2)^{3/2}} \right]$$

Model dip profiles can be computed for various depths z only by assuming a value for k . The sphere curves of Figure 6 assume a saturated k -value for a sphere radius of 50 ft. Obviously, a sphere having its center at a depth of greater than twice its radius generally will not be detectable. However, the filter operator aids in the recognition of a spherical conductor because it amplifies the anomaly, for the small sphere sizes

usually encountered in nature, assuming data spacing is 50 ft.

TOPOGRAPHIC EFFECT

Whittles (1969) recently described a topographic effect which may arise when surveying with VLF-EM in mountainous regions. The spatial wavelengths which result from the phenomenon he describes are greatly attenuated by the filter and generally do not appear on the contoured maps. Whittles advocates the use of first derivatives to remove the topographic effect. The filter operator described herein uses the first difference (i.e., the discrete first derivative) as one of its components.

ADDITIONAL APPLICATIONS

The simplicity of the calculations allows practical application of the filter to any form of ground geophysical data which yields zero-crossings over targets, such as vertical loop EM and Afmag. However, it is difficult to justify the use of the filter on vertical loop EM data because neither dynamic range of anomalies nor geologic noise is large. In Afmag, utilization of the filter is not recommended because of the varying direction of the primary field.

Airborne VLF-EM systems, which measure parameters yielding zero-crossings over targets, are being marketed. If the data were collected on magnetic tape, a computer could be used to apply the filter, thereby allowing contouring of the data. However, in this situation more sophisticated filter operators should be employed.

If the filter is to be applied to data other than ground VLF-EM, the sample interval should be selected to ensure that the passband of the filter is correct relative to the frequency components of the anomalies sought.

CONCLUSIONS

A consideration of geologic noise and conductor shapes illustrates that VLF-EM data should be collected at 50-ft intervals, and that the described filter operator should be employed. The filtered data, when contoured, provides a data presentation which simplifies interpretation. The filter also amplifies anomalies from near-surface, highly conducting ore pods which is an important feature in several mining districts such as at Tribag and Temagami, both in Ontario, and in Louvicourt Township of Quebec.

REFERENCES

- Fraser, D. C., 1966, Rotary field electromagnetic prospecting: Ph.D. thesis, University of California at Berkeley.
- Parry, J. R., 1966, A theoretical and experimental investigation of finite dikes in a uniform electromagnetic field: M.Sc. thesis, University of California at Berkeley.
- Fraser, D. C., and Ward, S. H., 1965. Investigation of finite dikes in a uniform electromagnetic field: Presented at the 35th Annual International SEG Meeting, Dallas, Texas.
- Ward, S. H., 1967, Electromagnetic theory for geophysical applications, in *Mining Geophysics*, Vol. II: Tulsa, SEG, p. 80.
- Whittles, A. B., 1969, Prospecting with radio frequency EM-16 in mountainous regions: *Western Miner*, February 1969, p. 51-56.

Underlying theory behind the VLF-EM method used in this survey.

(Reprint from section of "VLF Mapping of Geological structure")
(Telford et. al. 1977)

VLF MAPPING OF GEOLOGICAL STRUCTURE

W.M. Telford¹, W.F. King² and A. Becker³

Foreword

This paper is a summary of the work done by W. F. King while working under the direction of Dr. A. Becker as a graduate assistant for the Geological Survey of Canada during the summers of 1969 and 1970. The data described form part of his M. Sc. Thesis dissertation, working under thesis supervisor, Prof. W. M. Telford, Department of Mining Engineering and Applied Geophysics, McGill University. This paper is a product of the application of new geophysical techniques being adapted to the geological mapping mission of the Electrical Methods Section, Resource Geophysics and Geochemistry Division, Geological Survey of Canada.

L. S. Collett,
Head, Terrain Geophysics Program,
Resource Geophysics and Geochemistry Division

INTRODUCTION

It has long been observed that electromagnetic plane waves propagating along the earth's surface are locally distorted by near-surface discontinuities in electrical resistivity. In such cases the horizontal magnetic field components normally present induce in the ground a non-uniform eddy current distribution which results in an anomalous vertical magnetic field component. In the

extra low frequency range (ELF) this phenomenon is readily observable near coastlines (Weaver, 1963) while in the audiorange (AFMAG) the effect was first observed by Shaw (oral comm., 1961) in the vicinity of faults and shear zones. More recently, Collett and Bell (1971) have discussed how the AFMAG method can serve as a useful tool in structural mapping. Finally at very low frequencies (VLF) i.e. in the 10-20 kHz range the effect of geological structure has been observed by Becker (1967), Fraser (1969) and Patterson and Ronka (1971).

These effects were explained theoretically by Weaver (1963) who obtained closed form solutions for plane waves incident on a semi-infinite conducting medium divided by a vertical discontinuity into two regions of different resistivity. Weaver's calculations were later confirmed experimentally by Dosso (1976) on a laboratory scale model. Both authors forecast a sharp increase in vertical magnetic field component near an electrical discontinuity. This quantity exhibits a maximum value at the discontinuity and decreases gradually to zero away from it.

The rate of decrease is a function of the electrical properties of the material on either side of the discontinuity, being greater on the conductive side. More recently this problem was studied by Geyer (1972a, b) who found that the spatial variation of the vertical component was strongly influenced by the dip of the interface.

The purpose of the present study was to examine in some detail the variation exhibited by the field components of a plane electromagnetic wave in the vicinity of a fault. In particular we have elected to study the variation in the vertical magnetic component and in the surface wave impedance across the discontinuity. As will be shown later, in the results section, we were fortunate to be able to perform the measurements in relatively simple geological environments so that a good comparison could be made between our theoretical predictions of electromagnetic field behaviour and the observed variations.

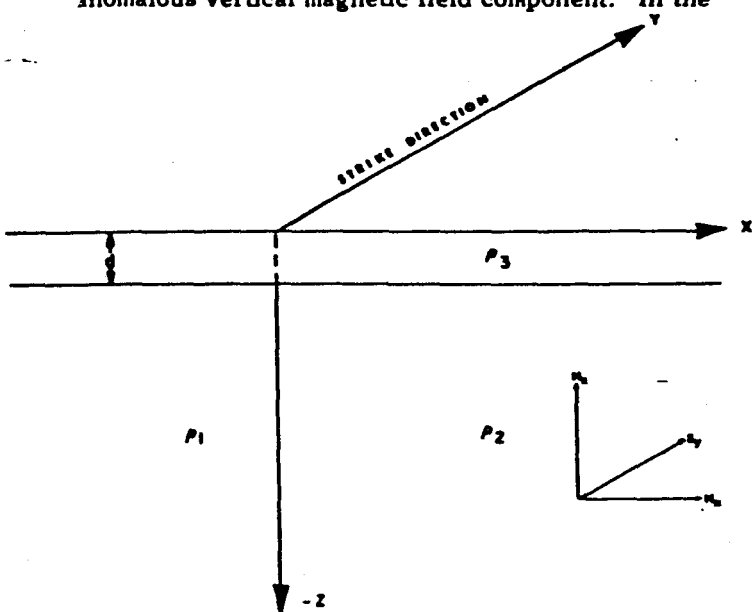


Figure 1. Two-dimensional fault with strike length infinite in y-direction: insert shows E polarization vectors.

¹Department of Geophysics, McGill University,
P.O. Box 6070, Station A, Montreal H3C 3G1, Canada

²Chevron Standard Company Ltd., 400 5th Ave. S.W.
Calgary, Alberta

³Managing Director, IREM-MERI, P.O. Box 6079,
Station A, Montreal H3C 3A7, Canada

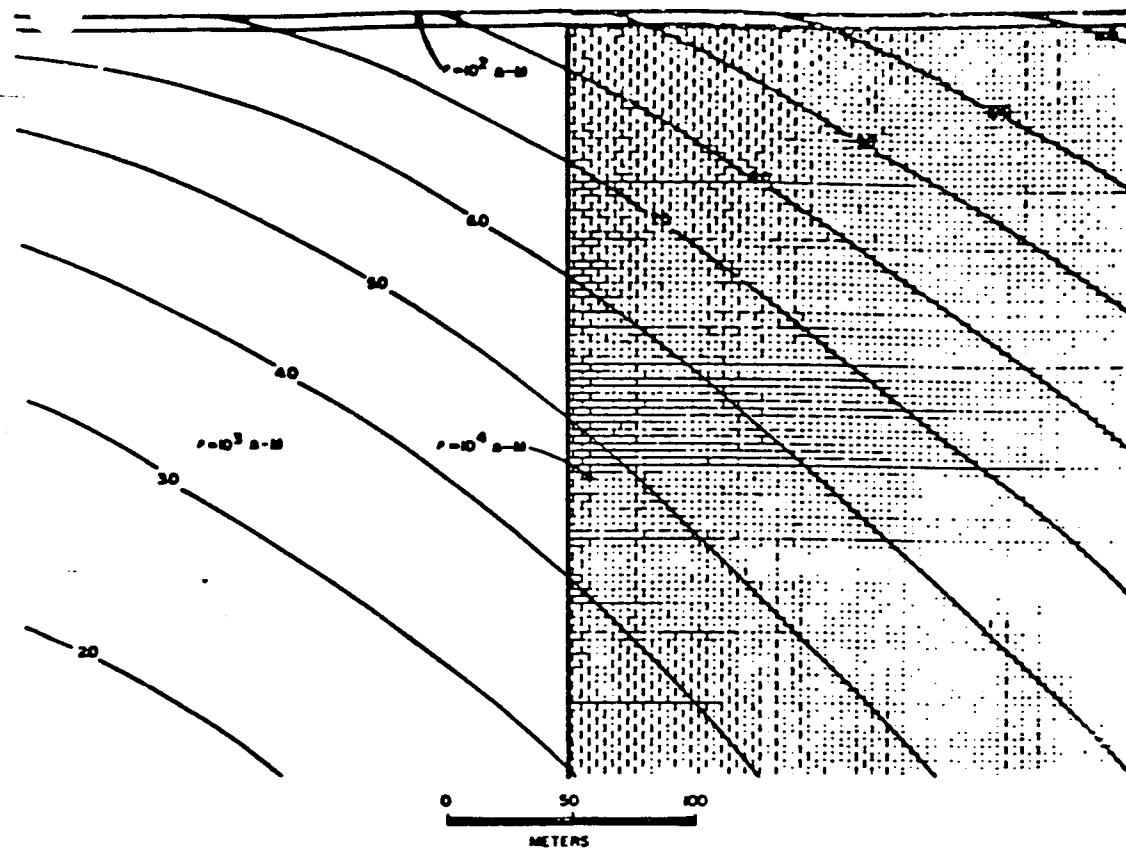


Figure 2.
Subsurface current flow (E_y , relative amplitude distribution) at 10 kHz in the structure of Figure 1.

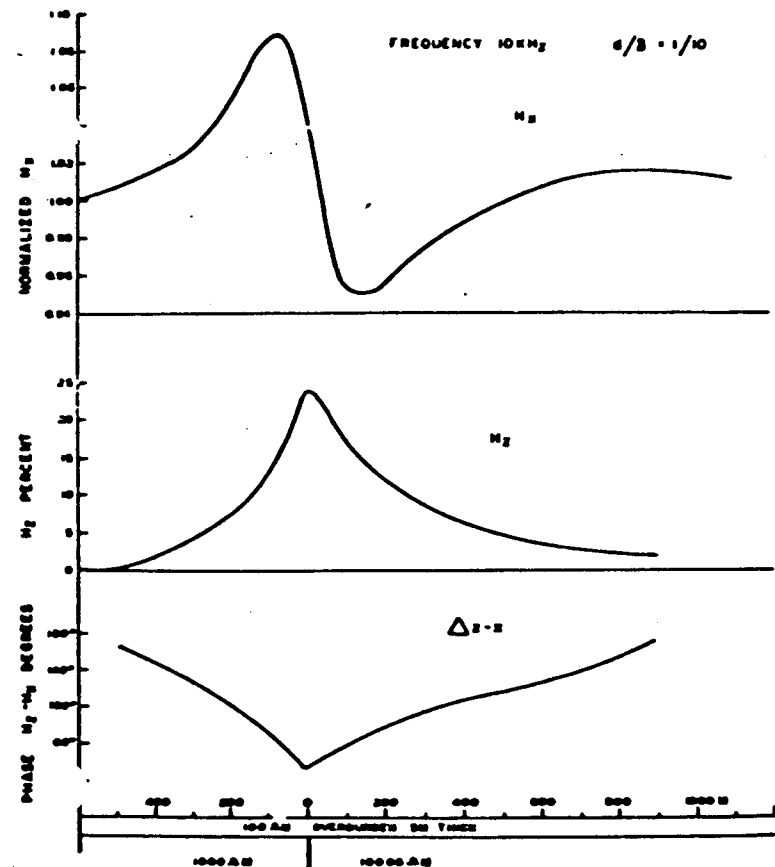


Figure 3. Theoretical profiles of H_x , H_z and Δ_{z-x} over structure of Figure 2.

THEORY

Vertical magnetic field variations

A number of authors (Jones and Price, 1970), Swift (1971) have discussed the mathematical basis for the distortion of an electromagnetic plane wave over a vertical discontinuity separating two half-spaces of different conductivity, with and without an overburden layer above. For a remote natural EM source the direction of E , the electrical and H , the magnetic horizontal vectors is random with respect to the co-ordinate system shown in Figure 1. These vectors, however, may be resolved into components parallel and normal to the contact. The appropriate Maxwell equations thus become:

$$\frac{\partial E_z}{\partial x} - \frac{\partial E_x}{\partial z} = j\omega\mu_0 H_y$$

$$\frac{\partial H_y}{\partial z} = -\sigma E_x \quad \text{for } E \text{ normal to strike (H polarization)}$$

$$\frac{\partial H_y}{\partial x} = \sigma E_z$$

and:

$$\frac{\partial E_y}{\partial x} = -j\omega\mu_0 H_x$$

$$\frac{\partial E_y}{\partial z} = j\omega\mu_0 H_x \quad \text{for } E \text{ parallel to strike (E polarization)}$$

$$\frac{\partial H_x}{\partial z} - \frac{\partial H_z}{\partial x} = \sigma E_y$$

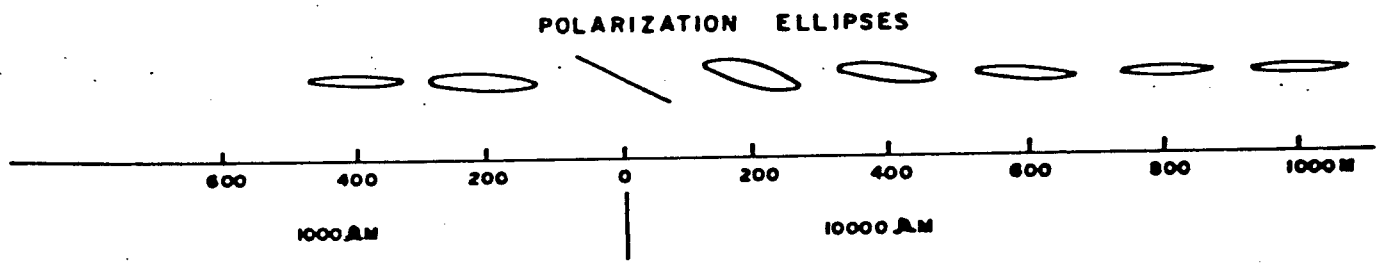
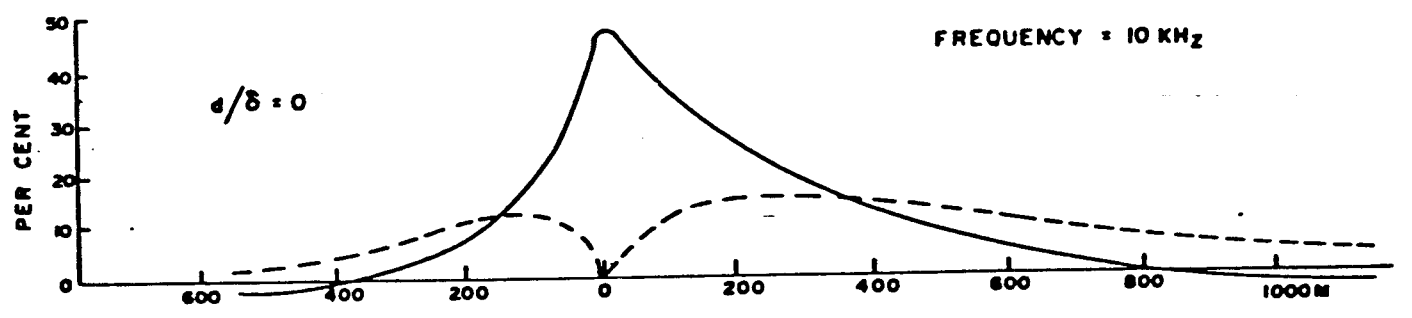
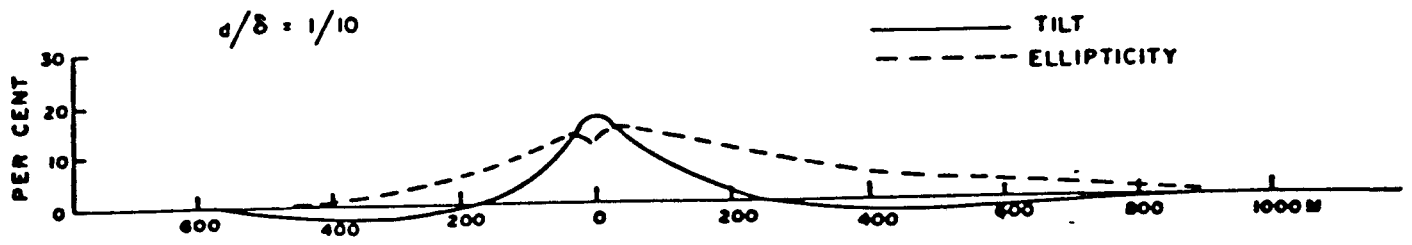


Figure 4. Tilt and ellipticity profiles for $d/\delta = 1/10, 0$ for the structure of Figure 2.

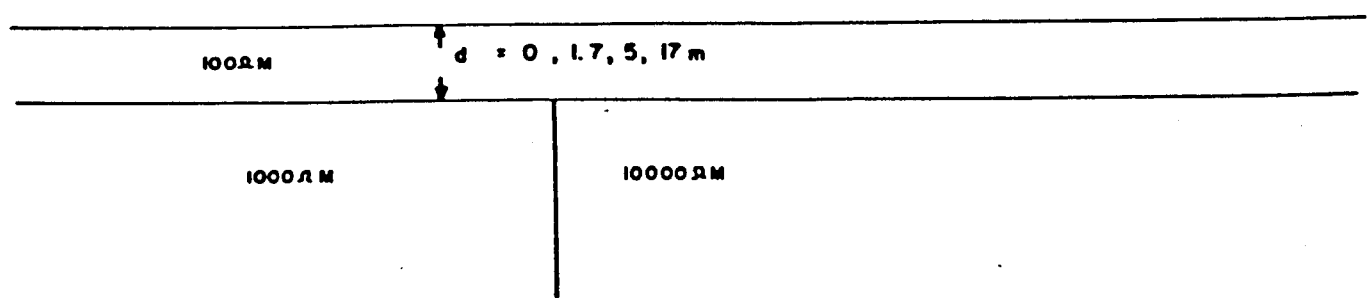
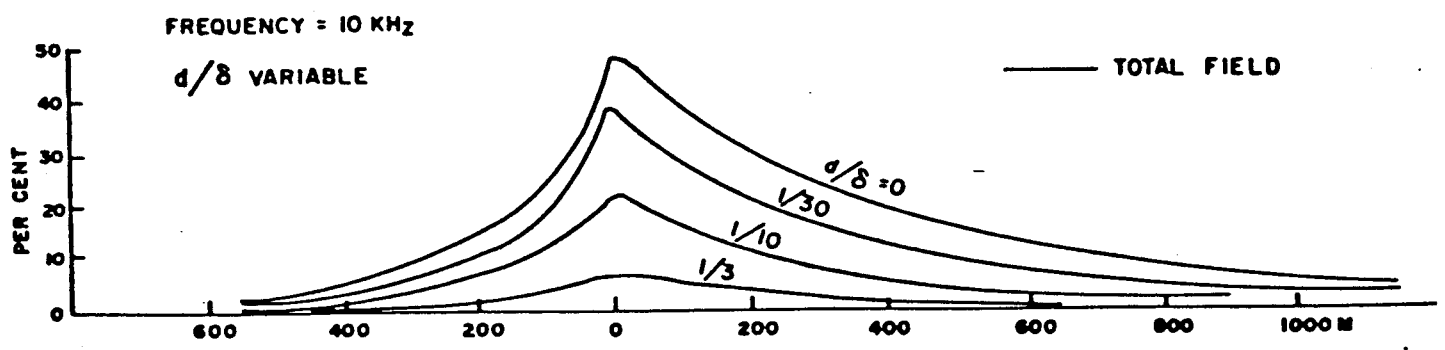


Figure 5. Total field, $|H_z/H_x|$, profiles over the structure of Figure 2 with $d/\delta = 0, 1/30, 1/10, 1/3$.

The E polarization is particularly convenient for the VLF method, which measures H_z and H_x . It is customary, where possible, to select a remote station whose H_x vector is roughly parallel to the survey lines, that is, the station location is more or less parallel to strike.

The VLF source field, propagating parallel to the earth surface and refracted vertically downward at the ground interface, thus provides H_x and E_y components approximately in the appropriate direction. The ground current flow may be readily illustrated by calculating with the aid of numerical techniques (Swift, 1967; Madden and Swift, 1969; Ku et al., 1973) the actual subsurface electric field distribution for a given geological situation.

Figure 2 shows the subsurface current flow (actually the E_y field amplitude distribution) at 10 kHz in the structure of Figure 1 with an overburden of 100 Ωm , 5 m thick and the contact separating beds of 1000 and 10 000 Ωm . Since the skin depth ($\delta = 500 \sqrt{\rho/f}$) for 100 Ωm and 10 kHz is about 50 m, the EM wave is not greatly attenuated in the overburden. Use is made of the ratio d/δ , where d is overburden thickness, since it involves all the significant overburden parameters.

Theoretical profiles of H_x , H_z and Δ_{z-x} over the same structure, are illustrated in Figure 3. As the fault is approached from the left (conductive side) the horizontal magnetic field increases to a maximum, falls sharply to a minimum as the contact is crossed and then increases slowly to background value as the traverse proceeds to the right. The slope is always steeper on the conductive side of the contact, although increasing overburden thickness and/or conductivity reduces the profile amplitude considerably. For very small values of d/δ the background value of H_x is actually larger on the conductive side than at large distances to the right.

The H_z field shows a peak directly over the contact which decays to zero on the flanks. Again the slope is steeper on the conductive side and the peak amplitude is controlled by d/δ . In the bottom profile, the phase variation, Δ , between H_z and H_x is roughly an inverted image of the vertical magnetic field, with a minimum of 32° above the contact and a more or less linear increase on both sides, the steep slope again appearing over the conductive bed. When $d/\delta = 0$ the phase shift is zero

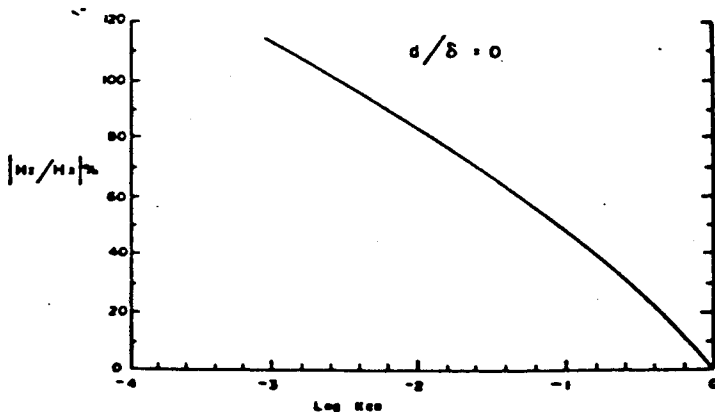


Figure 6. Peak amplitude of total field plotted against $\log K_{CR}$ for structure of Figure 2. No overburden.

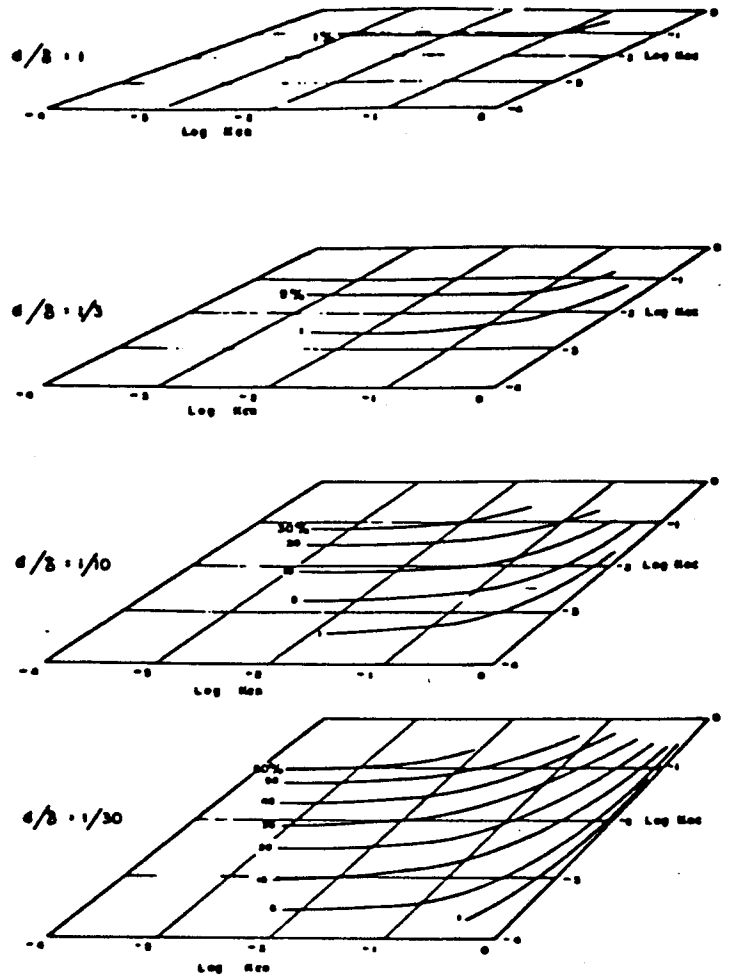


Figure 7. Peak amplitude of total field plotted against $\log K_{CR}$ and $\log K_{OC}$, for $d/\delta = 1, 1/3, 1/10, 1/30$ and structure of Figure 2.

at the contact; as this ratio increases, the cusp persists, although its phase increases.

Because H_z and H_x differ in phase in the vicinity of a conductive discontinuity, the resultant EM wave is elliptically polarized (Heiland, 1940; King, 1971; Paterson and Ronka, 1971). The wave tilt θ (inclination of the major axis with respect to the horizontal) and ellipticity r (ratio of minor to major axes) of the ellipse are given by:

$$\tan 2\theta = \frac{2R \cos \Delta}{1 - R^2}$$

$$r^2 = \frac{1 + R^2 - \sqrt{(1+R^2)^2 - 4R^2 \sin^2 \Delta}}{1 + R^2 + \sqrt{(1+R^2)^2 - 4R^2 \sin^2 \Delta}}$$

where $\Delta = \phi_z - \phi_x$ the phase difference between vertical and horizontal field components, and, $R = |H_z/H_x|$ is their amplitude ratio. With a little manipulation and assuming that H_x is considerably larger than H_z , which is generally the case, these relations become:

$$\tan \theta = R \cos \Delta$$

$$r = R \sin \Delta.$$

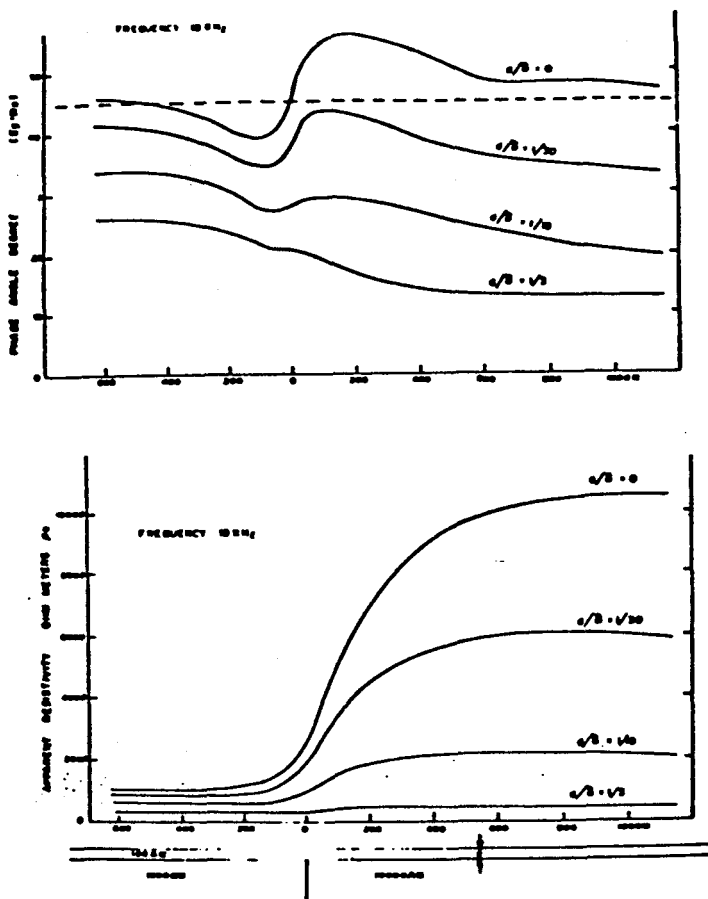


Figure 8. Theoretical profiles of ρ_a and ϕ over structure of Figure 2 for $d/\delta = 0, 1/30, 1/10, 1/3$.

In this case it is useful to note that the total normalized vertical field can be directly calculated from the measurements from:

$$R^2 = \tan^2 \theta + r^2$$

The parameters θ and r are related to "in-phase" and "quadrature" components of the secondary magnetic field (see section on instrumentation). Profiles of tilt and ellipticity, for $d/\delta = 1/10$ and zero (no overburden) are shown in Figure 4. The polarization ellipses at several stations along the traverse are included in the latter profile. Directly above the contact, if the value of Δ is zero, the ellipse degenerates to a straight line whose slope is H_z/H_x .

Clearly the overburden has a pronounced effect on both the tilt and ellipticity profiles. Figure 5 illustrates this point further, where the total vertical secondary field H_z , expressed as a percentage of the primary field, is plotted for increasing values of d/δ .

Two additional parameters may be employed to determine maximum response over the contact. These are K_{CR} , the ratio of resistivities in the conductive and resistive beds and K_{OC} , the ratio of overburden resistivity to the resistivity of the more conductive

bed. When $d/\delta = 0$, the maximum total field response is controlled by K_{CR} only; this is shown in Figure 6, where $|H_z/H_x|$ max is plotted against $\log K_{CR}$. Figure 7 displays total field values for variable K_{OC} as well as K_{CR} , corresponding to d/δ ratios of $1/30, 1/10, 1/3$ and 1 . When $d/\delta = 0$, the peak response will be 50% for any $K_{CR} = 1/10$ ($10 \Omega m$ vs $100 \Omega m, 1000 \Omega m$ vs $10\,000 \Omega m$, etc.); it should be noted, however, that the profile widths will be different. This will also be true for other values of d/δ when K_{CR} and K_{OC} are fixed.

From the foregoing discussion it is clear that, in areas where the overburden resistivity is large compared to rock resistivity or where $d = 0$, it would be possible to use the H_z measurements to determine the structure parameters from the $|H_z/H_x|$ max ratio, from the skewness of the profile, and from the profile width. A conductive overburden, however, affects these quantities greatly and other techniques are required. In general, we may summarize the behaviour of EM field components over a vertical fault as follows:

1. The total field response is an asymmetric peak over the fault and decays more rapidly on the more conductive side.
2. The in-phase component of the secondary vertical magnetic field is also an asymmetric peak above the fault and decays more rapidly on the more conductive side.

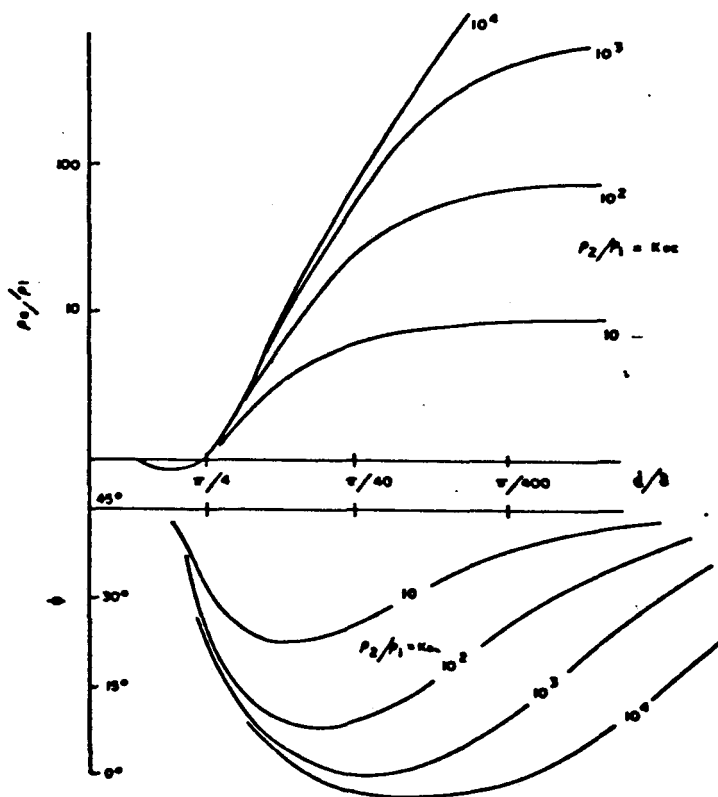


Figure 9. Variations of amplitude $|\rho_a/\rho_1|$ and phase ϕ for two-layer earth with resistive basement (after Cagniard (1953)).

3. The quadrature component displays a local minimum over the fault, the response being broader than that of the in-phase. The minimum becomes less pronounced with increasing depth of overburden.
4. Both in-phase and quadrature response decrease with increasing depth of overburden. The quadrature response becomes greater than that of the in-phase when the overburden thickness is more than approximately one-half a skin depth.
5. In-phase and quadrature response increase with increasing resistivity contrast across the fault.
6. Anomaly width decreases with increasing frequency, for a given resistivity contrast.

Surface impedance variations

Another method which can be useful for the mapping of lateral discontinuities involves the simultaneous measurement of E_y and H_x as in magnetotellurics (Collett and Becker, 1968). The surface impedance, Z , is the ratio of these two quantities and defines the "apparent resistivity" for the underlying terrain via

$$\rho_a = \frac{1}{\mu\omega} |Z|^2 \quad \text{in MKS units.}$$

Usually, Z is a complex quantity because E_y and H_x are not in phase with each other. Thus Figure 8 shows theoretical profiles for the apparent resistivity and the phase difference between E and H across the original contact of Figures 2 to 6 for the d/δ ratios used previously. It is again apparent that increasing depth of overburden influences the results by decreasing values of both ρ_a and ϕ on each side of the contact, while smoothing the profile slope directly over it.

Although the variation in the apparent resistivity near the contact can only be calculated numerically, the values of this quantity and the accompanying phase difference, remote from the fault, can be computed analytically. Variations of amplitude $|\rho_a|$ and phase ϕ for a two-layer earth - that is, the overburden layer remote from the fault - are shown in Figure 9. These are the standard master curves developed by Cagniard (1953), reproduced only for a conductive upper layer. Although magnetotelluric sounding normally involves measurement of horizontal orthogonal E and H fields over a range of frequencies, it is possible, by assuming a resistive bedrock, to estimate the overburden parameters from this master chart even when $|\rho_a|$ and ϕ have been determined only at a single frequency in the field.

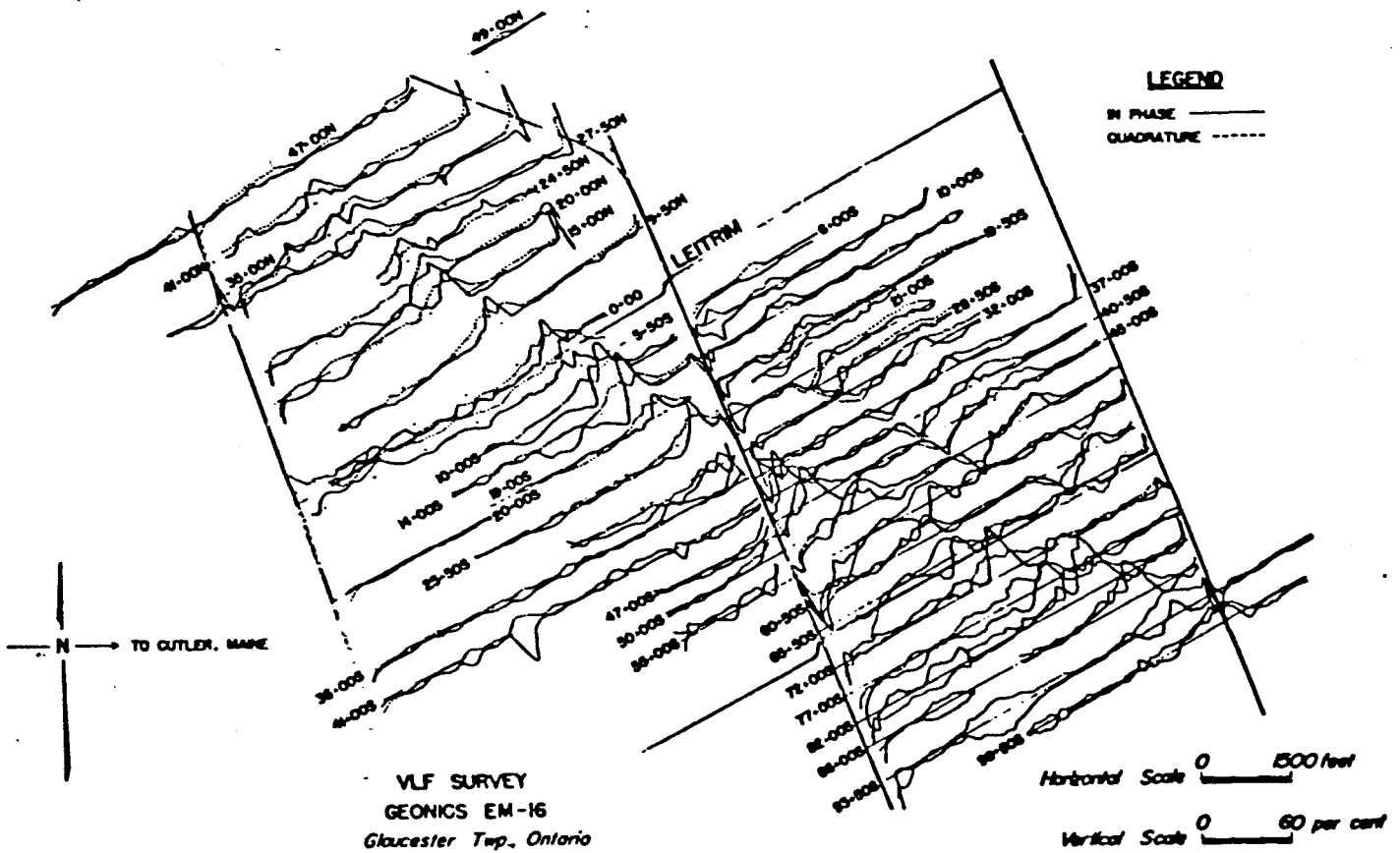


Figure 11. VLF in-phase and quadrature profiles, Leitrim area.